



The University of
Nottingham

UNITED KINGDOM • CHINA • MALAYSIA

**Adhesive Bonding of Discontinuous Carbon
Fibre Composites:
An Experimental Investigation**

TRISTAN KIT NICHOLLS, BEng

Thesis submitted to the University of Nottingham for the degree
of Doctor of Philosophy

DECEMBER 2013

Abstract

The excellent specific stiffness and strength of carbon fibre reinforced polymer composites means that the automotive sector has been investigating methods of implementing these materials into structurally demanding applications. The work detailed within this thesis supports ongoing research at the University of Nottingham into the automated manufacture of discontinuous carbon fibre reinforced polymer composite materials. Advances in the automation of composites manufacturing has meant that methods to effectively join these materials is required. This work provides a fundamental understanding of the differences that result from the adhesive bonding of a discontinuous fibre composite (DFC) compared to conventional fibre reinforced composite materials.

The main objective of the project was to characterise the behaviour of adhesively bonded DFC adherends. Using a single lap shear joint geometry, an optimised fibre architecture and joint geometry was identified with a 2-part low temperature curing epoxy adhesive being characterised for industrial application. To further improve the performance of the DFC substrates, a fibre alignment technique was implemented that achieved properties comparable to those of more traditional non-crimp fabric composites. From the experimental investigations conducted, the use of discontinuous carbon fibre reinforced composites in bonded assemblies shows promise with the potential for use in structural applications.

Acknowledgements

The author wishes to acknowledge the support of his main academic supervisors Dr. Mike Johnson and Prof. Nick Warrior. The assistance also offered by Dr. Tom Turner throughout the project is greatly appreciated.

Special thanks go to the technicians who facilitated so much of this work. The advice and wisdom of Roger Smith made the practical aspects and the time spent in the laboratory more pleasurable.

The author would also like to acknowledge the partners who funded the research as part of the larger Automated Structural Preforms (ASP) project: The Technology Strategy Board (TSB) and Aston Martin Lagonda PLC (AML).

My everlasting thanks go to my family and friends for their support and encouragement throughout the whole process.

Finally, this thesis is dedicated to my parents. No words can ever express the gratitude I have for everything they have done for me.

Nomenclature

AML- Aston Martin Lagonda

AMLC – Aston Martin Lagonda Cure Cycle

DCFP – Directed Carbon Fibre Preform

DoE – Design of Experiment

FO– Fibre Orientation

NCF – Non-Crimp Fabric

NVH – Noise and Vibration Harshness

ODCFP – Oriented Discontinuous Carbon Fibre Preform

P4 – Programmable Powdered Preform Process

RTM – Resin Transfer Moulding

SFO - Surface fibre orientation

SLS – Single-Lap Shear

S/N Ratio – Signal-to-Noise Ratio

SS - Stacking Sequence

VARTM- Vacuum assisted resin transfer moulding

Contents

CHAPTER 1. INTRODUCTION	1
1.1 Assembly Techniques employed at Aston Martin Lagonda.....	2
1.2 Potential for Growth of Composites within the Automotive Industry.....	3
1.3 Directed Fibre Preforming	5
1.4 The Advanced Structural Preforming (ASP) Project.....	7
1.5 Joining of Discontinuous Fibre Composites	9
1.6 Theme of Work	12
1.7 Novelty and Outline of Work	13
CHAPTER 2. LITERATURE REVIEW	14
2.1 Introduction.....	14
2.2 Joint Design	16
2.2.1 Common Joint Geometries	16
2.2.2 Single Lap Shear Joints.....	18
2.2.3 Effect of Bond Dimensions on Single Lap Shear Joints.....	20
2.3 Manufacturing Considerations.....	26
2.3.1 Surface Preparation.....	26
2.3.2 Adhesive Spew.....	31
2.3.3 Adhesive Cure Cycle	33
2.3.4 Environmental Effects	33
2.3.5 Bondline Defects.....	36

2.3.6 Failure Modes	38
2.4 Composite Adherend Properties	39
2.4.1 Volume Fraction	39
2.4.2 Laminar Composite Surface Fibre Orientation and Stacking Sequence.....	40
2.4.3 Discontinuous Fibre Composites	43
2.5 Conclusions.....	49
CHAPTER 3. PRELIMINARY ADHESIVE STUDIES.....	51
3.1 Introduction.....	51
3.2 Bulk Adhesive Tensile Testing.....	51
3.2.1 Results.....	53
3.2.2 Discussion	56
3.3 Surface Preparation.....	57
3.3.1 Results.....	58
3.3.2 Discussion	60
3.4 Post-Cure Study	61
3.4.1 Results.....	62
3.4.2 Discussion	65
3.5 Fibre Orientation Study.....	66
3.5.1 Results.....	67
3.5.2 Discussion	68
3.6 Conclusions.....	69
CHAPTER 4. EFFECT OF FIBRE ORIENTATION ON BONDED SLS JOINTS USING A CONVENTIONAL LAMINAR COMPOSITE SUBSTRATE.....	71
4.1 Introduction.....	71
4.2 Methodology	72
4.2.1 Manufacture of NCF Preforms	72

4.2.2	Resin Transfer Moulding	73
4.2.3	Cutting of Substrate	74
4.2.4	Assembly of Single Lap Shear Joints	74
4.2.5	Mechanical Testing	75
4.3	Test Results for NCF SLS adhesive Joints	76
4.3.1	Analysis of Failure Modes	76
4.3.2	NCF SLS Tensile Testing Results	78
4.3.3	Comparison of NCF Preform Performance	82
4.4	Discussion	83
4.4.1	Effect of Fibre Orientation.....	84
4.4.2	Effect of Changing Stiffness on performance of NCF SLS joints.....	85
4.4.3	Design of Experiment	86
4.5	Conclusions.....	87
CHAPTER 5. OPTIMISATION OF BOND PARAMETERS FOR DCFP SINGLE LAP SHEAR JOINTS.....		89
5.1	Introduction.....	89
5.2	Methodology	92
5.2.1	Manufacturing of DCFP Substrate.....	93
5.2.2	Resin Transfer Moulding	94
5.2.3	Cutting of Substrate	94
5.2.4	Manufacture of DCFP SLS adhesive joints	95
5.2.5	Mechanical Testing	96
5.3	Analysis of Joint Failure Modes	99
5.3.1	Settings for Optimising Adhesive joint failure mode	102
5.4	Representative Stress-Elongation Plots of Results	103
5.5	Results from Statistical Analysis	105
5.5.1	Settings for Optimising Shear Strength of DCFP SLS joints	106
5.5.2	Settings for Optimising Elongation to Failure of DCFP SLS joints	107

5.5.3 Recommended Settings for Manufacture of DCFP Substrate	108
 5.6 Discussion	110
5.6.1 The use of the Taguchi Method	110
5.6.2 Effect of Bond Overlap.....	111
5.6.3 Effect of Bond Width.....	112
5.6.4 Effect of Substrate Thickness	113
5.6.5 Effect of Tow Size	114
5.6.6 Effect of Fibre Length.....	115
5.6.7 Effect of Bond Gap	116
 5.7 Conclusions.....	117
 CHAPTER 6. EFFECT OF FIBRE ALIGNMENT ON THE SLS JOINT PERFORMANCE OF ORIENTED DCFP SUBSTRATES.....	119
 6.1 Introduction.....	119
 6.2 Methodology	120
6.2.1 Manufacture of ODCFP Substrate.....	121
6.2.2 Resin Transfer Moulding	121
6.2.3 Cutting of Substrate	122
6.2.4 Assembly of Single Lap Shear Joints	122
6.2.5 Mechanical Testing.....	123
 6.3 Test Results for ODCFP SLS Samples.....	124
6.3.1 Stress-Elongation Plots	125
6.3.2 Effect of Fibre Orientation.....	127
6.3.3 Effect Chopper Gun Height	128
6.3.4 Effect of Tow Size	129
6.3.5 Effect of Fibre Length.....	130
6.3.6 Interactions of Note.....	131
 6.4 Optimal Level Settings for ODCFP SLS adhesive joints	134
 6.5 Discussion	135
6.5.1 Interaction Effects.....	135

6.5.2	Fibre Orientation.....	136
6.5.3	Induced Alignment.....	137
6.5.4	Tow Size	138
6.5.5	Fibre Length.....	138
6.6	Conclusions.....	139
CHAPTER 7. DISCUSSION AND CONCLUSIONS		141
7.1	General Discussion	141
7.2	Major Conclusions	144
7.3	Future Work.....	148
REFERENCES		151
Appendix A.	Materials	159
Appendix B.	Adhesive Cure Cycles.....	163
Appendix C.	Analysis of adhesive joint failure loci	164
Appendix D.	Non-Crimp Fabric.....	165
Appendix E.	Optimisation of DCFP Substrate.....	172
Appendix F.	Investigation of SLS Joints manufactured using ODCFP Substrate	182

Chapter 1. Introduction

The implementation of more stringent regulations on vehicle emissions has led to much attention being paid towards ways of improving the fuel efficiency of vehicles whilst maintaining a high performance. One of the best ways of reducing vehicle mass is through targeted light weighting programs which is generally achieved through a system of careful materials substitution. By cutting a vehicles weight by 100 kg it is possible to save between 0.3 and 0.4 litres of fuel for every 100km travelled [1].

The high specific stiffness and strength of Carbon Fibre Reinforced Polymers (CFRPs) makes them highly appealing for use in high performance applications. By using these materials, the mass of a vehicle body structure can be reduced by between 50% and 70% compared to a conventional steel Body-In-White (BIW). In comparison, materials substitution to materials such as high strength steel or aluminium only have the potential to reduce weight between 23-35% and 40-55% respectively [1,2]. Reduction in the mass of the body structure has the additional effect of being able to reduce the weight of secondary systems such as the drive train, suspension and braking systems. The proliferation of vehicles with increased efficiency requirements (electric, hybrid and fuel-cell), as well as increasingly stringent CO₂ emission regulations will lead to further adoption of CFRP's.

There are a number of additional benefits of using composite materials in automotive applications other than weight saving. Owing to the ability to engineer the properties of fibre reinforced composite materials it is possible to consolidate the number of parts used within a vehicle assembly; thereby saving time, labour and additional joining costs. Fibre reinforced composites also have superior corrosion properties whilst also offering improved Noise, Vibration and Harshness (NVH) characteristics. Finally, there are the improved properties with regards to crash and impact properties. In impact, metals fail by folding or buckling; whereas, composites failure through a complex series of fracture mechanisms including; fibre fracture, matrix crazing or

Chapter 1 - Introduction

cracking, fibre/matrix debonding, delamination or inter-ply separation. These mechanisms can be controlled to increase the energy-absorption of the materials[3,4].

There remain challenges to overcome with respect to the adoption of composite materials when it comes to materials substitution away from the relatively well understood metallic options more frequently used in structural components within the automotive industry. The costs of changing from a predominantly metallic vehicle body structure to a fibre reinforced polymer one can be prohibitive for relatively small automotive companies, especially those already heavily invested in the infrastructure needed to assemble bodies from metallic materials. The concerns of increased cycle times associated with traditional polymer composite manufacturing can also act as an inhibitor; whilst, a lack of engineering experience or expertise within the field of fibre reinforced polymer composites compounds the problem.

1.1 Assembly Techniques employed at Aston Martin Lagonda

The Vertical Horizontal (VH) vehicle architecture employed by Aston Martin Lagonda (AML) is an evolution of the adhesively bonded, extrusion intensive structures previously used by manufacturers of other low volume niche vehicles. These are defined as those that produce less than 20000 vehicles in a given year [5]. Extrusion intensive structures are assembled using a combination of straight extrusions and sheet panels adhesively bonded to produce a single underbody. Examples of this type of structure are the Lotus Elise (1995) and its variant, the Vauxhall Speedster. This structure had a mass of only 75kg and was manufactured mainly of aluminium adherends joined using a single component hot cure adhesive [5,6].

The Aston Martin Vertical-Horizontal (VH) architecture was developed using this extrusion intensive approach. It allows for a vehicle architecture that can be easily modified in both length and width, thus providing a highly versatile system that allows for a variety of vehicle models to be produced using a similar architecture. The Aston Martin Vantage V8 (Figure 1) is one such example of a vehicle produced using the VH architecture. The body is constructed from a total of 172 individual extruded and sheet aluminium parts bonded using a single component hot cure adhesive and

weighing 142kg [5,6]. By using a composite-intensive alternative structure this part count could be greatly reduced.

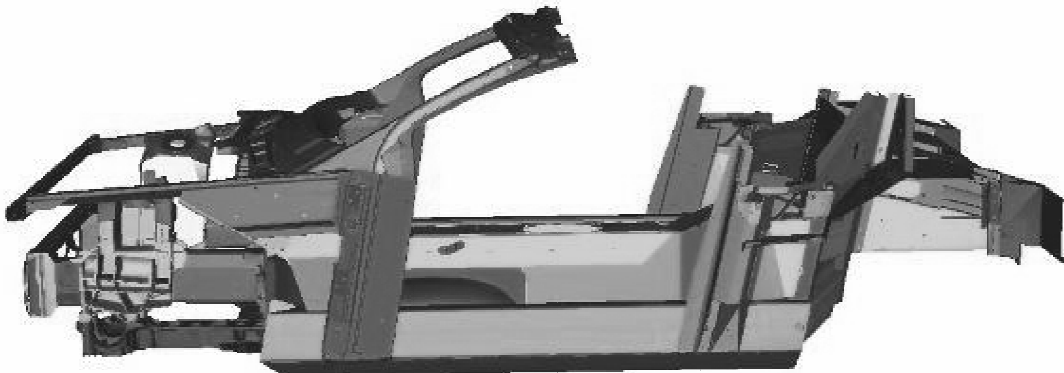


Figure 1 Underbody of Aston Martin V8 Vantage from [5]

1.2 Potential for Growth of Composites within the Automotive Industry

The use of composite materials within the automotive industry is expected to grow considerably in the near future as polymer composite materials become more prevalent within vehicle body structures. Currently the application of composite materials in mass produced passenger vehicles has been restricted to secondary structures such as body panels. These are mostly manufactured from sheet moulding compounds (SMC) or glass mat thermoplastics (GMT) using randomly oriented short fibre discontinuous glass reinforcements with volume fractions limited to approximately 30% [1]. These materials exhibit good formability and can be used in stamping processes similar to those used in the manufacture of metallic components; however, they are not well suited to structural applications.

Whilst the application of composite materials in the automotive industry has been well received for semi-structural secondary structures, the implementation of structural component substitution to composite materials has not been as readily accepted. This is partly due to a lack of understanding of the available manufacturing techniques but has also been limited by the cost of implementing changes in production and as a result of the perceived increase in manufacturing cycle times. Currently the use of carbon fibre reinforced polymer components in structural applications is limited to

Chapter 1 - Introduction

high value automotive applications [7]. A number of high profile research programs have been aimed at addressing some of these concerns.

Through the Technologies for Carbon fibre reinforced modular Automotive Body Structures (TECABS) project a floor pan structure was designed and manufactured making use of heavy tow carbon fibre yarns woven into a non-crimp fabric. A weight saving of approximately 50% was achieved with a parts count reduction of 70%. The manufacturing costs per part were higher than for conventional metallic floor pans; however, the reduction in parts had the potential to make savings in the moulding, stamping, joining and assembly processes. The problem of implementing the process into current manufacturing techniques was that the assembly of the preforms and resin transfer moulding (RTM) process meant production was limited to 50 parts per day [8].

The challenge of reducing cycle times has been investigated by the Automotive Composites Consortium (ACC), a research group comprising of the Chrysler Group, Ford and GM amongst other manufacturers. It forms part of the larger United States Council for Automotive Research (USCAR) with the aim of investigating new technology for implementation within the automotive industry. In 2012 the group announced the development of an underbody manufactured from a single composite part which could be mass produced with a 2.5 minute cycle time. It comprised a sheet moulding compound (SMC) system with long-glass fibre reinforcements being used in most of the part with chopped structural SMC used to reinforce the ribs in the component. This was envisaged to replace an under body that would typically comprise of 14-16 individual steel components resulting in a weight saving of nearly 10kg [9].

The High Volume road transport applications of lightweight structural COMPosite parts (HIVOCOMP) project is an EU Framework Program including 3 automotive manufacturers as well as materials suppliers and academic institutions that began in 2011. The aim is to develop new cost effective materials and processing solutions as well as simulation tools to allow for easier implementation of composite material manufacturing techniques into industry. The program involves work with thermosetting matrix materials as well as thermoplastic polymer composites intended

Chapter 1 - Introduction

to facilitate the manufacture of passenger vehicles. Initial progress reports are expected to be announced in 2013 [7, 10].

Resin Transfer Moulding (RTM) techniques with faster curing resins, novel out of autoclave processes and new preforming processes are all currently being researched and implemented within the automotive industry. Other techniques centre on using preforming techniques that allow for areas to be locally reinforced with high fibre volume contents [7]. This local reinforcement allows the preform to be tailored to compensate for specific load cases.

1.3 Directed Fibre Preforming

A technique that is attracting interest is the use of discontinuous directed fibre composites (DFC) to manufacture components. These are appealing as they represent cost advantages as well as more appealing manufacturing processes. The traditional uses of discontinuous fibre processes are in injection moulding, compression moulding and in processes where high performance is not required.

Owens Corning developed the Programmable Powdered Preform Process (P4) using a computer controlled chopper head mounted to a robotic arm to chop glass rovings onto a perforated screen to produce a preform. The method provided an alternative to conventional layup of fabrics and mats as well as sheet moulding compounds (SMC) and bulk moulding compounds (BMC). Owing to the versatility of the process it gained interest as a result of its consistency and repeatability. There were cost reductions, materials savings, reduced scrap, improved net shape preforming capabilities and reduced cycle times compared to conventional laminar composite manufacture [10,11].

Although the use of a chopped fibre processes was not new, this was the first time the process had been successfully automated. Previously, the fibres were deposited using hand held chopping devices. By using a programmable robot spraying fibres to manufacture composites it is possible to move a robotic chopper head along a predefined path thereby allowing for precise and repeatable control of the entire fibre deposition process [12]. During the manufacture of these preforms the primary parameters requiring control are the fibre volume fraction (Vf), tow size, fibre length

Chapter 1 - Introduction

and the fibre orientation. The fibre orientation is in itself governed by a set of complex interactions between the tow size, fibre length, fibre deposition rate, robot path and the chopper gun distance from the tool surface. All of these variables serve to define the eventual mechanical properties of the discontinuous directed fibre composite.

As part of the development process of P4 a number of case studies were used to prove the versatility of the manufacturing technique. Applications ranged from aerospace, automotive and marine applications to an improved fireman's protective helmet. The manufactured components were all infused using different techniques with the chosen process being tailored to each specific application. The problem was that all of these were non-structural parts manufactured using glass fibre rovings [10].

The Automotive Composites Consortium (ACC) developed P4 further with a focus on implementation of the process within the automotive industry. The aim was to design, analyse and develop a composite-intensive body-in-white (BIW) which offered a minimum weight saving of 60% over steel whilst not impacting on the manufacturing, assembly or process targets of the manufacturers. Originally this was aimed at high-volume production (100 000+) with the intended costs being similar to those of an equivalent steel structure [13,14].

In order to achieve the desired performance and weight savings needed for implementation in both the automotive and aerospace applications, the glass rovings would have to be replaced by carbon fibre. Investigations using the existing commercially available carbon fibre tows identified the lack of a suitable roving that could handle the manufacturing constraints of the P4 process. Once a suitable set of fibres had been developed alongside a number of suppliers, a set of demonstrator parts were manufactured to prove the manufacturing process [15].

A B-pillar was chosen as the demonstrator for the P4 process using both carbon and glass fibre rovings. The part demonstrated the ability to tailor the preform thickness from between 1.5mm and 8mm. Using a target volume fraction(Vf) of 40% the biggest challenge encountered was to maintain an even fibre coverage across the preforms at the desired Vf and at the low thicknesses. After infusion and assembly,

Chapter 1 - Introduction

the structural performance and dimensional tolerances of the part were shown to be equal to, or better, than the equivalent steel structure [13,14].

The Ford Programmable Preforming Process (F3P) has since been used by Aston Martin Lagonda to manufacture several composite components. Applicator System AB designed and fabricated the commercial scale preforming unit. Using glass and carbon fibre rovings, parts for the Aston Martin Vanquish, DB9 and V8 Vantage have been used in production models. However, to date the Volume fraction has been limited to between 35-40%, restricting the use to cosmetic and semi-structural applications. To achieve the 50-70% weight savings compared to steel, the process has to be developed further to allow for the manufacture of structural components[16].

1.4 The Advanced Structural Preforming (ASP) Project

The Advanced Structural Preforming (ASP) project builds on work previously carried out at the University of Nottingham into the manufacture of directed carbon fibre preforms (DCFP). The work had determined that DCFP had the potential for use in higher performance applications than the secondary structures it is currently used in. The ASP project seeks to determine the optimum mechanical properties that can be attained from this process along with the process developments required to achieve them. Historically the technique used glass fibre rovings; however, the process has been modified to exploit the beneficial properties of carbon fibres. The process consists of four stages: deposition, consolidation, stabilisation and extraction [17]. The manufacturing cell at the University of Nottingham is presented in Figure 2.

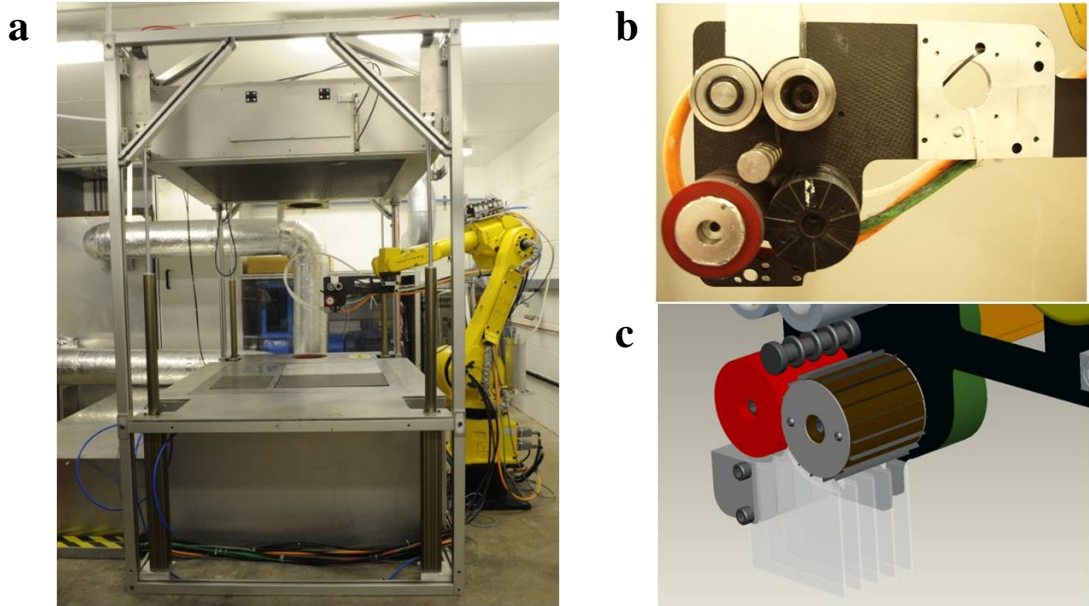


Figure 2 (a) DCFP cell at the University of Nottingham (b) Chopper Head (c) Alignment head for oriented DCFP

A schematic of the DCFP process used is presented in Figure 3. The process first draws carbon fibre tows directly from a bobbin and passes it through a chopper head mounted to a robot, depositing them on a perforated tool with a powdered binder. Air is evacuated from the tool allowing for the fibres to be held in position whilst the preforming process continues. Each single layer is made up using an orthogonal spray pattern comprised of an east-west pass followed by a north-south pass with each subsequent pass being offset by 50mm. In this manner it is possible to maintain a good degree of fibre coverage across the preform.

After the deposition process is complete a matching tool is lowered over the preform to consolidate the preform with the preform being heated to melt the binder. Once the preform is cooled it is extracted from the perforated tool and placed in rigid tool and infused with resin using a Resin Transfer Moulding (RTM) technique [17].

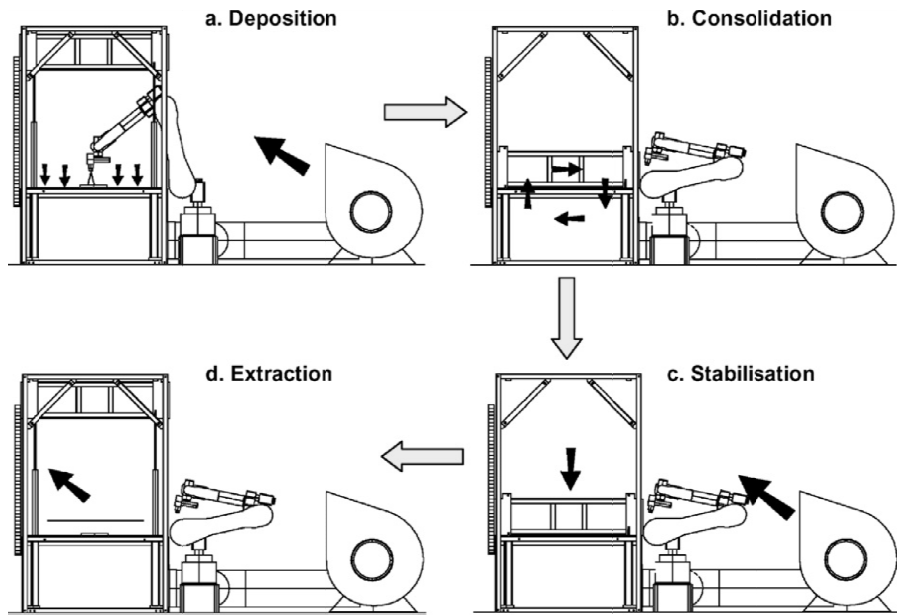


Figure 3 DCFP process schematic demonstrating the four production steps: (a) Fibre and Binder Deposition. (b) Binder Heating. (c) Binder Stabilisation. (d) Preform Extraction. Reproduced from [17]

The research program was divided into three distinct categories of research. The first area studied the critical process parameters. The work focused on the optimisation of the fibre architecture and matrix properties with particular attention being paid to optimising the fibre coverage and compaction of the preforms to improve the bulk material properties of the DCFP process. A separate area of research focussed on the development of a process model which simulated the entire fibre deposition process. The focus of the research presented in this thesis revolves around the development of adhesive bonding techniques for use with the DCFP composite material. The research centred on the modification of the DCFP fibre architecture to optimise the adhesive joint performance.

1.5 Joining of Discontinuous Fibre Composites

One of the largest challenges that remain with the substitution of metallic components for polymer composite ones is the problem of how to join these materials effectively. This is of particular concern for structural components. When considering the assembly of the traditional Body in White (BIW), the joining techniques commonly employed can be divided into 3 categories; warm joining techniques (welding operations), cold joining techniques (mechanical fastening) and adhesive bonding. As the focus of the present research project revolves around material substitution there

Chapter 1 - Introduction

will be many instances of the need to join dissimilar materials as well as similar materials. Cold joining and adhesive bonding offer the most versatile options with regards to joining many different types of material; however, this is not without its own challenges [18].

On average 20 different joining techniques are used in the manufacture of a lightweight BIW [18]. Whilst there is no universal adhesive option that will effectively bond all materials, careful material and adhesive selection can greatly reduce the manufacturing costs by reducing the number of techniques used overall. However, adhesive bonding will never be able to replace all of the joining operations associated with traditional BIW assembly. The use of structural adhesives within industries throughout the European market is predicted to grow by approximately 13% from 2008 to 2015 with significant growth being expected in the automotive and aerospace sectors [19].

There are a number of advantages to using adhesive bonding from a structural point of view. Primarily this is the ability to provide better joint efficiencies than mechanically fastened fixtures owing to the continuous nature of the join. This acts to provide a more effective method of load transfer as the stresses are more evenly distributed than other joining methods such as spot welding and riveting. If the joint is designed efficiently the bonded structure can sustain higher loads than traditional methods whilst also improving the overall stiffness of the joint. The adhesive joint can also improve the fatigue resistance compared to equivalent structures joined using mechanical fasteners. [18,20-22]

From an assembly point of view the choice of adhesive bonding can also offer a number of benefits. As previously mentioned the assembly of parts can be simplified owing to the ability to join dissimilar materials with the adhesive able to compensate for the stresses arising from different coefficients of thermal expansion. In turn this can increase production and quality whilst reducing the costs of manufacture. The low cure temperature of most adhesives means that they have the ability to join heat sensitive materials. The low thermal input required for curing also means the substrate structure remains unchanged resulting in no heat affected zone being present. Traditional welding operations typically result in a heat affected zone being present in the areas surrounding a join. The absence of mechanical fasteners can reduce overall

Chapter 1 - Introduction

weight whilst the continuous bondline of the adhesive can provide corrosion resistance and act as a sealant at the same time as reducing the noise, vibration and harshness (NVH) levels of a bonded structure [1,18,20,22].

The concerns expressed about adhesive bonding within both the automotive and aerospace industries centre around 2 main preoccupations. Primarily there remains concern over the fatigue and durability of bonded, structural components over a vehicles lifetime, whilst there also remains a lack of understanding of the fracture behaviour of adhesively bonded joints [22].

Through minimal design, substantial strength can be achieved using adhesive bonding for structural applications but the process of adhesive selection, validation, specification and performance must be studied. If not, it is possible to have an adhesive joint which passes the initial screening but which does not have the required durability. As such, it is important to understand both the initial and long term design requirements for a given joint. It is necessary to develop the entire system as a whole rather than treating the adhesive and substrate as separate entities as this allows for better control of the system; thereby improving the quality and service life of the bonded components [22]. The design of joints usually involves: the study of joint geometries, materials used, loading conditions, failure modes, temperature and humidity effects as well as additional computational analysis [20].

Conventional design approaches for adhesive bonding suggest that it is best to design bonded joints such that the adhesive can sustain loads greater than the unloaded strength of the substrate being bonded. This means the adhesive should be able to carry all possible load cases across the joint. In metallic substrates this is a valid design approach; however, the low inter-laminar strength of polymer composite materials means consideration of the underlying adherend is also important as this will define many of the failures observed both in testing and in service if the design is inappropriate [23].

As previously mentioned there is no adhesive that provides a universal solution to effective bonding. As such, the manufacturing processes require detailed attention as the requirements change depending on the adhesive in use. Surface preparation and curing are critical in ensuring there is consistent performance from the adhesive. This

Chapter 1 - Introduction

holds true for most adhesives. Inspection of defects of bonded structures by the Royal Australian Air force found that 53% of the significant defects found in these structures were associated with adhesive bond failures. These failures were primarily the result of poor surface preparation or improper joint design. When manufacturing the joint it is important to recognise that adhesives perform badly under peel loading and as such, measures must be taken to avoid this loading condition. [18,20,22]

One of the challenges with regards to the uptake of structural adhesives is the lack of confidence in adhesives demonstrated by some design engineers. As the performance of structural adhesive bonding is proven, this confidence will improve and the uptake will become more widespread [19]. In turn the resulting economies of scale will help drive down the costs of substituting more conventional joining methods with adhesive bonding.

1.6 Theme of Work

Aston Martin has an established understanding of structural adhesive bonding using aluminium substrates. Along with Hydro Automotive, it has used adhesive bonding dispensed through a robotic application system to assemble the vehicle tubs at Hydro Automotive and body panels at its Gaydon facility since 2003 [6]. The assembly of the vehicle tub was moved to Gaydon in 2005 to allow for greater flexibility in assembly of the VH architecture [5]. Currently the VH vehicle tubs make use of self-piercing rivets to locate the parts during cure; however, the use of similar rivets should be minimised when using composite materials in the future. Although DCFP has been shown to be less notch sensitive than conventional laminar composites, the presence of notches in the material results in undesirable areas of stress concentrations [24].

With the potential for more widespread use of DCFP in structural applications, the challenge remains to understand the best methods of joining DCFP with similar and dissimilar materials. This work seeks to gain an understanding of how the fibre architecture of discontinuous carbon fibre composites affects the overall joint performance of adhesively bonded composite structures. This performance is studied through a series of experimental investigations with the work split into a number of different sections that are detailed below.

1.7 Novelty and Outline of Work

The thesis details an extensive study into the effect of varying the fibre architecture of a discontinuous carbon fibre reinforced polymer composite material and its effect on the adhesive bond performance of these structures. The author is unaware of similar work being conducted in this area of research.

Using a randomly deposited DCFP substrate the fibre architecture and bond dimensions were varied. This allowed the effects of these parameter changes to be studied with respect to the joint strength and elongation to failure as well as the failure behaviour of the joint. It was demonstrated that it was possible to optimise the joint failure mode as well as the mechanical performance through variations in the fibre architecture of the randomly oriented substrate. This has not been demonstrated previously.

The work then progressed onto using a newly developed alignment technique to study the joint performance as a result in changes to both the fibre architecture and fibre orientation. Through the two different investigations a set of optimised fibre architectures and bond dimensions were identified that allows further detailed work to be conducted in this field.

Chapter 2. Literature Review

2.1 Introduction

When characterising an adhesive, a thorough research program is required to understand the performance of the adhesive when subject to different testing conditions. The normal approach is to determine the bulk adhesive properties through a series of tests and then to determine its performance in service using a number of specially designed joint geometries. In addition to the experimental work, stress analysis and a good understanding of the desired failure criterion are required. Finally, visual inspection of the failed adhesive joints provides an insight into the failure behaviour of the joint [25,26].

Modern structural adhesives can be broadly divided into two classes. The first are high glass transition temperature thermosetting resins such as epoxies that are high strength adhesives with a high modulus after cure but with a low strain to failure. It is possible to improve the impact performance and the strain to failure in these resins through chemical modification such as the addition of tougheners. The second class of adhesives are low transition temperature adhesives which are characterised by a low modulus and a high strain to failure, polyurethanes for example. These tend to not be as strong; however, their ability to absorb large strains makes them an appealing alternative to epoxies for bonding in structural applications. Traditionally they have been used in non-structural applications such as in the sealing and packaging industries. The most widely used adhesives in structural applications are epoxies, polyurethanes and methacrylates. An overview of the typical performance envelopes for these adhesives is shown in Figure 4 [18,22,27].

Structural polyurethane adhesives are desirable owing to very good fatigue and impact resistance and performance at low temperatures; however, they are limited by their strength. The adhesives are highly customisable with modifications to the polymer chemistry allowing for both the strength and elongation to failure to be engineered to

the desired specification. The large performance envelope in Figure 4 highlights this flexibility [25,28-30].

Methacrylates are a class of adhesives that exhibit good mechanical properties with an excellent ability to bond many different classes of material with minimal surface preparation. These have a good fatigue resistance and can be designed to have very short curing times; however, the main disadvantage to using these adhesives is the poor resistance to elevated temperatures and humid environments [25,29-31].

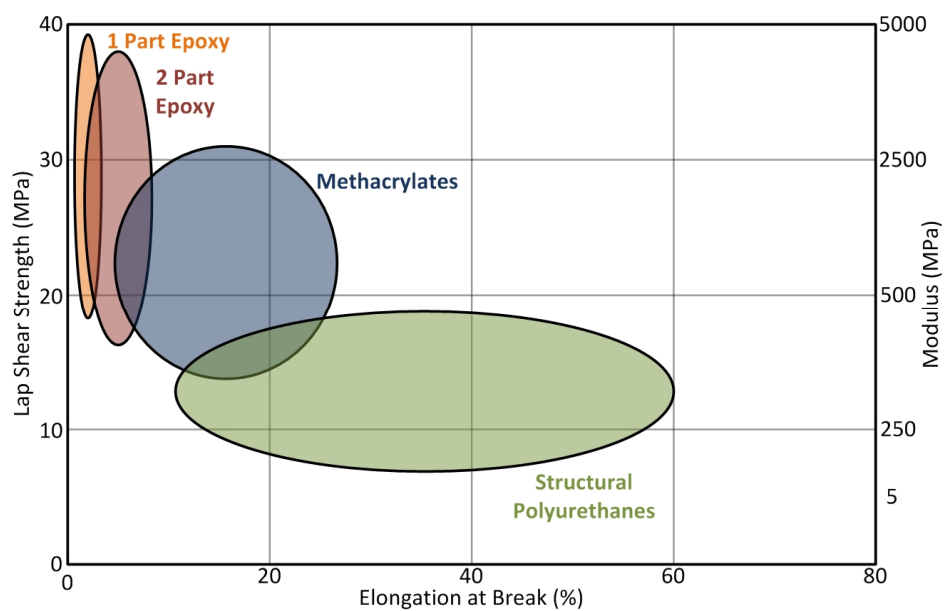


Figure 4 Typical Performance envelopes of structural adhesives. Modified from [30]

During the research investigation contained within this thesis, the focus has been on 2-part epoxy adhesives. The excellent mechanical properties and chemical and thermal resistance mean these adhesives are appealing for use in the automotive industry and are the most commonly used adhesives in automotive BIW production. Of the commercially available epoxy systems available, 2-part medium viscosity, room temperature curing adhesives are the most successful as they are relatively user friendly compared to most other adhesives. Currently Aston Martin utilise a single component adhesive which requires a high temperature cure; however, this is incompatible when bonding composite components. It is for this reason that a replacement 2-part epoxy was sought [25,28,30,32].

The adhesives studied in this research make use of an aliphatic amine curing agent. Although this has the benefit of curing at room temperature, without careful control the curing can be both incomplete and demonstrate low glass-transition temperatures.

Chapter 2 – Literature Review

Without modification to the adhesives, 2-part epoxy adhesives can require long cure times and can fail in a brittle manner. There is always the scope to modify the components depending on the desired properties; however, each change must be studied using the desired configuration of adhesive and adherend [25,29,32]. This can be both a costly and lengthy process.

2.2 Joint Design

The joint geometry and material properties of both the adhesive and substrate work in unison to define the behaviour of a bonded system. The strength of an adhesive joint also depends on the type of loading and stress distribution within the joint. For composite substrates the high through-thickness stresses at the joint overlap ends are the biggest concern to joint strength owing to the low through-thickness strength of most composite materials. There have been various attempts to control the stresses by varying both the joint geometry and material properties [25].

When designing adhesive joints for structural applications the aim is to reduce the number of factors that contribute to the stress concentrations arising as a result of the modulus mismatch between the substrate and adhesive. A poorly designed joint configuration results in the benefits of the high stiffness and strength of the adhesive structure being lost. The difficulties in identifying the optimal joint geometries that maximize the joint strength and the challenge of modelling these adhesive systems, means that the current use of adhesive bonding in structural components is limited [22,25].

2.2.1 Common Joint Geometries

Six commonly used adhesive joint geometries are shown in Figure 5. These joints are all used in different applications depending on the desired function. The most commonly studied adhesive joints are single-lap joints. These are discussed in more detail. Double-lap joints, single and double scarf joints and single and double strap joints are also encountered throughout literature. There are also many other geometries that have been designed to deal with unique load cases and requirements [25,33].

Chapter 2 – Literature Review

The scarf joints illustrated in Figure 5 present a challenge when used to bond composite materials due to the need to machine the adherends prior to bonding. They produce a variation in the stiffness of the substrate at the bond surfaces owing to the changes in fibre orientations at the bond interface which result as a consequence of machining. Large fluctuations in stress distributions can even occur within joints of the same laminate lay-up. Stress concentrations can build up as a result of the fibre discontinuities present across the bondline [25].

The strap joints illustrated are generally used to illustrate work undertaken to repair cracked structures. They are composed of either 1 or 2 composite patches applied to a cracked or divided assembly. Although not the most commonly used joints in adhesive studies, they are important to gain a good understanding of the behaviour of repaired components [34].

The high strength and stiffness of modern structural adhesives used to bond composite materials will usually induce failure within the composite substrate rather than in the adhesive owing to the low interlaminar strength of the adherend; this is something that must be considered when choosing a joint configuration.

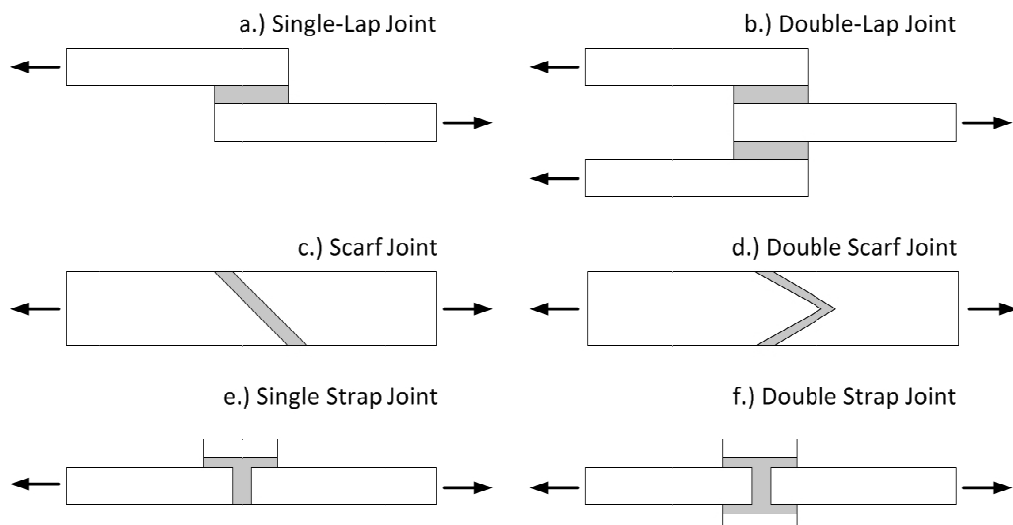


Figure 5 Schematic of commonly used joint configurations. a.) Single-Lap Joint b.) Double-Lap Joint c.) Scarf Joint d.) Double Scarf Joint e.) Single Strap Joint and f.) Double Strap Joint

2.2.2 Single Lap Shear Joints

The most widely studied test specimen used in tensile testing of adhesives is the single-lap shear (SLS) joint. When using the SLS joint configuration the measured adhesive shear strength cannot be used in design work as the failure is generally not controlled by shear but rather as a result of a combination of joint deflections, rotations and induced peel stresses; however, it is useful to compare different adhesive systems when selecting an appropriate adhesive configuration. Extensive work has been carried out both experimentally and through numerical techniques to optimise this joint design [25]. Although the numerical analysis of single-lap shear joints is not addressed specifically in this thesis, a brief summary of the previous work carried out in this area is included for reference purposes.

The earliest analysis that considered the non-uniform shear stress and strain distribution across the adhesive bondline was performed by Volkersen. This analysis assumed the adhesive only deformed in shear with the adherends deforming in both shear and tension. The problem with this analysis was that it did not take into account the bending effect caused by the eccentricity of the single-lap joint load path. The technique was refined further by Goland and Reisner which took into account the bending observed within the substrates. A graphical example of the shear and peel stresses calculated by Goland and Reisner is presented in Figure 6. By considering the bending moment and transverse loading the large deformations that occur in metallic adherends could be accounted for; however, the adhesive bondline was considered to be an infinitesimally thin bond. Hart-Smith [23] did consider the bondline and presented a modified form of the bending moment factor that accounted for the changing bondline thicknesses.[35,36]

The works by Volkersen, Goland and Reisner and Hart-Smith provided a significant advance in predicting the joint strength of single lap-shear joints; however, there were limitations. The models did not take into account through-thickness variations in stress through the bondline, meaning stresses at the adherend-adhesive interface were not considered [22]. This means that these estimates are not appropriate for composite adherends owing to the importance of being able to estimate the through-thickness shear stresses present near the surface of the adhesive-adherends interface. The

analyses also did not take into account the zero-stress condition at the overlap ends meaning the peak stresses are over estimated in the analyses thereby giving conservative failure load predictions. Assumptions were also made that the bond between the adhesive and adherend is perfect at the interface with no void content[37].

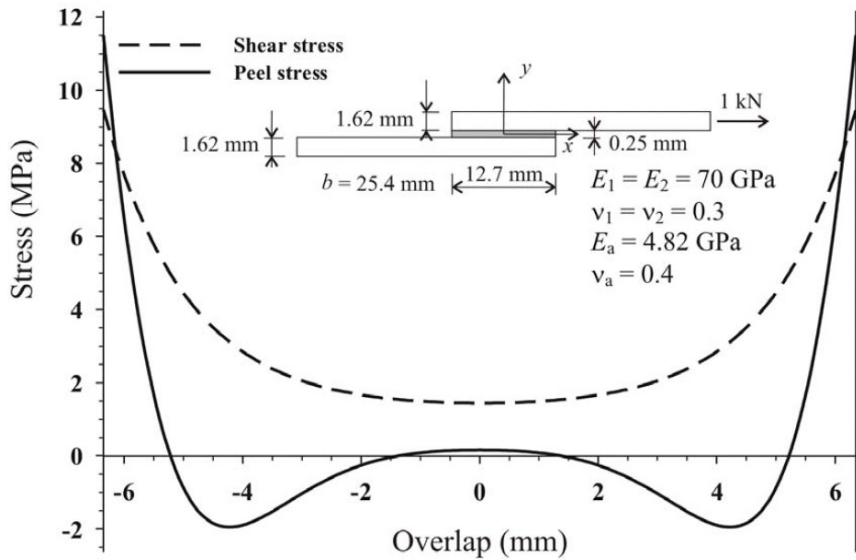


Figure 6 Example of Goland and Reissner's adhesive shear/peel stress distributions. From [36].

Attempts to optimise the performance of single lap shear joints have been carried out both experimentally and through numerical modelling to account for composite substrates. Tsai[38] proposed an improved form of the Volkersen and Goland and Reissner's solutions for single lap-shear joints. By including the shear deformation of the adherends, the solutions provide more accurate predictions of the adhesive shear distribution and maximum shear strength of the adhesive. These solutions offered better strength prediction, especially in the case of adherends with relatively low shear strength (such as polymer composite adherends).

Magalhaes[39] presented an evaluation of the stress concentration effects in single lap-shear joints when using composite adherends. In the work, 2-D finite element analysis was used to calculate the stress concentrations in critical areas of a bonded composite to composite joint. The author argues that with the application of a suitable damage model this would allow for more accurate prediction of failure mode for bonded composite joints manufactured using laminate composite adherends as the stresses at the adherend-adhesive interface would be considered.

Further work carried out by Mortensen[40] developed a unified approach for modelling a number of commonly used structural adhesive joints manufactured with a composite adherend. In the analysis the adherends were modelled as wide beams or plates in cylindrical bending. The laminate properties were derived from classical laminate theory and assumed to be linear-elastic in nature. The work examined both linear-elastic and non-linear solutions for the adhesive. The linear elastic solutions were shown to under-estimate the yield strength of the adhesive joint. When the non-linear solutions were applied the high stress concentrations observed in the linear elastic analyses were smoothed with the results matching closely to finite element analysis carried out on the same joints[40].

2.2.3 Effect of Bond Dimensions on Single Lap Shear Joints

Changing the adhesive bond overlap, bond width, bondline thickness or substrate thickness will have an effect on the overall joint strength and behaviour of an adhesive joint; as such, a summary of these effects is provided.

- Bond Overlap

The influence of bond overlap has been well documented in literature. The degree to which bond overlap influences the overall joint strength is dependent on a number of factors. The adhesive shear stresses along the length of a single lap shear joint are non-uniform, with high stresses observed at the joint ends with low shear stresses in the middle of the joint as illustrated in Figure 6. In theory extending the overlap length beyond a certain limit only serves to increase the low stress plateau in the middle [20]. The optimal overlap length of a single lap shear joint has been investigated with the main findings and observations summarised below.

When Da Silva[41] and Pereira[42] used metallic adherends to test the influence of bond overlap, the experimental and numerical analyses demonstrated a linear increase in the joint strength of SLS adhesive joints with increasing overlap length. These findings were tested from 12.5mm to 50.8mm. Pereira modelled the SLS joint and showed that an increase in bond overlap reduced the peak values of stress and strain near the overlap ends.

Chapter 2 – Literature Review

Song et al [43] studied 4 different overlap lengths when investigating the effect of varying manufacturing parameters on the shear strength of single lap-shear joints manufactured using a composite substrate. The overlaps ranged from 12.7mm to 50.8mm. In the study the shear strength of the SLS joints reduced from approximately 34MPa to 11 MPa as the overlap increased. Ferreira[44] observed similar when two different overlap lengths were studied, one of 30mm and the other of 60mm. The samples were subject both to static and fatigue tests. The 30mm overlap length outperformed the 60mm samples in both of these tests. The findings confirmed that there is a relationship between adhesive joint strength and the overlap length; however, the relationship could not be described as increasing linearly when using composite adherends.

Song theorised that as a result of the peak stresses at the overlap ends reducing gradually, and because the bulk of the load transfer occurs in this region there is an overall decrease in joint strength above a certain overlap length [43]. Meanwhile, De Goeij[45] explained the presence of an upper limit of overlap length in single lap-shear joints manufactured using composite substrates by arguing that the strength of the joint will increase only until the properties of the adherends are surpassed. At this point the failure becomes defined by the inter-laminar strength of the composite laminates, something proposed separately by Neto[46].

The influence of the overlap length does not operate independently of the other factors that define the geometry of an adhesive joint. Both the ductility of the adhesive and the bondline thickness have been observed to interact with the overlap length to change the behaviour of the bonded joints. The ductility of the adhesive coupled with the bond overlap length affected joint behaviour regardless of whether a metallic or composite adherend was used. Da Silva[41] noticed the influence of the overlap length when carrying out investigations using a metallic adherend. Neto[46] also observed the failure modes and load carrying ability of the SLS joints manufactured with a carbon-epoxy composite laminate affected. When a brittle epoxy adhesive was used, the adhesive joint failed through substrate delamination in joints with an overlap length greater than 20mm. No significant increase in strength was observed with the increased overlap length. For the more ductile polyurethane adhesive, cohesive failure

was observed up to the maximum overlap length tested (80mm) with an almost linear increase in strength.

Lee[47] observed that when a thin bondline thickness was used to manufacture a single-lap adhesive joint there was no significant increase in strength when the overlap was increased from 50 to 100mm. However, when the adhesive thickness was increased to 1mm there was a notable increase in strength (~45%). Although the type of adhesive is unspecified, it is assumed that this was a relatively flexible adhesive and the additional bondline thickness allowed the adhesive to sufficiently deform to achieve its maximum strength without surpassing the interlaminar strength of the GFRP adherends.

Previous work suggests the bond overlap is one of the most influential geometric factors that define the joint strength of an adhesively bonded single-lap shear joint. Although an upper limit has been identified, beyond which increasing the overlap is ineffective, this limit appears to be highly dependent on the substrate and adhesive material properties as well as the bondline thickness of the joint.

- Effect of Adhesive Bondline Thickness

In the past the adhesive bondline has been used to fill gaps when assembling components. Current research suggests this approach is both inefficient and detrimental to the performance of adhesively bonded components. Whilst this would not be important if assembling cosmetic or semi-structural components, in a structural application, greater bondline control is required. The review of literature identifies both an optimal bondline thickness and an explanation of why joint strength decreases with increasing bondline thickness.

Da Silva[41] identified the bondline thickness as having the second highest influence on joint strength after the adhesive bond overlap when using steel adherends and a bondline thickness ranging from 0.5mm to 2mm. Grant[48] also tested the sensitivity of adhesive bondline thickness using steel adherends. As the bondline thickness increased, so did the bending moment of the adhesive joints. For substrates with a greater degree of plastic deformation the overall strength of the joint was reduced.

Chapter 2 – Literature Review

This reduction was attributed to an increase in the proportion of peel stresses present within the joint.

Davies et al[49] investigated the influence of bondline thickness on the joint strength of adhesive joints using an aluminium adherend. The thicknesses studied were in the range of 0.2mm to 1.3mm. A significant decrease in yield stress and failure strain being observed for specimens with thicker bondlines. Using numerical analysis this decrease was shown to be the result of higher stress concentrations occurring within the larger bondline thickness. The authors proposed an upper limit of 0.6mm for the bondline thickness for samples tested in tension. Arenas[50] applied a Weibull distribution to identify the optimum adhesive bondline thickness in the region of 0.4mm-0.8mm for single lap-shear joints using an aluminium alloy substrate. From the results of the analysis an optimal thickness of 0.5mm was found to provide the most reliable shear strength for the joints.

When the substrate material is changed to a polymer composite, the optimum adhesive bondline thickness was observed to change. Lee[47] used four different adhesive bondline thicknesses ranging from 0.2mm to 2mm to bond GFRP single-lap shear specimens. Reducing the adhesive bondline thickness from 2mm to 0.2mm resulted in a 22% increase in joint strength when using a double lap joint. Cognard[51] also investigated the influence of bondline thickness in a composite to composite adhesive assembly subject to cyclical shear loading. Four different bondline thicknesses were analysed ranging from 0.36mm to 1.30mm. Cognard observed that the deformation observed was proportional to the adhesive bondline thickness and that the strength of the joint decreased with an increased bondline thickness.

Various authors have theorised as to the cause of the decrease in joint strength above a certain bondline thickness. De Goijer[45] proposed that an increased bondline thickness also increases the joint fracture resistance up to an optimum thickness. Beyond this the fracture resistance begins to decrease leading to more rapid crack propagation. Cognard[51] identified the presence of defects or the modification of the adhesive/substrate interface as being the most likely factors that influence joint strength when bondline thickness is increased. This has been contested by research by Davies[49], who suggests the size of bondline defects and the adhesive polymer microstructure have an insignificant effect on the bond strength with increasing

bondline thickness. The use of smaller bond gaps did however reduce the influence of test imperfections such as specimen misalignment[49]. Taib[33] reasoned that the observed decrease in strength as the bondline is increased is a result of the thin adhesive layers being more likely to be under plane stress conditions than plane strain. Consequently, as the bondline thickness is increased, so too does the likelihood of the joint being under plane strain thereby increasing the crack propagation as this condition favours brittleness.

The research carried out into the effect of bondline thickness appears to conclude that there exists an optimum bondline thickness above which the strength of the adhesive joint decreases. There is a degree of uncertainty over the main causes of this decrease in strength. Some theories have been detailed but it would seem that the optimum bondline thickness is dependent on a number of factors including the substrate properties, presence of defects, and the loading conditions close to the adhesive-adherend interface of the joint. This combination indicates that the optimum bondline thickness is specific to each adhesive-adherend configuration.

- Effect of Substrate Thickness

Increasing the substrate thickness of single lap-shear adhesive joints relates directly to the increase in stiffness of the substrate as well as the increase in the bending moment of the joint. The performance of a single lap shear joint is related to the bending effect and eccentric loading of the joint. The stiffness of the composite substrate is proportional to the cubic of its thickness; therefore, the thicker adherends result in higher joint strengths regardless of the increase in bending moment due to the eccentric loading. Finite element analysis (FEA) also demonstrates a decrease in von-Misses stress at the overlap ends as the thickness of the composite substrate is increased [43].

When Pereira[42] studied adhesively bonded single lap-shear joints manufactured from an aluminium substrate, increasing the thickness of the adherend naturally increased the joints rigidity and as a result increased its strength. Increasing the substrate thickness from 1mm to 1.5mm increased the failure load by about 18%. Numerical studies also showed that by increasing the substrate thickness the bending moment and adhesive yielding load increased. There was also a decrease in the angle

of rotation of the adhesive joint which, in turn reduced the plastic strain peak and increased the yield strength.

Song[43] investigated the effect of adherend thickness on the joint strength of adhesively bonded SLS joints using a quasi-isotropic composite substrate. In total, four different thicknesses were used. Experimental investigations and finite element analysis were carried out on the different joints. The findings concluded that as the thickness of the substrate was increased, so did the overall shear strength of the adhesive joint. The problem with bonding fibre reinforced composite adherends is the low interlaminar shear strength of the substrate. Keller[21] noted that the through thickness strength of the adhesive-adherend interface is considerably higher than the adherend through thickness strength in-between the composite layers. The increase in strength that results from the increase in substrate thickness will thus be limited to the point at which the shear stresses near the surface of the adherend surpass the interlaminar strength of the composite.

With the use of a discontinuous carbon composite substrate in this investigation, there will exist a maximum thickness at which the through-thickness strength of the laminate will be surpassed; the adhesive joint strength will be defined by this. If the behaviour of the adhesive joint is the same as for the material testing of the bulk substrate, there may also exist a minimum substrate thickness owing to the heterogeneous nature of the material resulting from an uneven fibre coverage [52].

- Bond Width

Most numerical techniques consider the stress distribution within an adhesive joint in a 2-dimentional sense, neglecting to study the distributions across the width of the joint. This assumption makes the numerical analysis simpler and is appropriate when considering a homogeneous substrate; however, the random nature of a discontinuous fibre reinforced composite material means the material properties at the surface of the adherend will change across the specimen width. Owing to this uncertainty, it is necessary to investigate this to ascertain whether there exists a minimum bond width below which edge effects affect the bonded joint performance. This may impact both the strength and variability of the results. De Goeij [45] observed that for an increasing joint width, the edge effect of the stress/strain peaks becomes less

significant as the peak stress towards the centre of the joint plateaus. Therefore, a minimum width must exist from which the energy release rate of the adhesive joint remains constant regardless of width. In an industrial setting, the minimum effective bond width will most likely not be of concern; however, it remains important for characterisation studies.

2.3 Manufacturing Considerations

2.3.1 Surface Preparation

It is generally possible to attain good joint strength in quasi-static testing with minimal surface preparation. When an adhesive joint is in service, it is necessary to modify the substrate surface to promote adhesion and to ensure minimal environmental degradation. The surface of the substrate and the preparation of this interface is perhaps the most important process that defines the quality of an adhesive joint. The principle of ensuring good adhesion is that the adherend surfaces should be free from contaminants, chemically active (to promote chemical bonding between adherend and adhesive) and resistant to environmental degradation during service. Currently, most adhesive failures can be attributed to poor processing conditions. Inadequate surface preparation techniques are the largest single contributor to these failures [20,25].

Hart-Smith[53] addressed the issue of good surface preparation when using composite adherends as a result of ineffective joint preparation observed within the aerospace industry. The Primary Adhesively Bonded Structure Technology (PABST) program was a research program carried out in the late 1970s and the early 1980s that aimed to address concerns about effective adhesive bonding when using metallic adherends. The research findings have since been implemented for aircraft development when bonding metallic structures; however, Hart-Smith argues that the composites industry is faced with similar challenges to those experienced prior to the PABST program. Premature failures in composite bonded joints caused by the use of peel ply as a surface preparation technique are presented as an example. Peel ply was originally intended to create a rough surface to bond to; however, it has been shown that on a microscopic level the furrows it creates are smooth. An additional problem identified was the nylon residue and other adhesion inhibitors that remained on the surface after the removal of the peel ply. The author investigated the implication of changing the

Chapter 2 – Literature Review

peel ply to a polyester fabric as well as studying the bond surfaces of abraded and sand blasted samples. Hart-Smith emphasised that the problems discussed have not been identified across the composites manufacturing industry and that the reasons for premature joint failure are yet to be fully understood.

- Surface Cleansing

The first step to ensuring good adhesion between adhesive and adherend is to have an uncontaminated bonding surface to adhere to. Prior to bonding, it is necessary to remove grease and other contaminants from the substrate surface. When using composite components it is also common to have traces of mould release present on the surface, which severely inhibits good adhesion. Some authors have recommended the use of a solvent or an aqueous detergent to clean the surface. The cleansing agent must be selected based on the contaminants which are expected to be present. The substrate must then be thoroughly dried prior to bonding. Health and Safety along with environmental concerns have led to some solvents being banned in the workplace. These are considerations which must be taken into account when selecting an effective cleaning product [54-57].

Davis[20] observed that the use of a detergent can introduce further contaminants onto the bonding surface if these are not completely removed from the surface. The choice of applicator was also identified as being important. A lint free cloth is recommended as some cloths contain lanolin or other chemicals that can also contaminate the bond area. Using a single cleaning process has been shown to be insufficient to ensure a good bond. Pereira compared substrates subjected to mechanical abrasion and chemical modification to substrates subjected to a single simple cleansing. The results demonstrated that when subject to tensile testing the samples treated with chemical processes and mechanical abrasion outperformed those specimens manufactured with a simple cleansing operation. This highlights the need for further surface treatment [42].

- Mechanical Abrasion

It is generally acknowledged that the minimum acceptable surface treatment when bonding to composite surfaces is some form of abrasive treatment. The aim of this is

Chapter 2 – Literature Review

two-fold; primarily, it removes loose polymer debris thereby increasing the surface area to bond to as well as exposing a fresh chemically active surface. The use of grit blasting and simple mechanical abrasion is discussed in further detail below [20,56,57].

The use of abrasion as a successful means of treating a surface prior to bonding can be attributed to a number of desirable interactions occurring at the interface. A proportional increase in adhesion may be observed so long as the roughness does not reduce the contact between the two surfaces to be bonded. When stressed, rough surfaces may be able to redistribute the stress so as to redistribute the energy dissipation when the adhesive joint fails. An increase in roughness can also change the failure mechanisms at a molecular level thereby influencing overall joint strength [58] .

Da Silva[41] chose to investigate three different surface pre-treatments when investigating the effect of surface treatment on the shear strength of adhesive lap joints manufactured using a steel substrate. Although the experiment used metallic adherends, meaning the chemical treatment methods proposed are inappropriate for use with composite materials, the study showed that the variation of surface pre-treatment can influence the resulting shear strengths. Of interest is the fact that mechanical abrasion of the samples resulted in strengths equal to, if not better, than those samples subjected to chemical pre-treatments.

Light grit-blasting has been shown to be the most effective method of removing the surface layer of a composite, providing the process is controlled and the blast pressure is not too high. If there is insufficient control of the process it is possible to damage the load-carrying fibres. Banea[25] recommended the use of shot blasting using aluminium oxide grit and performed in a dry nitrogen environment. This presents a manufacturing challenge as the controlled atmosphere adds additional costs to the manufacturing process. Research by Davis[20] concurred; however, the settings of the blast pressure and pass rate must be carefully controlled to avoid removing the entire polymer matrix from the bond surface as this can expose and damage the reinforcement fibres of the composite[52]. Simple surface preparation techniques that are more labour intensive involve the use of abrasive papers or cloths. When using these methods, care must be taken to ensure sufficient material is removed from the

Chapter 2 – Literature Review

surface of the composite while avoiding causing significant damage to the fibres embedded in the composite. Prior to bonding, it is essential the substrate is thoroughly cleaned after the abrasion process to remove any debris created through the removal of the surface layer [20,53].

It is generally accepted that either the use of grit blasting or mechanical abrasion will result in good adhesion between the substrate and adhesive. The limiting factor when choosing the preparation method for mechanical abrasion is the availability of a shot blasting facility with an inert gas delivery mechanism.

- Chemical Modification

Chemical modification of the substrate surface as a pre-treatment for bonding was not carried out in this piece of work; however, some of the methods currently being researched by others are briefly discussed. Examples of this type of treatment include: chemical etching, flame treatments, plasma techniques and the Ion assisted Reaction method.

Chemical etching as a surface pre-treatment modifies the composites' surface topography in order to promote good adhesion. Prior to any chemical etching it is good practice to thoroughly clean the parts to reduce contamination of the chemical solution and improve the interaction between the part surface and solution. There are no specific procedures describing how to effectively treat a composite substrate and as such extensive testing is required to identify the best possible chemical treatment. Chemicals which can change the adhesive properties of a composite include a number of acids, bases, oxidising agents and chlorinating agents, amongst others [54].

Flame treatments are a set of processes designed to render certain plastics adherable. In this method the composite component is passed over an oxidising flame. The flame is a mixture of a hydrocarbon gas and an excess of oxygen. These flame characteristics allow for hydrogen molecules to be removed from the polymer surface and be replaced with oxygenated functional groups. This chemical modification of the substrate surface increases the surface energy of the material in order to promote good adhesion [54].

Chapter 2 – Literature Review

Plasma is produced by exciting a gas with electrical energy and is a collection of charged particles which are electrically conductive and magnetically sensitive. The matter formed is very reactive and it is this characteristic that allows plasma to be used to modify the surfaces of polymeric materials. When treating a surface, the gas used varies depending on the chemical reactions desired but these usually include oxygen, helium and nitrogen. The reaction removes atoms from the polymer surface to produce a desirable surface to bond to. Literature states that plasma treated polymers create bonds that are two to four times stronger than conventional surface preparation techniques. In practice, this is demonstrated by a significant increase in the peel strengths of bonded joints caused by chemical bonding occurring between the polymeric substrate and the adhesive [54,59]. The use of cold plasma treatments on aluminium alloys has also been observed to produce a large reduction in surface contaminants. When subjected to up to two minutes of treatment the presence of contaminants was reduced by over 65% regardless of whether any initial surface cleansing had been carried out. Results were always better than a traditional surface cleansing operation when the treatment time was over 75 seconds. The author is unaware of similar studies using composite material substrates but postulates that similar results may also be observed [60].

The Ion Assisted Reaction (IAR) method is a technique which has been proposed to improve the mixed material bonding of carbon fibre reinforced polymer composites to an aluminium substrate. Research by Rhee[61] uses charged Argon ions (Ar^+) to alter the surface chemistry of a CFRP substrate to improve the fracture behaviour of the adhesive joint. The results of this work indicate that the joint behaviour was similar to an untreated substrate until the onset of crack growth. The fracture toughness of the treated joint improved by 72% compared to the untreated CFRP/aluminium joint. The failure mechanism also changed from an adhesive failure to a cohesive failure. Rhee reasoned that hydrophilic functional bonds such as carbonyl and carboxyl groups are more developed in the treated CFRP which thus improved the adhesive strength between the CFRP and adhesive causing the cohesive failure of the joint [61].

2.3.2 Adhesive Spew

Spew is defined as the adhesive that is squeezed out of the overlap region of an adhesive joint when a joint is closed. Figure 7 shows a number of the most common spew geometries encountered in literature. The spew geometry can affect a number of properties relating to the strength of an adhesive joint. The main effects of the inclusion of spew fillets are summarised below.

When using a steel substrate, changing the spew geometry can reduce the magnitude of peel stresses by up to 5 times and reduce shear stresses by 2 times [22]. Grant et al[48] carried out a series of tests and finite-element analyses to investigate the effect of using a structural adhesive instead of spot welding for the manufacturing of metallic structural components in the automotive industry. The method used single lap shear samples using mild steel adherends with varying overlap length, bondline thickness and the inclusion of a 45° adhesive fillet radius. The research showed that when using a very small bondline (0.1mm) the inclusion of an adhesive fillet did very little to vary the strength of the joint. However, as the bondline thickness increased the effect of the spew played a larger role in changing the strength of the join. As the bondline thickness approached 3mm the strength of a square-ended joint (without spew) was less than half that of the joint with the triangular fillet included [48].

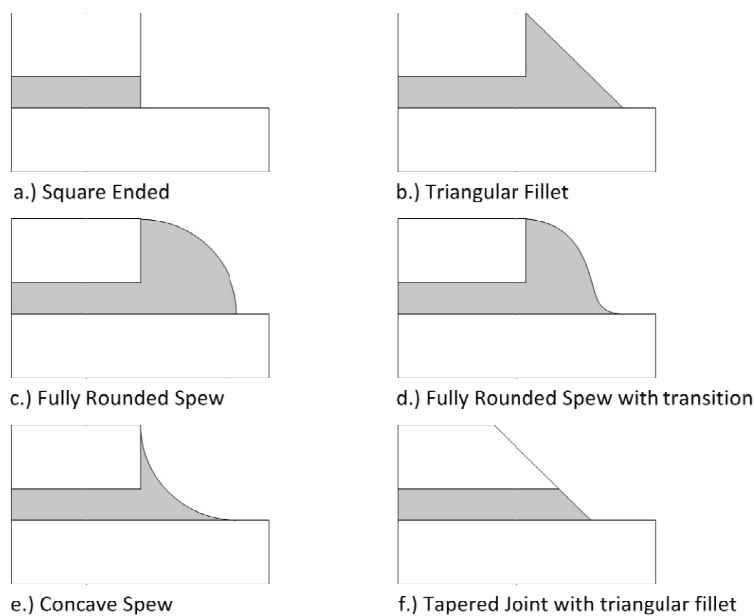


Figure 7 A selection of typical spew fillet configurations

Chapter 2 – Literature Review

Belingardi[62] studied the fillet angles between 15° and 75° in order to identify an optimal spew geometry. The 45° fillet angle was identified as the best compromise between ease of manufacture and reducing peak stresses at the joint ends. While there is a continual reduction in peak stresses with a decreasing fillet angle the manufacturability must also be considered. Kelly[1] identified that using a standard 45° fillet the joint strength increased by 28% when using a carbon fibre reinforced composite adherend. The best improvement was observed for a fully rounded fillet with a rounded adherend which creates a smooth transition; this resulted in a 60% improvement in joint strength compared to square ended joints. This required both the manipulation of the adhesive spew as well as the adherend geometry in order to grade the modulus near the joint ends and reduce the peak stresses located in this region. Whilst theoretically this may be an appealing approach, dimensional control of this nature would be very hard to maintain in an automated production environment.

Wang et al[63] used a Digital Image Correlation (DIC) technique to measure the strain fields near the over-lap ends of a laminated composite single lap-shear joint. Wang used this technique to study the effect of adhesive spew on the stress distribution of the adhesive joint. The spew fillets were shown to carry a portion of the tensile, shear and peel loading which resulted in a decrease in the stress concentrations at the overlap ends.

Lang and Mallick[64] investigated the effects of spew geometry with respect to single lap adhesive joints manufactured using a sheet moulding compound (SMC) composite adherend. Through the use of finite-element techniques it was shown that an increase in spew size resulted in a significant reduction in the stresses observed across the specimen. This is caused by the larger spew size being able to carry a greater load thus reducing the peak stresses at the joint overlap ends. The shape of the adhesive spew also plays a role in reducing stress in the join. This was demonstrated by studying a triangular and arc fillet compared to a normal rounded spew. Despite the triangular and arc spews having less adhesive in the region, the two configurations demonstrated significantly lower peak stresses compared to the rounded spew. Having a smooth transition across the joint was shown to significantly reduce the peak stresses.

Chapter 2 – Literature Review

The effect of spew fillets on joint strength and performance is reasonably well understood with extensive research having been carried out investigating the inclusion of fillet radii using a variety of fillet geometries. When carrying out further research, the consequences of the inclusion or exclusion of spew should be considered when designing experimental procedures.

2.3.3 Adhesive Cure Cycle

There are 3 different ways of adhesively joining a composite material. These are: Secondary bonding, co-bonding and co-curing. Secondary bonding uses a layer of adhesive applied to 2 parts that have already been cured, the traditional interpretation of adhesive bonding. Co-bonding is a joining method used where one composite part has previously been fully cured whilst the second part is uncured. The parts are joined together with an adhesive and the entire assembly is subjected to a full cure cycle to ensure cure of both the laminate and adhesive. Co-cured joints are manufactured using 2 individual composite parts that are in their uncured state. The 2 components are fixed together and then cured together, in this process an adhesive may or may not be used [43,65].

The focus of this research is on secondary bonded applications using a 2 part epoxy adhesive. An adhesive is required to join composite-composite materials as well as dissimilar materials involving metallic adherends where co-bonding or co-curing the parts would not be viable. A customised cure cycle was developed to consider the minimum thermal exposure a vehicle would be exposed to during manufacture. A vehicle tub was instrumented with thermocouples and the lowest temperatures recorded across the body as it passed through the paint ovens. This was used to determine the proposed cure cycle. The final cure profile is provided in Appendix B.

2.3.4 Environmental Effects

When designing an adhesive joint for use in automotive applications, they will be exposed to a number of environmental conditions over their service life. As such, an understanding of the effects of these climatic changes on the joint performance is necessary. The environmental concerns that are raised with adhesives relate to both temperature and humidity, this is due to the sensitivity of adhesives to their operating

environment. Whilst hot and humid environments are the most challenging conditions to ensure joint stability and longevity, at low temperatures adhesives can be equally problematic. Adhesives often become brittle at low temperatures whilst at elevated temperatures the modulus can drop and the adhesive begins to creep. In the presence of moisture the effects can be amplified [18,22]. The main concerns with regards to the adhesive bonding of composite joints are summarised below.

- Temperature

Exposure of adhesives to elevated temperatures can have a serious effect on the performance of adhesively bonded joints as the adhesive joints are reliant on the glass transition temperatures of the adhesive. If the joint is exposed to temperatures below the adhesives' glass transition temperature the effects are generally reversible and no lasting damage will occur; however, above this temperature the effect can lead to irreparable damage of the adhesive[25] .

Zhang[66] studied the effect of elevated temperature testing on the performance of double lap-shear joints using a glass fibre reinforced substrate bonded using a 2-part epoxy adhesive. The results demonstrated that at low to ambient temperatures (-35°C to 40°C) the overall shear strength of the joints were not significantly affected by the changes in temperature. When the joints were tested at temperatures above the glass transition the reduction in joint performance was similar to the decreases observed when the bulk adhesive was subject to dynamic mechanical thermal analysis (DMTA). Along with the decrease in performance, the variability of the results was also observed to increase along with changes in the failure modes of the joints. At the lower temperatures the failures were recorded as interlaminar failures within the composite substrate, at room temperature (approx 25°C) fibre pullout near the composite surface was observed whilst above the glass transition temperature, all of the failures occurred as adhesive failures.

To address the problems encountered when bonding structures to be used through a wide temperature range Da Silva [67] proposed a dual adhesive solution building on previous work proposed by Hart-Smith [68]. By placing a stiff high temperature adhesive in the middle of the adhesive joint and a low temperature adhesive with a low modulus at the joint edges where the areas of high stress concentrations are

located, the performance of the adhesive is enhanced when exposed to extreme fluctuations in temperature. Overall, the joint was shown to perform better than the high temperature adhesive alone at low temperatures and better than the low temperature adhesive at high temperatures; however, the results showed that the joint does not perform better than a single low temperature adhesive at low temperatures or a high temperature adhesive alone at high temperatures [67].

- **Humidity**

The effect of moisture on an adhesive joint can either be reversible or irreversible depending on the temperature at which the adhesive is subject to the humid environment. The irreversible damage to adhesives exposed to elevated temperature and humidity can result in degradation of the adhesive performance, swelling of the adhesive and possibly plasticization [25].

When bonding composite materials the substrate can also absorb moisture which can lead to degradation in the composite as well as the adhesive. Although aspects pertaining to bonding of metallic adherends, such as the corrosion of substrate may not be applicable to composite materials, Pujol argues that in some respects the challenges of optimising bonding to composite materials is similar in ways to bonding to anodised aluminium substrates' owing to their porous nature and ability to absorb moisture prior to bonding. Studies have confirmed the degrading effects on joint performance of composite laminates exposed to pre-bond moisture. This includes laminates that had been stored for extended periods of time. A degas cycle when using anodised aluminium substrates drives off any moisture present within the anodised layer prior to bonding [5]. When using composite adherends the moisture could also be removed through the use of a similar post cure prior to bonding [25].

Ashcroft [69] used composite laminates manufactured using both uni-directional and multi-directional fibre orientations to study the effect of moisture and elevated temperature testing on the performance of adhesively bonded joints. The research demonstrated that if a joint is exposed to high humidity below the glass transition temperature of the adhesive the results were not severely affected by the environmental exposure. Above the glass transition temperature the performance of the adhesive joints were seriously degraded. Guidance indicates that for every 1%

Chapter 2 – Literature Review

of moisture absorbed into the adhesive the glass transition temperature is reduced by approximately 20°C.[69] As such, consideration of the adhesives propensity to absorb moisture must be accounted for when specifying an adhesive to be used in situations where exposure to elevated temperature and humidity will be encountered.

The review of literature indicates that a good understanding of the environment in which the adhesive joints are going to be exposed to is required before selecting a candidate adhesive. The use of a dual-adhesive joint proves a challenge to manufacture and is not necessarily the best option if the adhesively bonded structures are not going to be subjected to large variations in temperature. The temperature has been shown to not only influence the adhesive performance but also plays a role in defining the failure behaviour of adhesively bonded composite structures, changing the failure from adhesive through to substrate failure. The research also highlighted a need to understand the effects of climatic exposure on joint performance for the specific adhesive-substrate configurations to be used. This means a combination of environmental, fatigue and fracture testing should be carried out to validate the use of the chosen adhesive-substrate configuration.

2.3.5 Bondline Defects

Weak bonds are adhesively bonded joints where there is no sign of a weakness although the joint itself is not effectively bonded. The fact there is still contact between the 2 adherends means these defects are hard to identify through NDT techniques. Witness coupons that are manufactured alongside components attempt to provide an indication of joint integrity and are tested prior to approving the quality of a component. This is a technique currently employed at AML to control joint integrity. The cause of weak bonds is usually the result of poor surface preparation such as the inclusion of contaminants, mould release (in composite adherends) or oxide layers (in metallic adherends) [53,70].

Porosity is a defect caused by the entrapment of moisture and volatiles within the adhesive joint during cure. Similarly, voids are caused by the entrapment of air when manufacturing the joint or by the lack of sufficient adhesive in the joint. Although present in most bonded systems, the void content must be controlled as this can have a detrimental effect on the strength of a joint. Pujol[5] identified the presence of pre-

Chapter 2 – Literature Review

bond moisture within the substrate and adhesive as a factor that can lead to void formation and porosity. He concluded that humidity in the environment and exposure time were the determining factors that affected void formation when bonding anodised aluminium substrates[5].

Another source of bondline defects can be attributed to regions of poor cure within the adhesive. For smaller regions this can be due to incorrect mixing of the adhesive. For larger regions of poor cure, incorrect adhesive formulations or a lack of thermal exposure during cure can be the cause. Sometimes these regions can fix themselves as the chemical reactions between the adhesive components continue; however, at low temperature this can be very slow [32]. Adhesive cracks can be caused in cure or in service. In cure the cracks can be explained by thermal shrinkage whereas in service they can be caused by large stresses.

Moura[71] conducted experimental studies as well as stress analysis on adhesively bonded single lap shear joints so as to evaluate the effect of bond defects on the residual strength of an adhesive joint. The experimental results demonstrated a constant joint strength regardless of the defect size; however, joint strength diminished as the defect moved closer to the joint overlap ends. Stress analysis showed that peak stresses within the bondline decreased almost linearly with the defect size. When bonding composite materials the presence of defects within the substrate must also be acknowledged. Pethrick[57] observed that interlaminar shear strengths (dominant when testing single lap shear joints) reduced by 7% for every 1% of void content up to a total void content of 4% within the substrate.

It has been shown that traditional ultrasound and NDT techniques may not be appropriate for application as a monitoring device for discontinuous chopped composites such as the one used in this research. Hot spots identified when using an ultrasonic imaging technique did not effectively identify the failure location of the specimens despite successfully identifying flaws within the material [72]. This demonstrates that not all defects cause premature failure of a substrate or of an adhesive joint. The size of the defects, position in the joint and the loads the joint is placed under all play a role in determining what effect a defect will have on the strength of a joint. The presences of defects are more an indication of improper manufacturing techniques and should lead to a review of the manufacturing process.

2.3.6 Failure Modes

The failure of an adhesive joint may occur in a number of locations and is dependent on a number of different factors that define this. It is important to study the failure modes of an adhesive joint as this allows for the weakest part of the joint to be identified [5].

When investigating the failure modes of adhesive joints with composite adherends, they are notably different to metallic mainly due to the fact that the metallic adherends will only fail in 3 ways; substrate failure, fracture in the oxide layer or through corrosion of the substrate[5]. With a composite material the failures are more complex. The possible failure modes within a composite adhesive joint can be categorised as illustrated in Figure 8 [25,29].

The failure mode can consist of a number of different failure modes occurring simultaneously. They can be affected by the poor cure of either the composite substrates or the adhesive with the presence of bondline defects exacerbating the problem. To simplify the failure modes they are usually defined between cohesive or adhesive failure modes; however, with a composite material, the nature of substrate failures is also of interest. The failure modes used in this investigation are detailed in Appendix C.

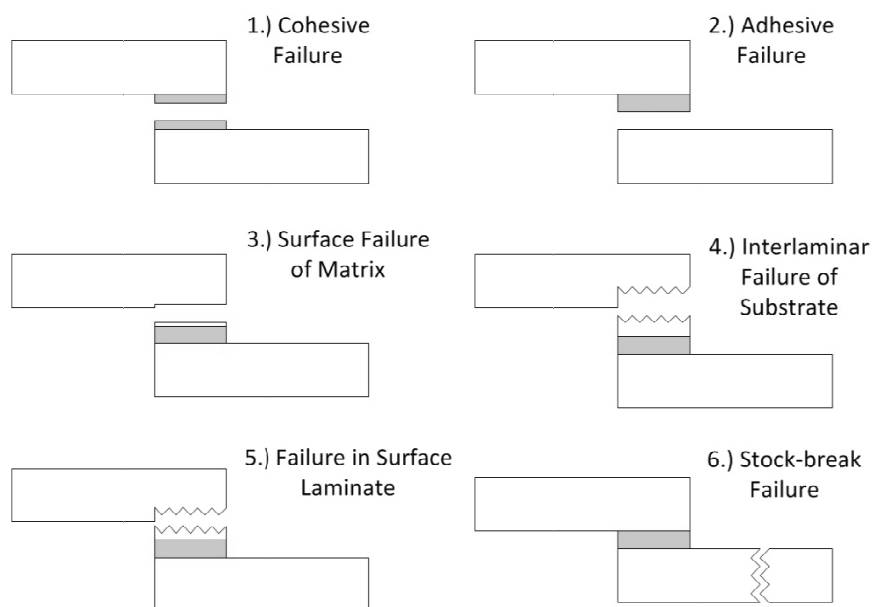


Figure 8 Typical Failure modes in bonded FRP composite joints.

2.4 Composite Adherend Properties

With the focus of the research focused on the optimisation of the fibre architecture of a discontinuous carbon fibre composite to maximise joint performance, a review of the effects the reinforcements can have on the mechanical performance of the adhesive joints and substrate material is presented. A review of the effect of fibre volume fraction, fibre orientation and stacking sequence in conventional laminate joints is provided before focussing on the effect fibre architecture has on the properties of discontinuous fibre composites. Very little work has been undertaken studying the joining of these meso-scale discontinuous composites. As such, the effect of varying the tow size, fibre length and fibre orientation on the mechanical properties of the substrate material is provided.

2.4.1 Volume Fraction

The effect of fibre volume fraction (V_f) on the in-plane properties of traditional composite materials has been studied by a number of researchers [73]. When studying the effect of increasing the fibre volume fraction of a discontinuous carbon fibre composite material Harper[73] found that there was a strong linear relationship between increasing the volume fraction and an increase in the in-plane material properties. Jacob[3] did not observe this relationship, the increase in V_f did not always result in better properties; above a certain limit a decrease in properties was measured. This was most likely the result of problems related to the infusion of the manufactured preforms because the permeability of the preform will decrease with increase V_f . This can lead to dry areas of the preform with insufficient matrix to properly wet-out the fibres. This can decrease the overall interlaminar strength of the composite. What follows are interlaminar cracks forming at lower loads which result in a decrease in the energy absorption of the composite laminates. When considering the effect this will have on the adhesive joint strength, the limit at which the interlaminar strength begins to decrease will be the point at which adhesive bond strength will also start decreasing. To ensure consistency in this investigation, the V_f of the DCFP was maintained constant, at a target volume fraction of 50%.

2.4.2 Laminar Composite Surface Fibre Orientation and Stacking Sequence

The effect the surface fibre orientation and the stacking sequence has on the behaviour of adhesive joints manufactured using conventional laminar composite adherends has been addressed in some detail within literature. However, the majority of the results discussed can be considered to be application specific with the changes in performance as the fibre orientation moves off axis being dependant on the fibre, matrix and adhesive properties.

An experimental study conducted by Mathews and Tester[74] investigated the effect of changes in a composite laminates' stacking sequence on the joint strength on a composite SLS adhesive joint. The work conducted used 3 different laminate thicknesses and 12 different fibre orientations. This allowed both the effect of the laminates' bending stiffness and the effect of fibre orientation to be investigated.

Mathews and Tester[74] observed that, as suggested by Hart-Smith [23], an increase in laminate bending stiffness resulted in an increase in joint strength. This was done by comparing 2 different thickness substrates. The effect of the stacking sequence was then studied by comparing laminates of the same thickness but with different ply orientations. It was observed that by changing the position of the laminate fibre orientations, the joint strength could be influenced. A link was observed between the failure load and maximum shear stress derived from Classical Laminate theory; however, as the high stresses occurring at the corners of the lap joint and the through thickness stresses at the free edges of the adherend were neglected, it was of limited success. This approach was only able to show the highest and lowest performing adherends with those in-between not correlated with the theoretical analysis. The authors concluded that a complex three dimensional stress analysis would have to be conducted to fully explain the failure behaviour. This approach has been investigated and is discussed below.

The problem with having varying orientations in the composite laminate is the stress concentrations that can arise from having differing local stiffness's between the layers that can cause premature failure of adhesive joints manufactured using a composite laminate. Mortensen[75] studied the effect of changing the stacking sequence of the

plies in a laminate numerically. The findings demonstrated that the transverse normal stresses within the adhesive layer increased by up to 58% at the overlap ends when the stacking sequences were changed from 0° to 45°. The shear stresses also increased by up to 39% when the stacking sequences were changed. This highlighted the importance of having a 0° surface layer as this limited the deformation in the top layer of the composite laminate which in turn reduced the stresses imparted into the adhesive layer.

Taib[33] studied the effect of fibre orientation on the joint strength of single lap-joints using two different fibre orientations. Using a [0°, 90°]_s and [+/- 45°]_s composite laminates the failure loads were 29% higher for those laminates using a [0°, 90°]_s stacking sequence. The failure modes also changed with the fibre orientation from a cohesive failure initiating in the spew fillet for the 0° surface fibre orientation to an inter-laminar failure for those specimens with a 45° surface fibre orientation. The elongation to failure was higher for the 45° specimens as the fibre orientation allowed for more deformation of the substrate despite the failure load being lower[33]. Conversely, only a small influence was observed when the stacking sequence was studied by De Goeij [45].

Meneghetti[76] modified the near surface layers of a composite material to change the adhesive/substrate interface. The static and dynamic properties of the joints were then analysed. The authors manufactured 2 different types of substrate, one substrate with a [+45°, 0°, 0°] near surface fibre orientation and the other with a [+45°, +45°, 0°] fibre orientation. The presence of the extra 0° layer changed the failure mechanism of the samples when tested. In the [+45°, 0°, 0°] samples, simultaneous damage occurred in both the bond and within the substrate. For the [+45°, +45°, 0°] samples, the failure occurred entirely within the substrate itself. Although these results provide useful data for the specific testing, it is not possible to draw conclusions about the effect the different orientations have in bonded systems as the substrate failure does not allow for the failure mechanisms within the joint to be investigated. When Kelly[1] investigated the effect of surface fibre orientation on the joint strength of quasi-isotropic composite SLS adhesive joints, decreases in strength of up to 50% were observed when the surface fibre orientation was changed from being parallel to the load path to being perpendicular to it. Kelly proposes that this is the result of there

Chapter 2 – Literature Review

being no fibre reinforcement when the fibres are aligned perpendicular to the load path. As a consequence the strength is governed entirely by the matrix material properties[1].

De Goeij[45] observed that when composite joints were subject to cyclic loading the fatigue life of specimens was larger when the surface fibre orientation was 0° compared to +/- 45° surface laminates which still outperformed those with a 90° configuration. The failure modes were also similar to those observed by Taib [33] with the 0° surface laminates failing at the interface or in the adhesive whilst for the +/-45° orientations the failures occurred either in the surface ply or between the +/-45° layers as inter-laminar failures[45].

When investigating the effect fibre orientation has on the bond strength of a fibre reinforced composite multiple researchers have found that lay-up patterns with larger effective moduli carry greater loads [43-45,76,77]. This will be more pronounced when testing Single Lap Shear joints as the resulting increase in stiffness within the composite should reduce the bending effects of the sample under tensile loading which in turn should lead to a greater load carrying ability. With the exception of the numerical analysis proposed by Mortensen[40] the results of investigations into the effect of surface fibre orientation and stacking sequence are application specific. It is well established that a 0° surface layer will provide the best performing joint; however variations of stacking sequences were not very comprehensive and usually only carried out as a side study in a larger investigation. By using a quasi-isotropic laminate to study the effect of varying the stacking sequence a more thorough understanding of how this affects joint performance may be gained without having to consider the changes to the overall mechanical properties of the substrate.

Boss[78] proposed a method of reducing the peak stresses through modulus grading of the composite material during manufacture. Using braided preforms where the braid angle was varied the local modulus around the bond area was modified. The finding demonstrated that by modifying the substrate modulus in the bond area it was possible to reduce the peak stresses by approximately 20% compared to a substrate with a uniform modulus. The modulus grading was also compared to grading the substrate thickness around the bond area. Those substrates with a graded substrate modulus

demonstrated the lowest peak shear stresses whilst also being a simpler method than grading the joint geometry. Baldan[22] proposed interleaving the different fibre laminates as an alternative way of reducing the stress concentrations located between the layers of composite laminates by distributing the adhesion mechanisms over a number of plies adjacent to the adhesive layer. This has been shown to become more effective as the ply count of the laminate is increased.

2.4.3 Discontinuous Fibre Composites

The aim of using a discontinuous fibre composite is to compete with conventional metallic manufacturing techniques with regards to cost and cycle times whilst retaining mechanical properties that approach those of conventional continuous fibre composite materials. Whilst the factors described previously will affect the performance of adhesive joints manufactured using a discontinuous fibre laminate, there are a number of other factors that may also influence the joint performance. The performance of discontinuous fibre composites is dependent on the homogeneity of the preforms. This is controlled through the fibre orientation, fibre distribution, fibre length and by ensuring a good level of adhesion between the fibres and reinforcing matrix [79]. To date very little work has been carried out studying these effects in bonded joints.

The failure behaviour of the discontinuous composite materials is different from conventional laminar composites. When fibres end, the load carried axially must be transferred to another fibre through shearing within the resin and the fibre/resin interface. As such, with larger bundle sizes the large number of fibre ends finishing simultaneously will mean the load transfer is greater than when using a smaller bundle size. This can cause large stress concentrations and lead to cracking and failure between ply interfaces; however, at the same volume fraction the number of individual segments will be fewer. As such the optimal fibre architecture will be a compromise between having fewer fibre segments and having large numbers of fibre ends simultaneously ending [11].

- Tow Size

Fibre tow size has been observed to heavily influence the strength of discontinuous fibre composites. Whilst there has been no published attempts to characterise its' influence on the bond strength of structural composite joints, reviewing the literature available on the subject, a number of different factors can induce changes in bulk material properties. Those that have the potential to influence the adhesive joint performance of a composite single lap shear joint are discussed in greater detail. Characteristics such as the overall material homogeneity, the tow size aspect ratio and the presence of material discontinuities are all discussed.

As the bond surface is considered to be critical to successful adhesive bonding, the effect of material homogeneity at the composite surface is of importance. Dahl[14] investigated the effect of tow size on the material distribution in 2 separate studies. Using light transition measurements to determine the effect of tow size on the coverage of the material Dahl was able to demonstrate that a reduction in filament count results in improved material distribution of the material. Using a 3k filament count there was complete fibre coverage of the preform. Something not observed for the larger 6k filament count[80]. By having a more even fibre coverage there is the potential for having more uniform mechanical properties; which in turn would reduce the variability in performance of bonded joints.

The effect tow size has on a discontinuous carbon fibre composite was investigated further using a number of experimental rovings. A 36k carbon fibre roving was manufactured by joining together a number of smaller tow sizes (0.5k, 1k, 1.5k, 3k, 6k and 12k) to study the effect of tow size when the additional manufacturing parameters were the same. The resulting findings confirmed that a reduction in the tow size served to increase the homogeneity and as a consequence the mechanical performance of the composite materials [81]. Similar observations have been made using both glass and carbon fibre reinforcements by a number of researchers [13,14,82].

Jacob[3] studied the effect of tow size on the energy absorption of a discontinuous carbon composite laminate using 12k and 48k tow sizes. The work demonstrated that an increase in tow size resulted in decreased energy absorption; however, the effect was decreased with increasing fibre lengths which indicates the presence of an

interaction between the 2 different factors. There was an observed reduction in energy absorption between the 24k and 48k tow sizes at a 25.4mm fibre length; however, this did not occur when the fibre length was increased to 50.8mm.

The linear density of the carbon tows will invariably change with the tow size and as a result the number of fibre bundles present within a composite preform changes depending on the tow size. This will lead to a change in the number of fibre ends and other phenomena that may affect the load transfer at the adhesive/substrate interface in an adhesive joint. Analysis of the substrate surfaces after failure will indicate the location of the failure, either within the adhesive or the substrate. Owing to the non linear stress distribution throughout the overlap, the location of localised substrate failure should provide an indication of where future work in joint strength optimisation in DCFP can take place.

- Fibre Length

Typically, discontinuous composites can be divided into 2 classes. In short fibre composites, the fibre length is typically considered to be less than 5mm; whilst long fibre composite fibres can range from 10mm to 150mm in length. Short fibre reinforcements are generally found in injection moulding compounds and some bulk mouldings compounds (BMC) and are usually single filament dispersions within the matrix. Long discontinuous fibres are more commonly found in sheet moulding compounds (SMC), chopped strand fabrics and in the case of this research, DCFP [83]. The reinforcements are typically deposited in fibre bundles with the fibres used in DCFP being drawn directly from a roving through a chopper gun as previously described. The effect of fibre length on the mechanical properties of discontinuous fibre composites appears to be relatively well understood; however, there does not appear to be literature describing how the bond strength is affected by this important variable in the manufacture of discontinuous fibre composite joints. Similar to the tow size effects, the changes in fibre length affects the homogeneity of the substrate through the thickness of the laminate.

Pan[84] considered the effect of fibre length on scale effect and critical length are discussed. If studying individual fibres then the increase in fibre length should lead to a reduction in the mechanical properties owing to the higher occurrence of critical

Chapter 2 – Literature Review

flaws. Described as Weibull effects, Pan proposes that as the fibre length is increased the mechanical properties should decrease owing to the higher probability of critical flaws existing in the individual filaments. Pan observes that both the sizing and bundling of multiple filaments into tows will make the effects less pronounced. Harper[73], observed a significant improvement in the mechanical performance of DCFP preforms with decreasing fibre length owing to a reduction in the number of critical flaws and a more even fibre coverage. This result was achieved through the use of a filamentisation device to break up the fibre bundles; thus improving the coverage further, this was easier achieved when using a shorter fibre length.

Hitchen[85] tested the effect of fibre length on a randomly oriented discontinuous composite using 3 short fibre length (1mm, 5mm and 15mm). The strength of the composite increased with fibre length with the stress-strain curves for 5mm and 15mm fibre lengths increasing linearly. For the 1mm there was non-linear behaviour observed. The fibre deposition in this study were not robotically sprayed rather deposited using a glycerine solution deposited onto a steel mesh and then dried with multiple sheets stacked to obtain the desired VF (approx 20%). For the manufacture of structural components it is anticipated these fibre lengths are too short to achieve the desired mechanical properties. When Boylan[31] studied the effect of fibre length on the properties of Sheet Moulding Compounds at a Vf of approximately 20% the strength of the materials were observed to increase as the fibre length increases in the range of 12.7mm to 50.8mm. The surface quality of the composite was also influenced by fibre length with the surface roughness increasing with fibre length[31].

By increasing the fibre length and consequently the mass of the individual fibres the trajectory of the fibre flight from the chopper gun to the preforming surface changes. Harper carried out a study on the areal density variations within DCFP plaque manufacture using 3 different fibre lengths. The variability in areal mass was observed to increase with fibre length. The largest variation occurred when increasing the fibre length from 25mm to 50mm, the increase then appears to level off with only a nominal increase in variability observed when increasing the fibre length from 50mm to 75mm [73].

Feraboli[52] observed that the chip length of a chopped discontinuous carbon fibre prepreg composite affected the overall strength of the composite with an increase in

the average tensile and flexural strength with increasing fibre length in the range of 12.7mm to 76.2mm observed. Feraboli did note that there was a compromise between increasing the mechanical properties and achieving the optimum manufacturing settings as increasing the fibre length can lead to fibre kinking, resin rich or starved areas and void formation[52].

Similar to the discussion with variations in fibre tow size, the changes in the fibre length of the composite results in the number of material discontinuities present within the adhesive joint changing. It is anticipated that the fibre length change will impact upon the overall SLS joint strength with the shorter fibre lengths showing a larger drop-off in load carrying ability; however there may be a number of interactions between the fibre length, tow size and principal fibre orientations present. The use of longer fibre bundles should provide a more constant load transfer mechanism when compared to the use of shorter fibre lengths when the testing is carried out with fibres aligned to the fibre direction. Of interest is the change in the joint strength with changing fibre length when the fibres are aligned off-axis. The shorter fibre length may result in a better load carrying ability owing to the presence of the discontinuities across the bond providing reinforcing mechanisms.

• Fibre Orientation

When manufacturing composites using a discontinuous fibre architecture, the historical Vf limit when using a random fibre arrangement has been between 35 % and 40 %. If an alignment process is utilised it is possible to increase this to between 55 % and 60 % as the fibres are packed better with fewer fibre crossover points. The alignment process has also demonstrated the potential to allow up to a 90 % stiffness and 50 % strength retention compared to unidirectional continuous fibre composites. To achieve this, a combination of good fibre alignment, fibre distribution and fibre lengths are required as well as the ability to successfully infuse the preforms with the matrix without severe fibre distortions. Owing to the sensitivity of the process to different variables, dry fibre placement methods will be reviewed; however, there exists other means of orienting fibres such as through liquid dispersion and electrical techniques [11].

Chapter 2 – Literature Review

During the development of the P4 process described in Section 1.3, Owens-Corning developed a directed fibre preforming process to process glass rovings. The design used a similar layout to the conventional P4 machine with an additional orientation fixture attached to the chopper unit. The process used a perforated tool with a vacuum applied to hold the fibres in position; however, no compaction of the preforms occurred. The process achieved fibre orientations with 90% of the fibres aligned within 5° of the principle axis but no mechanical performance figures were published [86].

Throughout the development of P4 to accommodate processing of carbon tows, the design of the orientation devices were changed with 3 different types of orientation devices used. The strength retention ranged from 36% to 50% and the mechanical stiffness from 74% to 94% depending on the device and fibre length used at a normalised volume fraction of 55%. Only the 3k carbon tows were used as these provided the best performing preforms in a separate study [79]. Rondeau had demonstrated that a 3k tow size was the most desirable having tested 3k, 6k and 12k filament counts. The fibre length was also varied ranging from 51mm to 127mm. The results showed an increase in mechanical performance with increasing fibre length with a potential plateau being reached between 102mm and 127mm [11].

As previously mentioned, it is possible to align fibres in discontinuous composite materials through a number of different means; however, in this investigation it has been achieved using a simple alignment head mounted to the chopper gun. This was a development from a nozzle design described in [73,83]. This previous design employed an air-curtain to ensure the tows exited the alignment fixture. The problem was that this induces high levels of fibre filamentisation with deposition rates limited to 150g/min. The importance of fibre alignment and its relationship with the fibre length and tow size means that this will inevitably affect the joint performance of adhesively bonded discontinuous fibre composites. The author is not aware of previous investigations into this relationship.

2.5 Conclusions

Having reviewed the literature relating to adhesive bonding for composite materials, there is a lack of available resources pertaining to adhesive joining of discontinuous carbon composite materials. With the development of these materials for use in structural applications an understanding of their bonded behaviour is necessary.

The single-lap shear configuration was used in the investigation as there is an established understanding of the expected behaviour of these joints both with regards to metallic and composite substrates. As such, there exist both experimental methods that are used to determine the optimum fibre settings as well as the scope to develop numerical models to predict joint performance in the future. The complex shear and peel modes of the specimens means that if the material substrate can be engineered to surpass the SLS requirements, it should perform well in additional testing with little additional development work. The screening removed adhesive spew as this ensured that the peak stresses at the overlap ends were maximised. The adhesive fillets' shape and dimensions are hard to control in a manufacturing environment and the peak stresses are reduced with the inclusion of a fillet meaning additional gains can be made if good control of spew can be achieved. The simple configuration means the substrates do not require special manufacturing techniques and if successful, the assembly methods can be easily adopted for coupon testing in a production environment.

Prior to investigating the different fibre architectures as described below, a set of candidate adhesives were tested in Chapter 3. Owing to the cure requirements of the current single part adhesive in use at Aston Martin Lagonda, a new candidate adhesive had to be identified from a set of low temperature curing 2-part epoxy adhesives. Using the findings from the literature review, a set of preliminary investigations were performed to establish a common joint preparation technique that could be used in the subsequent work. This allowed for a number of important variables to be controlled throughout the investigations.

The work then progressed onto using a non-crimp fabric to determine how an adhesively bonded conventional laminar composite material behaved when the surface fibre orientations and stacking sequences were varied. A quasi-isotropic stacking

Chapter 2 – Literature Review

sequence was used to retain a constant substrate bending stiffness. The importance of a sound laydown strategy was shown with the influence of the fibre orientation below the surface also being demonstrated. The findings from this chapter were used as a reference for a more detailed investigation using a highly oriented DCFP substrate as described in Chapter 6

Different aspects of the discontinuous fibre reinforced composite substrate were studied with an initial parametric study, detailed in Chapter 5. The investigation focussed on randomly oriented DCFP, studying both the effects of bond dimensions as well as the fibre architecture. A set of optimised bond dimensions and fibre architectures were identified for use in future adhesive trials.

The fibre orientation of the discontinuous fibre laminates was then investigated as a means of further optimising joint performance in Chapter 6 with another set of recommended fibre architectures being produced using this work.

The results of these experimental investigations were then compiled in a final discussion in Chapter 7 to understand how bonding to a DCFP laminate differs from using a conventional composite adherend.

Chapter 3. Preliminary Adhesive Studies

3.1 Introduction

The objective of this chapter was to provide an overview of the rationale behind studying the fibre architecture of composite substrates as a means of improving adhesive joint performance. The initial screening of a set of adhesives to determine bulk properties was followed by validation of the surface preparation and post-curing methods before the effect of surface fibre orientation and stacking sequence were briefly examined. The failure modes of the adhesive joints produced in these initial studies resulted in the focus shifting from enhancing bulk adhesive properties to examining methods that can be used to improve the joint performance of both conventional laminar composite materials as well as DCFP by varying the fibre architecture of the substrates.

3.2 Bulk Adhesive Tensile Testing

The aim of studying the mechanical properties of the bulk adhesive was to determine which of the candidates was most suited to being used as a replacement two-part epoxy adhesive for the current one-part adhesive in use at AML. The adhesive used at present is not compatible with bonding composite materials as a result of its 190°C cure cycle. The bulk tensile testing of the five candidate adhesives aimed to compare the performance of the adhesives when subjected to two different adhesive cure cycles. The two cure cycles studied were; ambient cure and the AMLC cure cycle. The AMLC cure cycle would be the minimum elevated temperature cure a chassis would be subjected to during assembly meaning any candidate adhesive would have to be able to at least retain its mechanical integrity following this cure regime.

The tensile strength, elongation to failure and tensile modulus were investigated to identify how each of these properties was affected by the different cure cycles. Not

only did this provide valuable data for comparing the adhesives with no substrate effects but this also allowed for initial judgements to be made with regards to the potential performance of the adhesives.

A mould was produced using PTFE, owing to its self releasing nature, containing 18 cavities that allowed for the manufacture of a set of bulk adhesive tensile specimens. Figure 9 shows the specimen dimensions used whilst Figure 10 shows the final specimen mould. The testing standard EN ISO 527-3:1995 was used to select the dimensions of the specimens (Specimen 1B).

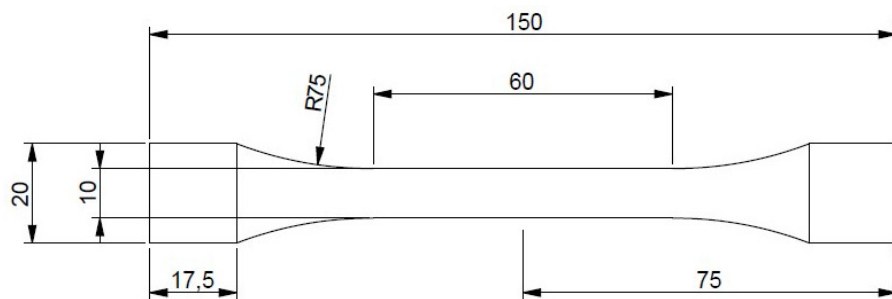


Figure 9 Standard bulk adhesive test specimen from EN ISO 527-3:1995

The adhesives chosen for this study were: BM 2096, BM 2098, DP 460, DP 490 and Loctite 9461. The first cure cycle used was a 7 day ambient temperature cure, this provided data to describe the adhesive performance following no elevated temperature cure. The second was the AMLC adhesive cure cycle described in Appendix B. Following injection and cure, the sprue and any flash was removed prior to testing.

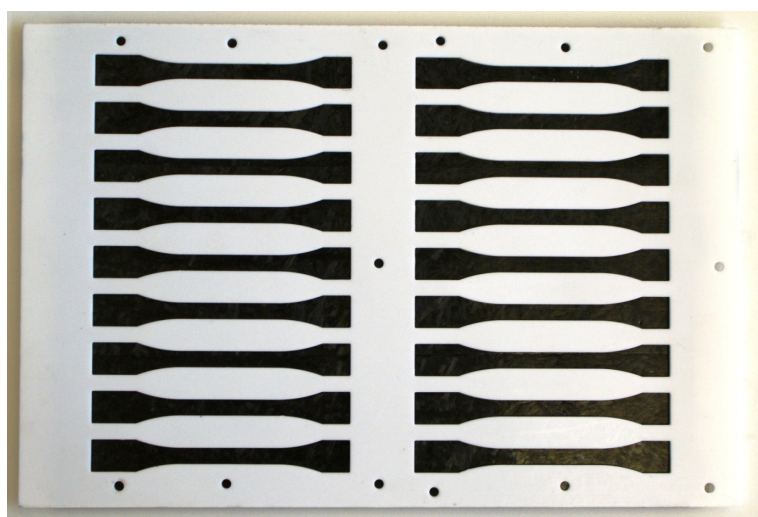


Figure 10 Specimen mould for bulk adhesive tensile specimens

An Instron mechanical testing machine was used for the tensile testing of the bulk adhesive specimens. Prior to the test, each sample's dimensions were measured at 3 different locations. The specimen was loaded into the jaws and a 50 mm extensometer attached to the neck of the specimen. A fixed displacement of 2mm/min was used to test the adhesive specimen to failure with the load being collected using a 50kN load cell. A minimum of five replicates were tested with any specimens containing flaws such as entrapped air being discarded and another sample tested.

3.2.1 Results

The results of the tensile strength of the candidate adhesives are presented in Figure 11. With the exception to the BM 2096 adhesive, the tensile strength of the other adhesives were relatively similar when exposed to the ambient temperature cure; however, the inclusion of an elevated temperature cure using the AMLC cure cycle changed the performance of the adhesives considerably. The biggest changes occurred in the BM 2096, BM 2098 and DP 460 adhesives with 25%, 22% and 26% increases in the tensile strength being observed with the inclusion of the higher temperature cure. The Loctite 9461 adhesive only had a small 8% gain in strength following the additional cure cycle whilst for the DP490 adhesive there was a 7% reduction in strength when an elevated temperature cure was used.

The change in the standard deviation of the specimens following the AMLC cure cycle was studied to identify which adhesives are enhanced by the AMLC cure cycle. The BM 2098 adhesive was the adhesive with the largest reduction in variability as a result of the AMLC cure cycle with a 77% reduction in the standard deviation compared to those samples manufactured using an ambient cure. Similarly, there were considerable reductions in the standard deviation of the specimens manufactured using the DP 460 and Loctite 9461 adhesives, being a 64% and 65% reduction respectively. Finally, the BM 2096 adhesives standard deviation was reduced by 29% with the AMLC cure cycle whilst, for the DP 490 adhesive, the standard deviation increased by 142% as a result of the use of the AMLC cure cycle.

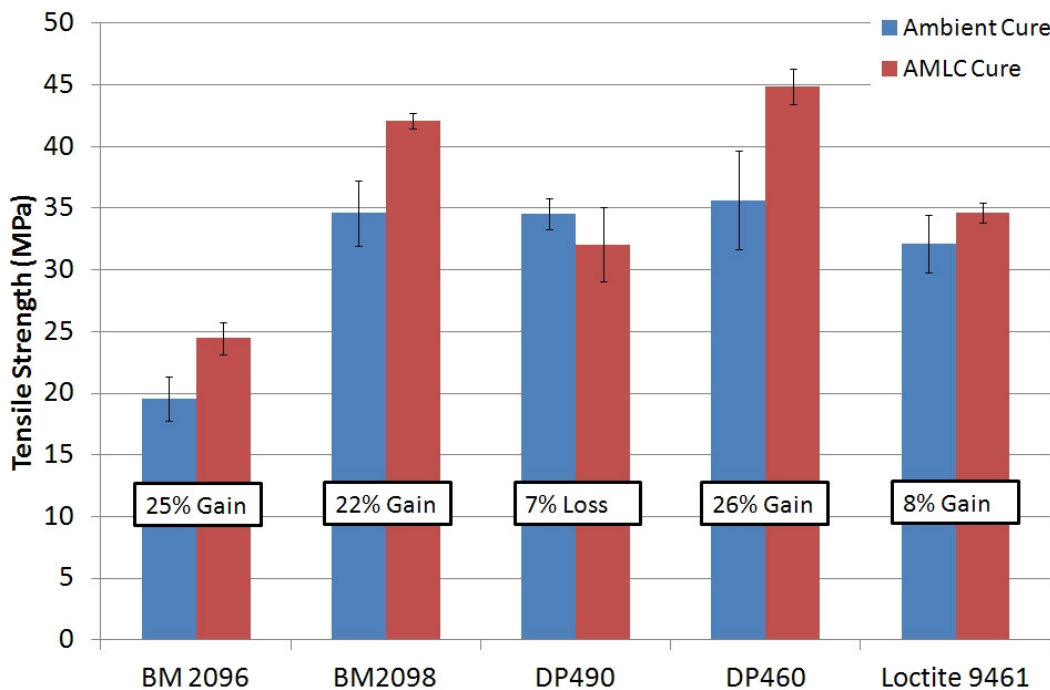


Figure 11 Comparison of Tensile Strength for Bulk Adhesive tensile specimens

The analysis of the elongation to failure of the different candidate adhesives is presented in Figure 12. The largest changes between the ambient temperature and AMLC cure cycles occurred with the DP 460 and BM 2098 adhesives, there were 81% and 71% increases in performance for the adhesives respectively. Meanwhile, the Loctite 9461 and BM2096 adhesives had 33% and 11% increases in the elongation to failure. Whilst for the DP 490 adhesive a drop in elongation to failure was observed when the AMLC samples were tested against the ambient cure temperature specimens.

The changes in the standard deviation of the elongation to failure as a consequence of the AMLC cure cycle were mixed. The only 2 adhesives to have a reduction in the standard deviation of the samples were the BM 2098 and Loctite 9461 adhesives. For these specimens the standard deviation of the samples was reduced by 55% and 90% respectively. The other 3 adhesives observed increases in the standard deviation of the elongation to failure as a result of using the AMLC cure cycle. This ranged from a 9% increase for the BM 2096 specimens to a 79% increase for the DP 490 adhesive specimens.

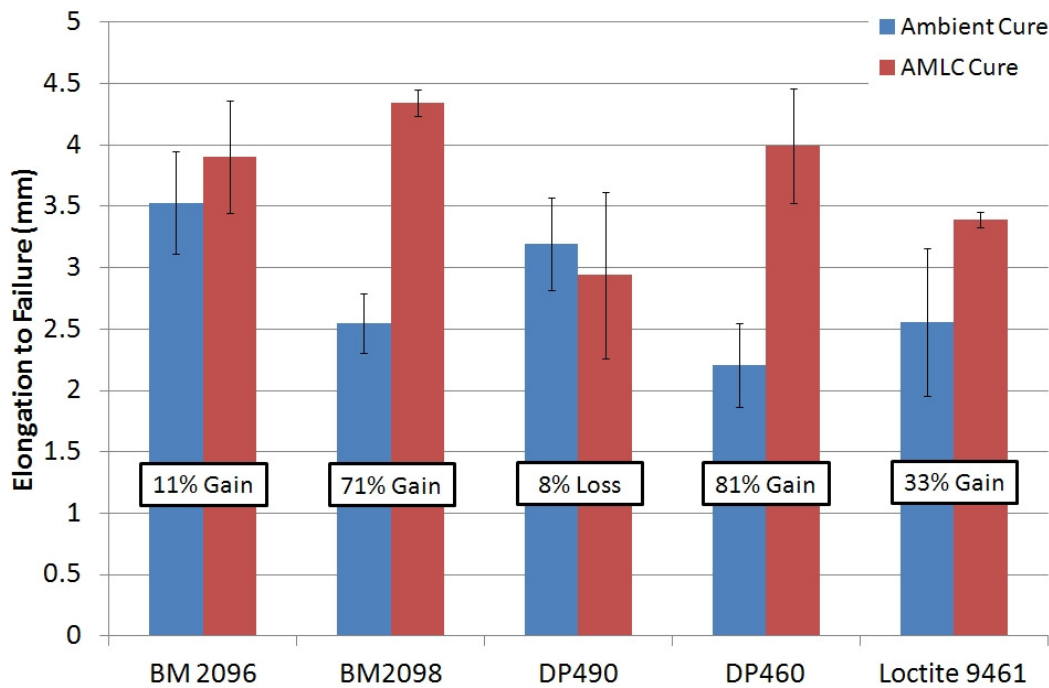


Figure 12 Comparison of Elongation to Failure of Bulk Adhesive tensile specimens

The tensile modulus of the bulk adhesive specimens was the least affected by the change in cure cycle. The comparison of the tensile modulus for the candidate adhesives is presented in Figure 13. Whilst the BM 2096 adhesive had a 16% increase in the tensile modulus, regardless of the increase this was still the lowest performing adhesive with respect to the tensile modulus. The only other adhesive to observe an increase in tensile modulus was the Loctite 9461 adhesive, which only increased by 1%. The BM 2098 and DP 490 adhesives had 4% decreases in the tensile modulus whilst for the DP 460 adhesive the tensile modulus was reduced by 10%.

Despite the trend for reductions in the tensile modulus with the use of the AMLC cure cycle, when the variability of the results was studied, there were generally large improvements in the standard deviation of the tensile specimens. The only adhesive to demonstrate an increase in the standard deviation of the samples when the AMLC cure cycle was used was the Loctite 9461 adhesive. For this adhesive the standard deviation of the samples increased by 66% compared to the samples manufactured at ambient temperature. The largest reduction in standard deviation of tensile modulus occurred with the BM 2098 adhesive which had an 87% reduction in standard deviation when the AMLC cure cycle was used. For the BM 2096 and DP 460 adhesives the reduction was measured at 59% and 52% respectively; whilst, for the DP 490 adhesive the standard deviation was reduced by 21%.

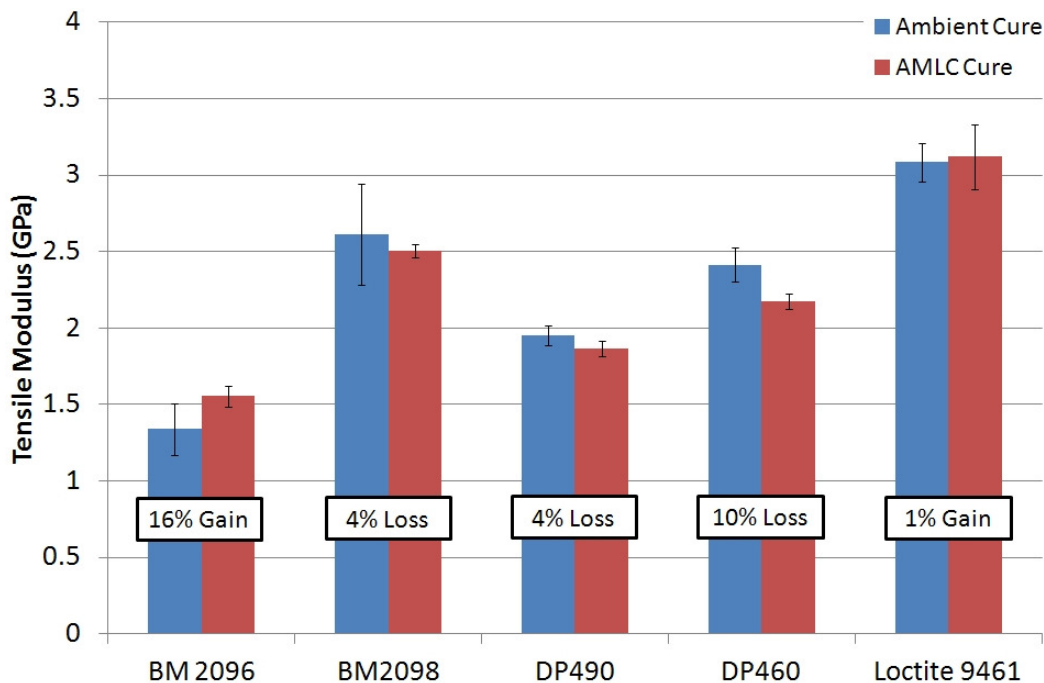


Figure 13 Comparison of Tensile Modulus of Bulk Adhesive tensile specimens

3.2.2 Discussion

Throughout the bulk tensile testing the two candidate adhesives that performed best were the DP 460 and BM 2098 adhesives, making these the two preferable adhesives following the bulk tensile testing.

Another adhesive that showed promise was the Loctite 9461 adhesive; however, in separate investigations carried out to study the effectiveness of bonding dissimilar materials, in this case an anodised aluminium substrate and DCFP, problems arose and as such the adhesive was removed from the subsequent studies. The DP 490 candidate adhesive is commonly used within industry to bond composite materials at low temperatures; however, the results showed that the variability in performance increased when exposed to the AMLC cure cycle. As such, despite its wide-spread availability and common usage, the DP 490 adhesive was removed from the adhesive candidate list. The BM 2096 adhesive was removed from the candidate adhesive list for a number of reasons. Primarily, the required tensile strength and modulus stipulated by AML at the beginning of the research project was not achieved. However, of more concern were issues pertaining to crystallisation of the adhesive that occurred during storage.

3.3 Surface Preparation

The screening of the surface preparation method aimed to validate a method a simple surface preparation method that was both quick and easy to implement and which could be used regardless of the substrate materials used. Three different adhesives were used in the study as a means of assessing the sensitivity of different adhesives to changing surface preparation methods.

Two DCFP plaques were manufactured using the substrate properties described in Table 1. Two different surface preparations were then tested on the substrates. The first was a simple cleaning operation where ScotchBrite abrasive pad soaked in acetone was used and then the adherend surface wiped clean using a lint free cloth. The second procedure was more thorough. Following the extraction of the substrate, the specimens were cleaned in water to remove the majority of the contaminants that arose from the cutting process. The bond area was abraded using 500 grit abrasive papers followed by a ScotchBrite 7496 pad soaked in acetone. This ensured any remaining mould release, cutting fluid and loose debris were removed from the bond area. Finally, the specimens were wiped with a clean cloth soaked in acetone before the specimens were allowed to dry prior to bonding. The adhesives used in the study were: DP 460, DP 490 and DP 620.

Table 1 Substrate Properties for initial DCFP manufacture

Parameter	Specification
Tow Size	6k
Fibre Length	60 mm
Thickness	3 mm
Volume Fraction (Vf)	50%

For each surface preparation method five replicate SLS adhesive joints were manufactured. The bond dimensions used were 25mm x 10mm x 0.2mm and the AMLC cure cycle used to cure the adhesive joints. After a 7 day period the specimens were subject to mechanical testing using a 2mm/min test speed. Following the testing the failure mode of each of the specimens was recorded to compare the failure characteristics of the different surface preparation methods.

3.3.1 Results

The results from the surface preparation study are displayed in Table 2. When studying the effect of surface preparation on the shear strength of DCFP SLS adhesive joints, it is immediately apparent that there is a significant improvement in the load carrying capability of SLS adhesive joints when the surface of the DCFP substrate is thoroughly abraded in comparison to those which are simply cleansed. This was observed regardless of the adhesive formulation as can be seen in Figure 14. Unlike the shear strength results, not all of the adhesives demonstrated the same trends when studying the effect of surface preparation on the elongation to failure of the DCFP SLS adhesive joints. The results are presented in Figure 15.

Table 2 Summary of SLS tensile testing results comparing surface preparation methods

	Shear Strength (MPa)	StDev (MPa)	Elongation to Failure (mm)	StDev (mm)
DP 490	19.40	0.99	1.97	0.72
DP 490 A	21.84	2.86	1.58	0.27
DP 460	17.30	7.18	1.15	0.47
DP 460 A	21.36	2.56	1.43	0.33
DP 620	15.16	2.59	1.07	0.18
DP 620 A	17.58	2.45	1.53	0.57

The analysis of failure modes also provided a good insight into the effect of surface pre-treatment on the eventual failure mode of the DCFP SLS adhesive joints studied. The distribution of failure modes for the non-abraded specimens is presented in Table 3.

Table 3 Distribution of Failure Modes of Abraded and Non-abraded SLS tensile specimens

	DP 490	DP 490 Abraded	DP 460	DP 460 Abraded	DP 620	DP 620 Abraded
Adhesive	50%	-	75%	-	75%	-
Cohesive	-	25%	-	-	-	50%
Substrate	25%	75%	25%	100%	25%	50%
Mixed	25%	-	-	-	-	-

The shear strength of the SLS adhesive joints manufactured with DP 490 adhesive was improved by over 13% when the substrate surface was properly abraded instead of simply being cleansed. It must be noted however that the standard deviation of the

tests almost trebled when the abrasive surface preparation method was used. There was also a 20% decrease in the elongation to failure of the specimens with a 60% reduction in the standard deviation of the specimens when the abrasive surface preparation technique was used. The differences in performance can be attributed to the failure modes being either cohesive or substrate failures when the abrasive technique was used indicating the specimens became more reliant on the structural integrity of the substrate rather than on the adhesive type or surface preparation method. With the abraded specimens, 75% of the specimens failed within the substrate indicating the full strength of the adhesive was not being attained.

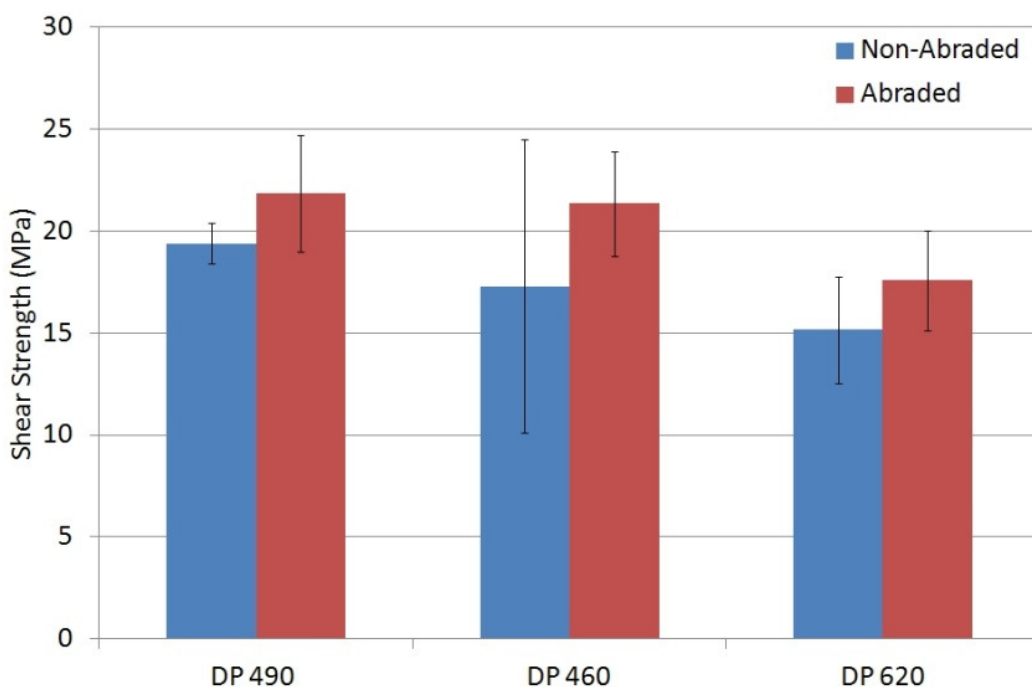


Figure 14 Comparison of SLS Shear Strength for different surface preparation techniques using 3 different adhesives

When the DP 460 adhesive was used to bond the DCFP SLS adhesive joints, the surface preparation technique changed the distribution of failure modes considerably. For the non-abraded specimens some 75% of the joints exhibited an adhesive failure mode, with the remaining 25% being failures within the DCFP substrate. When the specimens were abraded, there were no observed adhesive failures with all of the failures manifesting themselves as substrate failures. As a result, the SLS adhesive joints' shear strength was improved by 24% when the surface of the DCFP substrate was abraded. Additionally, there was a 65% reduction in the standard deviation of the samples when the abrasive method was used compared to the cleaning of the substrate.

There was also a 24% increase in the elongation to failure of the specimens with a 30% decrease in the standard deviation of the specimens.

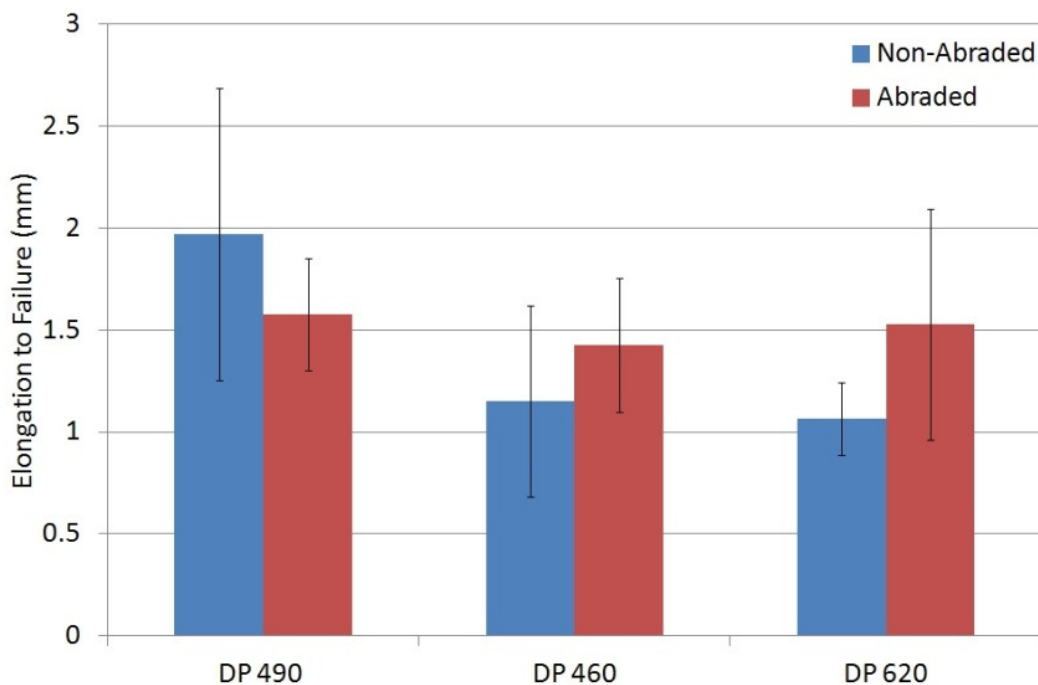


Figure 15 Comparison of Elongation to Failure of SLS joints prepared using different surface preparation techniques for 3 different adhesives.

Using the DP 620 adhesive for manufacturing the DCFP SLS adhesive joints, a big change in failure behaviour was observed between the non-abraded and abraded surface preparation techniques. When the non-abraded surfaces were tested 75% of the joints manifested adhesive bond failure with the remaining 25% being substrate failures. When the bond area was thoroughly abraded there were no recorded adhesive failure; instead, 50% of the failures were cohesive failures and the remaining half being failures within the substrate. The shear strength of the joints also improved by 16% when the substrate was abraded, with very little change observed in the standard deviation of the samples. The elongation to failure increased by approximately 44% with the abrading of the substrate; however, the standard deviation did also double when mechanical abrasion was used as a means of surface preparation.

3.3.2 Discussion

The aim of the surface preparation investigation was to validate a simple method to ensure consistent results with regards to the surface preparation methodology. The

mechanical performance and failure modes of adhesively bonded SLS joints were analysed with two differing surface preparation methods and three different adhesives.

The mechanical testing results highlighted the fact that a simple mechanical abrasion surface preparation was sufficient to ensure an increase in the shear strength of the adhesive joints ranging from 13% to 24%. The effect on the elongation to failure was less clear with the DP 490 adhesive having a 20% reduction in the elongation to failure whilst the DP 460 and DP 620 adhesives had considerable increases in the elongation to failure.

The lack of any adhesive failures following the mechanical abrasion of the substrate surface prior to bonding indicates this method is sufficiently robust to ensure a good bond between the adhesive and the substrate. The high incidence of substrate failures during testing indicated good adhesive compatibility and surface preparation. These failures show that the adhesive strengths are higher than that of the substrate material in the SLS joint configuration. This highlighted that rather than the surface preparation being an issue that needed to be addressed, the substrate properties and the manner in which failure modes could be controlled was of more interest.

3.4 Post-Cure Study

The purpose of studying the effect of the substrate post-cure was to validate a regime that was being used in the manufacture of the DCFP substrate and to identify any problems that may arise when bonding the material as a result of it. The post-cure study tested two different aspects of the material properties. The first studied the bulk substrate material properties to gain an understanding of the effect of the post-cure on the substrate whilst the second was a study of the adhesively bonded SLS joint properties using three different adhesives. To determine whether the effect of a substrate post-cure was common regardless of the choice of adhesive three different adhesives were used. These were: DP 460, DP 490 and BM 2098.

In the study, four DCFP Preforms were manufactured following the process described in Section 1.4 using the fibre properties detailed in Table 1; however, only two of them were subjected to the 4 hour post-cure at 75°C.

Bulk Tensile specimens measuring 220mm x 25mm were extracted from the DCFP plaques with five specimens tested from both the post-cured and non-post-cured substrates. A total of 5 SLS adhesive joints were also manufactured for each of the adhesives. The bond dimensions used were 25mm x 10mm x 0.2mm with the AMLC adhesive cure cycle used to cure the adhesive (Appendix B).

The specimens were subjected to tensile testing using a 2mm/min displacement. A more detailed description of the test method is contained in Section 4.2.5. Following testing, the failure mode of each specimen was recorded to study the influence of post-curing the substrate on the eventual failure mode of the SLS adhesive joints.

3.4.1 Results

The results from the bulk substrate testing are presented in Table 4. Using a post-cure following the moulding of the DCFP substrate served to enhance the bulk material properties of the material. When considering the tensile strength of the DCFP substrate there was a 6% increase in the tensile strength when the post-cure was used with a 60% reduction in the standard deviation between the specimens. The elongation to failure of the DCFP substrate was also increased by 8% when a post-cure was used with a 30% reduction in the standard deviation of the specimens. Finally, there was a 3% increase in tensile modulus with an 18% reduction in variability as a consequence of the post-cure cycle. This testing confirmed that when using a DCFP substrate a post-cure is beneficial as it improves the overall material properties of the material.

Table 4 Tensile Properties of Bulk DCFP substrate

	Tensile Strength (Mpa)	St Dev (MPa)	Elongation to Failure (mm)	StDev (mm)	Tensile Modulus (GPa)	St Dev (GPa)
DCFP	132	53	2.40	0.5	37	4
DCFP PC	140	21	2.59	0.4	38	3

When studying the failure modes of the SLS adhesive joints, it is important to note that there were no adhesive failures indicating good compatibility of the substrate and adhesive. The distributions of the adhesive failures are presented in Table 5. The role of the post-cure with respect to the failure modes of the SLS joints is not entirely clear,

Chapter 3 – Preliminary Adhesive Studies

mostly owing to the bulk of the failures for both sets of tests being located within the substrate.

Table 5 Distribution of failure modes of non-post-cured and post-cured DCFP SLS adhesive joints

	BM 2098	BM 2098 Post- Cure	DP 460	DP 460 Post- Cure	DP 490	DP 490 Post- Cure
Adhesive	-	-	-	-	-	-
Cohesive	-	-	-	-	80%	60%
Substrate	40%	100%	100%	60%	20%	-
Mixed	60%	-	-	40%	-	40%

The effect of a substrate post-cure on the performance of adhesively bonded DCFP joints is less clear than for the bulk material properties. The shear strength and elongation to failure of the SLS adhesive joints were compared as well as the resulting variability between specimens. The results of the testing are presented in Table 6. The comparison of the shear strength and elongation to failure for the non-post-cured and post-cured specimens are presented in Figure 16 and Figure 17 respectively.

Table 6 Tensile properties of post-cured and non-post-cured DCFP SLS adhesive specimens

	Shear Strength (MPa)	StDev (MPa)	Elongation to Failure (mm)	StDev (mm)
BM 2098	25.15	2.6	1.69	0.2
BM 2098 PC	23.87	4.1	1.51	0.3
DP 460	31.25	4.8	2.73	0.4
DP 460 PC	23.71	5.0	1.96	0.4
DP 490	24.77	3.5	2.00	0.3
DP 490 PC	25.03	3.8	1.98	0.3

When the BM 2098 adhesive was used there was a 5% decrease in the mean shear strength of the adhesive joints. There was also a significant increase in the variability of the samples with the standard deviation increasing by nearly 60%. The use of a substrate post-cure also resulted in an 11% reduction in elongation to failure and a 36% increase in the standard deviation of the specimens. The post-cure would appear to have made the substrate more brittle thereby changing the failure mode from a combination of substrate and mixed failures to being entirely substrate related.

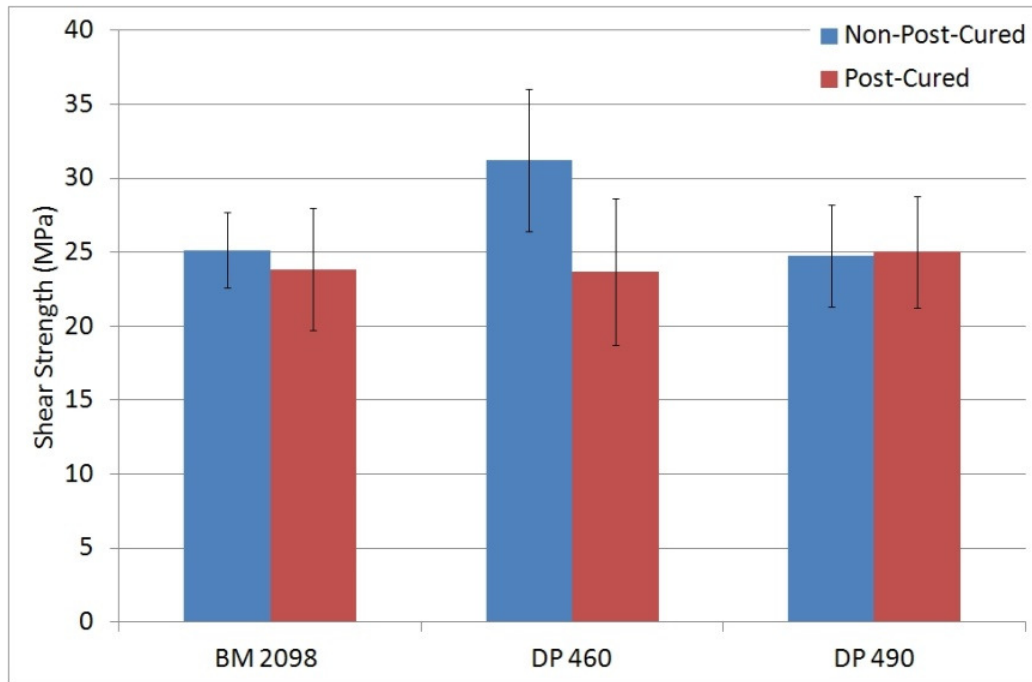


Figure 16 Shear Strength comparisons of post-cured and non-post-cured DCFP SLS adhesive joints

The most sensitive adhesive to the substrate post-cure was the DP 460 adhesive. A 24% reduction in the SLS joints' shear strength was observed when a post-cure was applied to the substrate but with an almost negligible change in the standard deviation between the 2 sets of specimens. There was also a 28% reduction in the elongation to failure of the specimens with the standard deviation of the post-cured specimens increasing by 43%.

The DP 490 adhesive was the least sensitive adhesive to the substrate post-cure. There was a 1% increase in shear strength when the post-cure was applied with a similar increase in the standard deviation of the specimens. The elongation to failure of the SLS adhesive joints manufactured using the DP 490 adhesive were again the least sensitive to the post-curing of the substrate. There was a 1% increase in the elongation to failure of the specimens and a 17% reduction in the standard deviation of the samples.

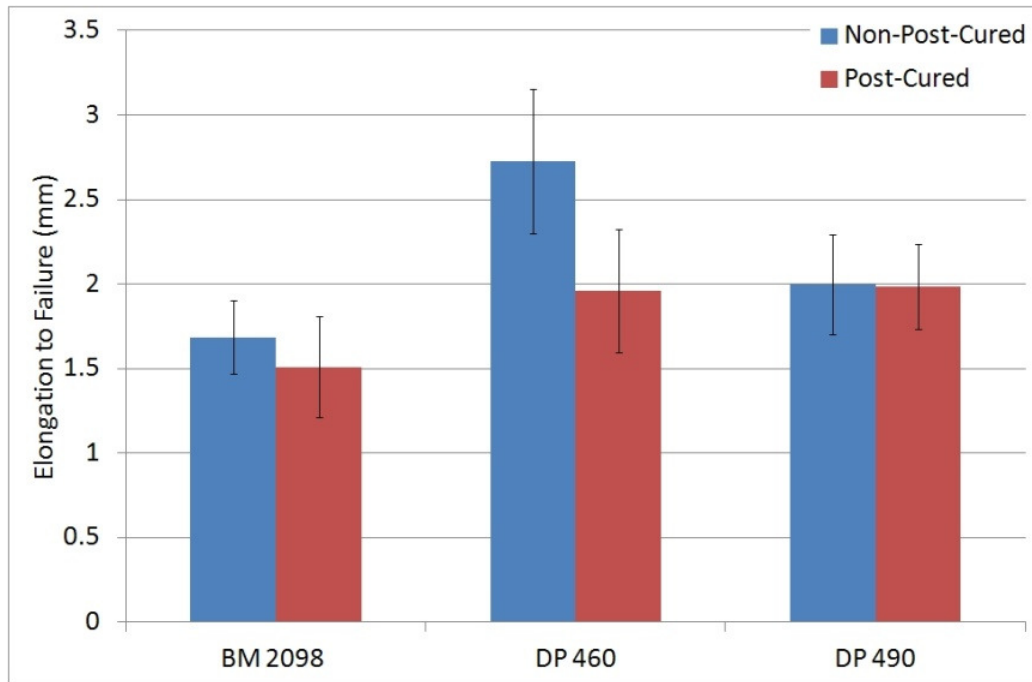


Figure 17 Comparison of Elongation to Failure of post-cured and non-post-cured DCFP SLS adhesive joints

3.4.2 Discussion

The post-curing of the DCFP substrate was a requirement that arose from issues surrounding the mechanical performance of the substrate when subjected to mechanical testing. As this process was deemed necessary for the manufacture of structural DCFP components a small study was carried out to better understand how the post-curing of the substrate affected the joint performance of SLS adhesive joints manufactured using a DCFP substrate. Three different adhesives were studied to ascertain whether the effects were specific to the adhesives.

The effect of post-curing on the bulk strength of the DCFP substrate was confirmed through a series of mechanical tests. When the substrate was post-cured there was an increase in material properties that was coupled with a reduction in the variability of the results. This highlighted the importance of a post-cure to achieve the best mechanical performance and stability from the DCFP substrate.

The effect of a post-cure on the failure modes of the different specimens was not easily identifiable. The fact that the substrate and mixed failure modes were so dominant throughout the testing served to highlight that the weak link in the joint studies was the substrate performance and not that of the adhesives being tested. The

bulk mechanical testing of the adhesives has shown the adhesive performance should be sufficient to achieve the desired joint strengths; however, without an improvement in the substrate properties the full strength of the adhesive will not be achieved. The stochastic nature of the DCFP means it would be expected to be harder to control compared to other adhesive joints manufactured using a metallic or laminar composite substrate. As a result the content of this thesis sought to improve the performance of bonded composite materials through the effective use of the reinforcing fibres of the substrate rather than chemical processes that arise between the composite matrix and the epoxy adhesive.

3.5 Fibre Orientation Study

An investigation into the effect of fibre orientation and stacking sequence had the aim of identifying how these components influence the load bearing capability of SLS adhesive joints manufactured using a uni-directional carbon fibre prepreg substrate. In this study a single adhesive, DP 490, was used to manufacture the adhesive joints. The three different plaques all had different stacking sequences which are described in Table 7. By comparing the performance difference between Plaques 1 and 2 the effect of surface fibre orientation can be identified whilst the comparison between Plaques 2 and 3 tests the influence of the stacking sequence changes in the substrate.

For the substrate manufacture, an MTM49-3 unidirectional pre-preg manufactured by ACG was used. The laminates were layed up between 2 metal plates and cured using a vacuum bagging technique, as illustrated in Figure 18. The plaques were cured under vacuum for 1 hour at 120°C before being removed from the vacuum bag and being placed in an oven to post-cure for a further 2 hours at 120°C.

Table 7 Fibre Stacking Sequence for UD prepreg substrate manufacture

Plaque ID/ Stacking Sequence	1	2	3	4	5	6
1	+45°	-45°	+45°	-45°	0°	90°
2	0°	90°	0°	90°	+45°	-45°
3	0°	90°	+45°	-45°	0°	90°

Following the manufacture of the laminates, specimens measuring 100mm x 25mm were extracted for use as substrate in the manufacture of the SLS joints. The joints

were assembled using a bond area of 25mm x 10mm x 0.2mm on the underside of the laminate and the specimens were cured using the AMLC cure cycle described in Appendix B.

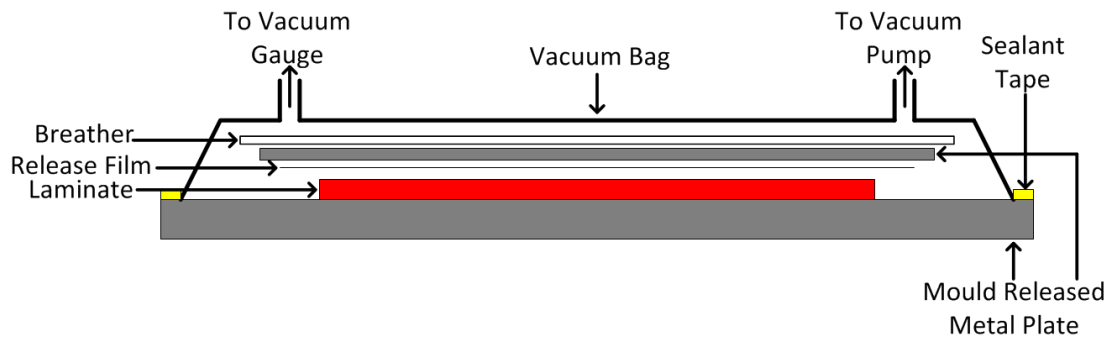


Figure 18 Schematic of Vacuum Bagging for UD prepreg substrate manufacture

The specimens were tested at a 2mm/min extension rate with the failure modes of each of the specimens being recorded for comparison between the three different laminates. The methodology for the SLS testing is described in more detail in Section 4.2.5.

3.5.1 Results

The distribution of the different failure modes are presented in Table 8. For Plaque 1 the joints all demonstrated failure within the substrate as being the dominant failure mode. The fibres were removed from the adhesive joint along the 45° fibre direction. For Plaque 2 the failures were distributed between cohesive failures (60%) and a mixed failure mode (40%) where part of the SLS joint failed cohesively and part failed within the substrate. Plaque 3 had the most varied set of adhesive failure modes. A total of 40% of the joints manifested cohesive failure behaviour. A further 40% were failures located entirely within the composite substrate whilst the final 20% were mixed failures combining aspects of the cohesive and substrate failure modes.

Table 8 Distribution of failure modes of 3 different UD prepreg SLS adhesive joints

	Plaque 1	Plaque 2	Plaque 3
Adhesive	-	-	-
Cohesive	-	60%	40%
Substrate	100%	-	40%
Mixed	-	40%	20%

The results from the testing are presented in Table 9. The highest performing substrate with regards to shear strength was Plaque 2, which also the plaque with the least variability between the samples. There was a 30% overall reduction in shear strength when the surface fibre orientation of the specimens was changed between plaques 1 and 2. There was also a 23% reduction in the shear strength of the SLS adhesive joints when the stacking sequence near the surface of the substrate was changed from [0°, 90°, 0°, 90°] to [0°, 90°, +45°, -45°] (Plaques 2 and 3). This highlighted that both the surface fibre orientations and subsequent stacking sequence exert a large influence on the final adhesive joint performance.

Table 9 Tensile properties of UD prepreg SLS adhesive joints

	Shear Strength (MPa)	StDev (MPa)	Elongation to Failure (mm)	StDev (mm)
Plaque 1	20.64	2.6	1.20	0.3
Plaque 2	26.92	1.5	1.56	0.3
Plaque 3	20.83	4.0	1.40	0.5

Studying the elongation to failure, the highest performing plaque was again Plaque 2, with the [0°, 90°, 0°, 90°] surface layers, also the plaque with the lowest inter-specimen variability. The lowest performing plaque was Plaque 1, with the [+45°, -45°, +45°, -45°] near surface fibre orientations. Plaque 3 performed slightly better but the variability was also considerably higher than that of Plaques 1 and 2. When comparing Plaques 1 and 2, to study the effect of surface fibre orientation, there was a 30% difference between the plaques indicating a significant influence on the elongation to failure. There was also a 10% difference between Plaques 2 and 3 as a result of the changes in the stacking sequence.

3.5.2 Discussion

A small study was carried out to validate the concept of using reinforcing fibres as a means of changing both the joint performance and failure modes of these joints. Three different laminates were manufactured and SLS joints prepared and subjected to mechanical testing. This allowed for orientation effects and the effect of stacking sequence to be validated with a limited number of laminates.

When the failure modes of the 3 plaques were studied, differences were observed between them as a consequence of the changes in fibre orientation and stacking sequence. Whilst Plaque 1, with a +45° surface fibre orientation, only had substrate failures, for Plaques 2 and 3, with 0° surface layers, a combination of failure modes was observed. This demonstrated the ability to alter the failure modes by modification of the fibre orientation.

When Plaque 1 and Plaque 2 were compared to check the effect of fibre orientations there was more than a 30% reduction in shear strength as a result of the change in fibre orientation of the surface fibre orientations from 0° to 45°. Similarly, there was a 30% reduction in the elongation to failure of the specimens. This would be the result of the delamination of the 45° surface layers as the substrate strength becomes more dependent on the matrix properties as a result of the off axis fibre orientation.

When Plaque 2 and Plaque 3 were compared to study the effect of stacking sequence on the joint performance of SLS adhesive joints a 30% reduction in shear strength was also observed. There was a 10% reduction in elongation to failure as a result of the change in stacking sequence of the composite substrate. This result along with the reduction in the cohesive failures would indicate the fibre orientation below the surface layers is also important in defining joint strength and failure behaviour as they facilitate the efficient load transfer both between substrate layers and across the joint.

The results highlighted the important role fibre orientation can play in defining both the joint strength and elongation to failure as well as controlling the failure modes of the SLS adhesive joints. As a consequence, this coupled with the results from the post-cure study led to the thesis presented being focussed on the fibre orientation of composite substrates and the role it plays in defining joint behaviour.

3.6 Conclusions

The work contained within this chapter aimed to place the work carried out in a greater context of the project and to explain the reasoning behind why the focus of this thesis is around the role fibre orientation, stacking sequence and fibre properties have on defining the joint performance of adhesively bonded SLS joints.

Chapter 3 – Preliminary Adhesive Studies

Prior to continuing research into the substrate fibre properties it was necessary to select a single two-part epoxy adhesive with which to carry out further investigations. Alongside colleagues at AML and the University of Nottingham, it was decided that owing to its consistent performance as well as the technical help provided by the adhesive supplier, the BM 2098 adhesive would be used throughout the remainder of the research investigations.

The use of a simple surface preparation technique to improve the performance and consistency of composite SLS joints was validated. Using a simple mechanical abrasion prior to bonding resulted in no recorded adhesive failures. This was the first time the problem of extensive substrate failure was observed within this experimental investigation.

The post-cure study identified that application of a post-cure to the DCFP substrate had a detrimental effect on the joint strength and elongation to failure of the adhesive joints as a result of the failure modes tending toward a substrate failure with the variability of the results also increasing. However, as this is a requirement to produce the best performing composite substrates, the post-cure cycle was maintained throughout the experimental investigations. There is the potential for future investigations into the possibility of enhancing joint strength through co-curing or post-curing the substrate with the adhesive joints already manufactured.

The study of three different composite plaques with differing fibre orientation and stacking sequences highlighted the importance of gaining a better understanding of the role the fibre reinforcements play in defining the joint behaviour and performance of SLS adhesive joints. This was the first of the studies involving changes to the fibre arrangement within the composite material to be carried out in this research investigation. More detailed studies of the effects of changing fibre properties on SLS adhesive joint performance are addressed in the subsequent chapters.

Chapter 4. Effect of Fibre Orientation on Bonded SLS Joints using a Conventional Laminar Composite Substrate

4.1 Introduction

The aim of the experimental investigation was to determine the effect of surface fibre orientation and stacking sequence on the joint behaviour of SLS adhesive joints manufactured using a fibre reinforced composite substrate. Prior to investigating the role of fibre orientation on the joint behaviour of oriented DCFP adhesive joints, a study was designed to gain a greater understanding of the behaviour of adhesively bonded SLS joints manufactured using a non-crimp fabric fibre reinforced composite substrate.

By using a conventional fabric instead of a discontinuous fibre composite substrate a number of factors identified as being influential on the joint strength of adhesively bonded DCFP substrates could be controlled. The presence of material discontinuities, uneven fibre areal density distribution, different discontinuous fibre properties and factors related to the automated manufacture of DCFP preforms were removed from the study to allow for the effect of fibre orientation and stacking sequence to be better isolated.

With regards to the substrate properties, the thickness of the substrate, matrix and fibre properties were all maintained constant. The study varied both surface fibre orientation and the stacking sequence of a quasi-isotropic composite substrate as a means of assessing the extent the fibre orientation can alter a SLS joints behaviour. The use of a quasi-isotropic laminate meant that the strength increases predicted by Hart-Smith[23] and observed by Mathews and Tester[74] as a result in changes to the bending stiffness would be limited.

4.2 Methodology

A quasi-isotropic stacking sequence was chosen for the investigation as this allowed for the overall substrate strength and stiffness to remain relatively unchanged as the stacking sequence of the composite was varied. These properties only change between the laminate layers. A total of 8 different preforms were designed to test the behaviour of the SLS adhesive joints as the stacking sequences changed. In order to increase the number of different stacking sequences investigated, each of the preforms were tested at both the 0° and 90° orientations. A set of 5 replicates of the SLS joints were prepared for the 16 different configurations.

Table 10 Stacking sequence for manufacture of NCF Substrate

Preform #/ Layers	1	2	3	4	5	6	7	8
1	0°	0°	45°	90°	-45°	-45°	90°	45°
	90°	90°	-45°	0°	45°	45°	0°	-45°
2	0°	45°	90°	0°	-45°	-45°	0°	90°
	90°	-45°	0°	90°	45°	45°	90°	0°
3	0°	0°	90°	45°	-45°	-45°	45°	90°
	90°	90°	0°	-45°	45°	45°	-45°	0°
4	0°	45°	-45°	0°	90°	90°	0°	-45°
	90°	-45°	45°	90°	0°	0°	90°	45°
5	0°	90°	0°	45°	-45°	-45°	45°	0°
	90°	0°	90°	-45°	45°	45°	-45°	90°
6	0°	90°	45°	0°	-45°	-45°	0°	45°
	90°	0°	-45°	90°	45°	45°	90°	0°
7	0°	0°	45°	-45°	90°	90°	-45°	45°
	90°	90°	-45°	45°	0°	0°	45°	-45°
8	0°	45°	0°	-45°	90°	90°	-45°	0°
	90°	-45°	90°	45°	0°	0°	45°	90°

4.2.1 Manufacture of NCF Preforms

The manufacture of the NCF plaques can be divided into two distinct manufacturing operations. These are the assembly of the fabric preforms and the injection of the preform to produce the finished plaques.

The different stacking sequences for the manufactured NCF preforms are described in Table 10. The layers were cut at the desired fibre orientations with approximate dimensions of 300mm x 400mm. They were then assembled with the thermoplastic

binder being evenly distributed between each of the layers to facilitate handling of the preforms at 5% by fibre weight in total.

Once the desired stacking sequence was assembled two preforms were consolidated simultaneously by placing the preforms side by side between two sheets of release film in a press preheated to 120°C. The press was then closed with a 10 ton clamping force being applied for 5 minutes to melt the thermoplastic binder. This equated to a consolidation pressure of approximately 4 Bar. The preform was then removed and allowed to cool to room temperature.

$$\text{Pressure} = \frac{\text{Mass (kg)}}{\text{Area (m}^2\text{)}} = \frac{10000}{2 \times 0.12} = 41667 \text{ kg/m}^2 = 4.08 \text{ Bar} \quad \text{Equation 1}$$

A stamping tool measuring 300mm x 400mm was then used to remove any excess material from the preform edges before being placed into the RTM mould tool ready for injection.

4.2.2 Resin Transfer Moulding

The Resin Transfer Moulding (RTM) of the laminates was maintained constant throughout the research investigations to ensure continuity with regards to the matrix properties. The injection procedure was carried out using a stainless steel mould assembled using a 3mm thick picture frame. A CiJect One™ resin injection machine manufactured by Composite Integration was used to inject the preforms.

Release agent was applied to the tool parts and was allowed to thoroughly dry. The preform was then placed in the tool and loaded into a heated press with a 50ton clamping force. The press and tool were pre-heated to 50°C prior to injection. The resin was preheated to 80°C to maintain a low viscosity whilst an initial injection pressure of 0.5bar ensured the preforms were fully wet out. A vacuum pump attached to the exhaust port via a catch pot helped with infusion of the resin through the preforms. When the resin ran clear in the exhaust port the injection was stopped and the temperature of the press ramped to 120°C for 1 hour. The tool was then cooled and the manufactured plaque removed. A post-cure of 75°C was carried out for 4 hours to ensure the plaques were fully cured prior to bonding.

4.2.3 Cutting of Substrate

The specimens were extracted from the moulded preforms using a Diamant Boart diamond cut-off saw. The dimensions of the Lap-shear specimens were 100mm x 25mm x 3mm. The specimens were extracted at 0° and 90° to the principal fibre direction to double the number of unique fibre orientations. The dimensional tolerances were +/- 0.5mm for the specimen width and +/- 1mm for the specimen length. If a specimen fell outside of these dimensions it was deemed flawed and another specimen extracted.

4.2.4 Assembly of Single Lap Shear Joints

Following the extraction of the substrate, the specimens were cleaned in water to remove the majority of the contaminants that arose from the cutting process. The bond area was abraded using 500 grit abrasive papers followed by a ScotchBrite 7496 pad soaked in acetone. This ensured any remaining mould release, cutting fluid and loose debris were removed from the bond area. Finally the specimens were wiped with a clean cloth soaked in acetone before the specimens were allowed to dry prior to bonding.

The specimens (Figure 19) were mounted into the bonding jig (Figure 20) and a bead of adhesive was dispensed onto the substrate. The adhesive was spread across the bond area and two 0.2mm wire spacers were placed within the bond. The joint was then closed and the bond overlap dimensions checked. Once the 10mm overlap length was achieved any excess adhesive was removed using a sterile blade. This ensured a constant spew geometry as the adhesive joints had no fillet radii. The bonded joint was secured with bull clips and allowed to cure at room temperature for a 24 hour period before being cured using the AMLC cure cycle described in Appendix B. After a 7 day period at room temperature the specimens were subject to tensile testing.

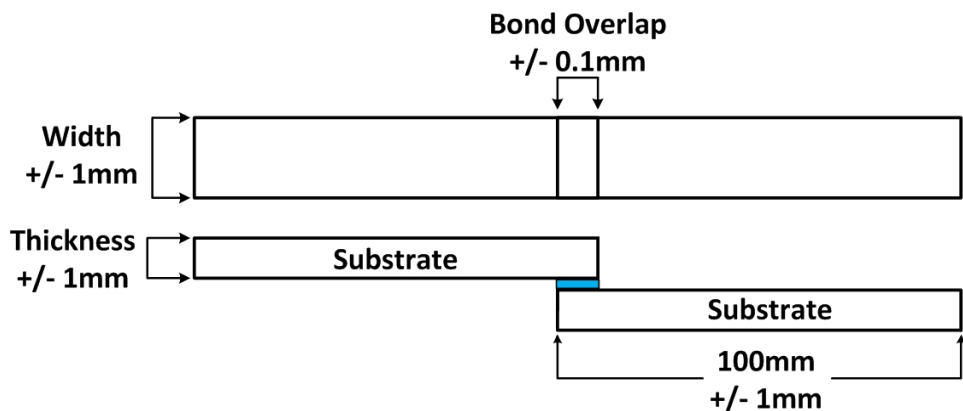


Figure 19 SLS Joint Configuration

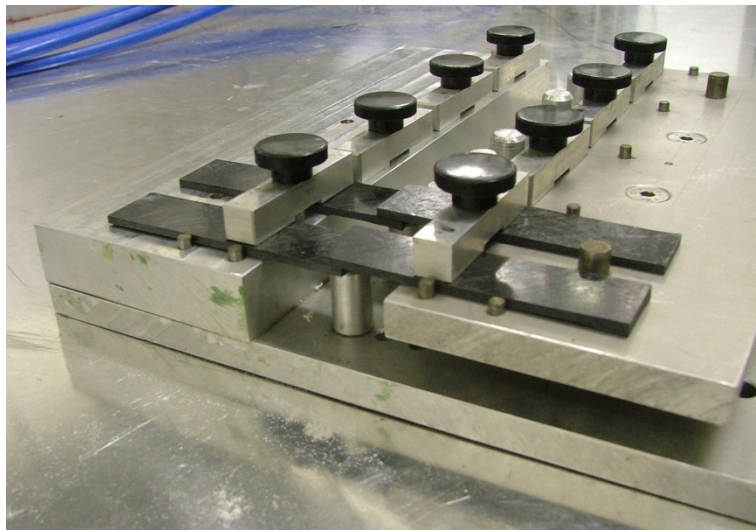


Figure 20 SLS adhesive joint bonding rig

4.2.5 Mechanical Testing

The tensile testing was carried out using an Instron mechanical testing machine. The test speed was set to 2mm/min, as a means of ensuring the capture of good images intended for use with Digital Image Correlation (DIC). The load was measured using a 50kN load cell whilst the extension was measured from the cross-head displacement. Although the cross-head displacement is not the most accurate form of measuring strain and displacement, owing to the SLS joint configuration it was not possible to use a conventional extensometer effectively.

In order to minimize the peel forces present in SLS tests, spacers were used in the jaw faces. This ensured that the load path passed centrally through the adhesive bondline.

A 96mm gauge length was set to maintain a constant distance between the two jaw faces. A schematic of the tensile test setup is included in Figure 21 .

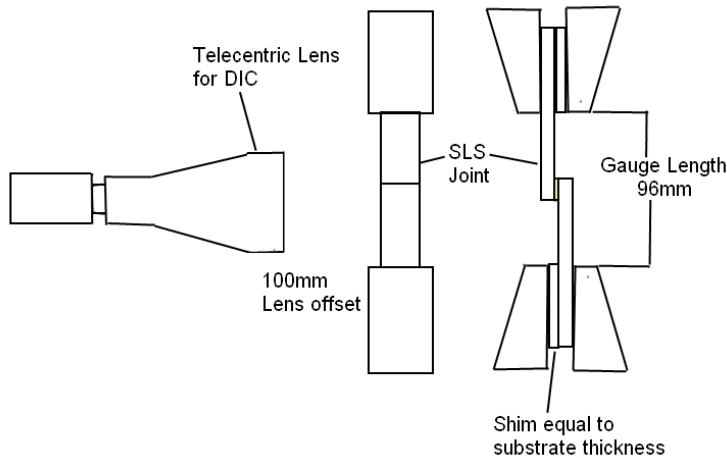


Figure 21 Schematic of SLS mechanical testing setup

4.3 Test Results for NCF SLS adhesive Joints

4.3.1 Analysis of Failure Modes

The surface fibre orientation was studied to determine the influence this has on the overall failure mode of the adhesive joint. The joints were studied with the failures being recorded as a percentage of the failures at each fibre orientation. Images of common failure modes observed during testing are presented in Figure 22. When studying the substrate it was noted that the majority of substrate failures occurred between the first and second layers of the NCF substrate. It is important to observe that there were no adhesive failures recorded throughout the testing indicating a good compatibility between the adhesive and composite substrate.

The analysis of the failure modes separated by the surface fibre orientation is presented in Table 11 and provides an insight into how influential the fibre orientation is on the failure behaviour of the NCF SLS adhesive joints.

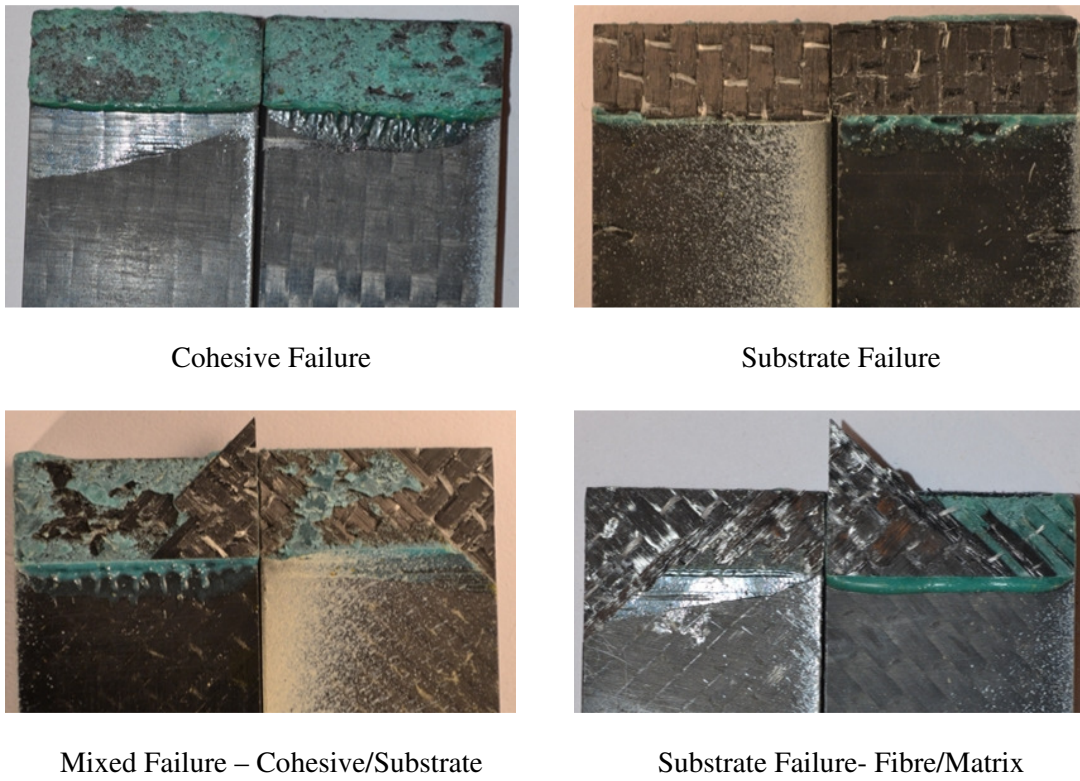


Figure 22 Example of Common Specimen Failure Modes for NCF SLS Joints

At the 0° fibre orientation, 64% of the failures observed were cohesive failures. This was followed by 24% of the specimens exhibiting failure within the substrate and the remaining 12% being a mix of both substrate failure and cohesive failure. With regards to the substrate failures, these failures were mostly the matrix being removed at the surface leaving the tows intact on the substrate indicating a poor adhesion at the fibre/matrix interface. Some part bundles were also removed hinting that the substrate may not have been thoroughly wet-out through the resin transfer moulding process.

When the fibres were aligned at 45° to the load path the failure modes were dominated by substrate failure. A total of 77% of the specimens failed in this manner. The remaining failures were 13% displaying mixed failure and the final 10% being cohesive. The substrate failures observed for the 45° surface fibre orientation mostly consisted of the surface layer being removed with the failure initiating at the joint overlap ends. Sometimes this failure manifested itself as a mixed failure with only the corner of the joint having the 45° layer removed and the remaining bond failing in a cohesive manner.

For the specimens oriented perpendicular to the load path all of the failures occurred within the substrate. The majority of the specimens had entire fibre bundles removed with either the first or both the first and second layers of the NCF material being removed from the remaining substrate.

Table 11 Distribution of failure modes (%) for the first layer fibre orientation of NCF SLS adhesive joints

	0°	45°	90°
Adhesive	-	-	-
Cohesive	64%	10%	-
Substrate	24%	77%	100%
Mixed	12%	13%	-

4.3.2 NCF SLS Tensile Testing Results

When studying the effect of stacking sequence on the joint shear strength a number of trends are apparent that can be used in future adhesive bond studies to improve the performance of composite-composite adhesive bonds.

The top performing plaque from the tensile testing was plaque NCF 5 90° with a stacking sequence of [0°, 90°, -45°, 45°]. The apparent shear strength of the preform was 31.73 MPa. In contrast, the worst performing preform was NCF 7 90°. This had a stacking sequence of [90°, -45°, 45°, 0°] with a mean shear strength of 14.77 MPa. The extent of the difference in performance is represented graphically in Figure 23 detailing the Stress-Elongation plots of 2 of the tested samples. There was more than a 50% reduction in shear strength and elongation to failure indicating that the stacking sequence and surface fibre orientation of the composite substrate had a significant influence on the shear strength of the SLS adhesive joints subject to tensile testing.

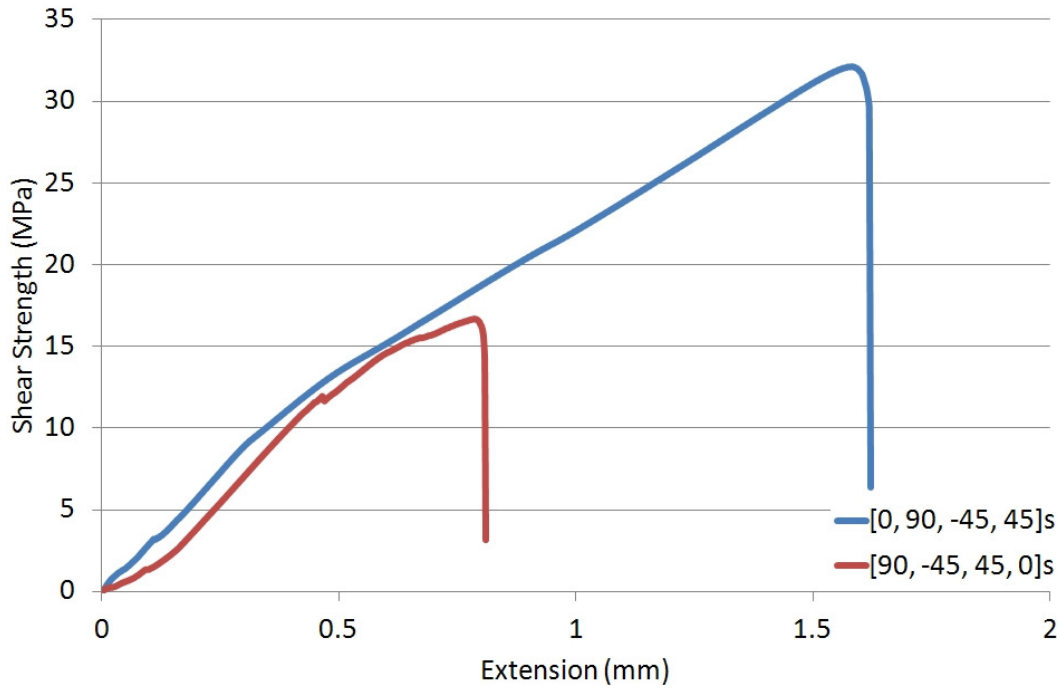


Figure 23 Comparison of Stress-Elongation of Best (NCF 5 90°) and Worst (NCF 7 90°) Performing SLS joints

From studying the rankings of the shear strength of the 16 different stacking sequences, some general trends became apparent. The mean shear strengths of the different NCF SLS adhesive joints are presented in Figure 24. The top 3 performing preforms, NCF 5 90°, NCF 1 0° and NCF 3 0°, all had a 0° surface fibre orientation (with a 90°, 45° and 90° second layer respectively.) The fourth highest performing preform was NCF 2 90° which had a stacking sequence of [-45°, 0°, 90°, 45°]_s. This was followed by preforms NCF 6 90° and NCF 7 0°, which had a 0° surface layer with a 45° second layer. The preforms that followed had predominantly 45° and -45° surface layers with those 2 preforms which had a 90° surface orientation having a 0° second layer.

The worst performing preforms with regards to the shear strength of the SLS joints tested were NCF 6 0°, NCF 1 90° and NCF 7 90°. All 3 plaques had 90° surface layers with a 45° or -45° second layer. The data indicates that the surface layer played an important role in defining the shear strength of an SLS joint with the subsequent layers also exerting a degree of influence over the load bearing capacity of the SLS joints studied.

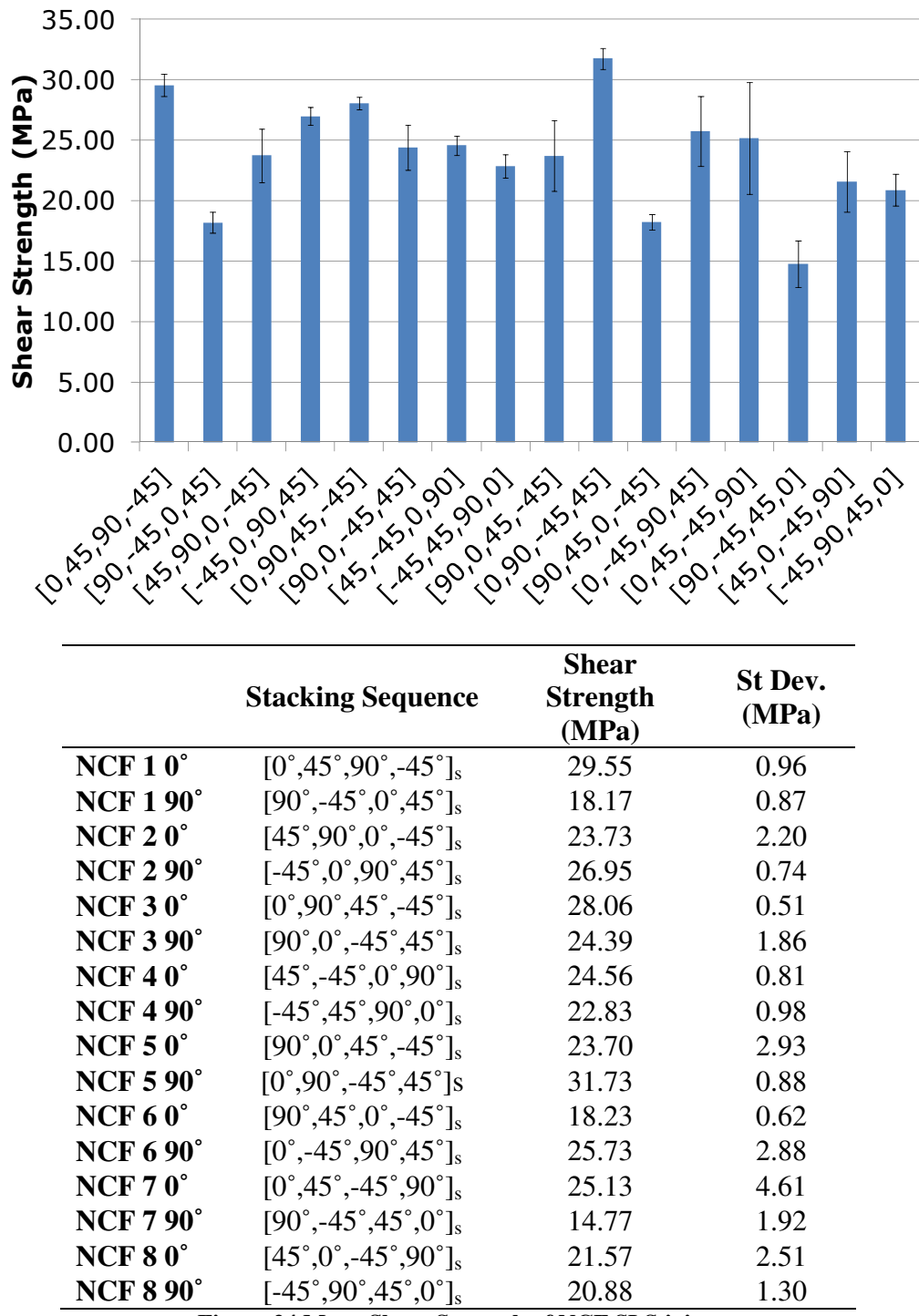


Figure 24 Mean Shear Strength of NCF SLS joints

The effect of stacking sequence and surface fibre orientation on the elongation to failure of SLS joints subject to tensile testing is less clear than for the shear strength of the adhesive joints. The mean extensions to failure of the specimens are presented in Figure 25.

The preform with the highest elongation to failure of the SLS joints was NCF 3 0° which had a stacking sequence of [0°, 90°, 45°, -45°]_s whilst the lowest performing preform was NCF 7 90° which had a stacking sequence of [90°, -45°, 45°, 0°]_s. For NCF 3 0° the mean elongation to failure of the samples was 2.09mm and for NCF 7 90° the mean elongation to failure was 0.71mm which equates to a decrease of nearly 70% in the average elongation to failure. The top 3 performing preforms (NCF 3 0°, NCF 1 0° and NCF 5 90°) all had 0° surface layers with NCF 3 0° and NCF 5 90° having a 90° oriented second layer whilst NCF 1 0° had a 45° second layer.

The worst 3 performing plaques were the same as for the shear strength with NCF 6 0°, NCF 1 90° and NCF 7 90° having the lowest elongation to failure of the samples tested. All 3 plaques had a 90° surface layer fibre orientation and either a 45° or -45° fibre orientation for the second layer.

From the testing it was possible to deduce that the 0° surface fibre orientation offered the best performance for elongation to failure whilst the 90° surface fibre orientation offered the lowest elongation to failure of the specimens studied. The role of the subsequent layers within the composite substrate was less clear with a mix of orientations being present within the highest performing plaques.

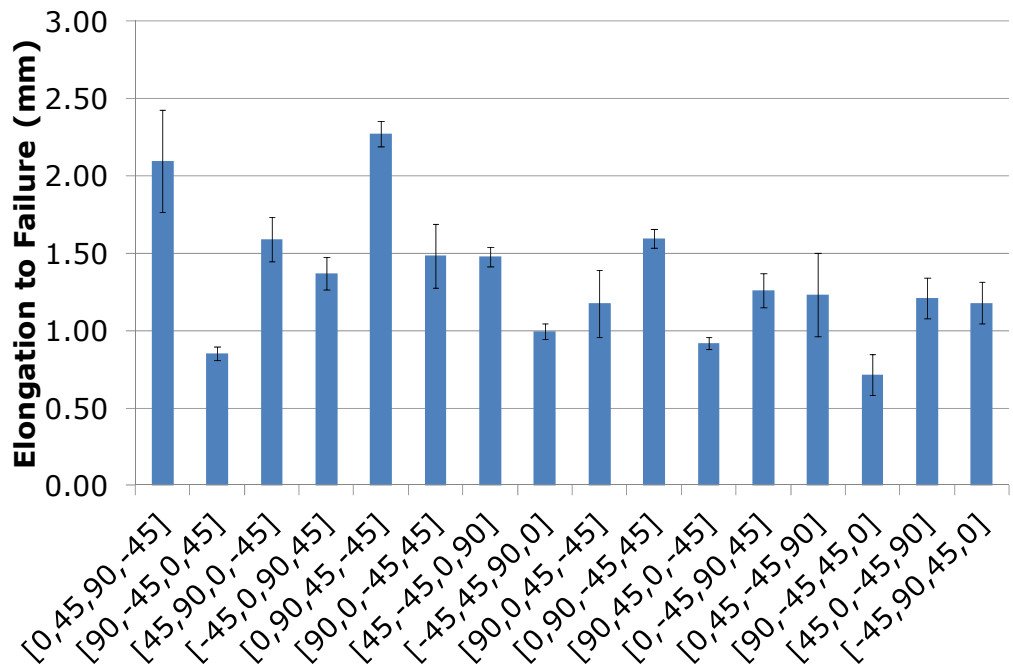


Figure 25 Mean Elongation to Failure of NCF SLS joints

4.3.3 Comparison of NCF Preform Performance

The results from the testing were combined to provide a cumulative ranking of properties in order to identify the best and worst performing preforms from the testing and the difference in properties between them. To simplify the data, those plaques

with similar stacking sequences but with opposite 45° layers were merged to provide a plot of the 12 unique stacking sequences.

In order to normalize the data, the results for each plaque were divided by the highest value of each property and then converted to a percentage of the maximum value achieved for the property. The shear strength and elongation to failure were then summed and the total value obtained was ordered to organise the plaques into a ranking. The data was then plotted on the cumulative bar chart presented in Figure 26. This method assigns an equal weighting to properties studied. This could be revised in the future depending on the requirements of the testing.

The $[0^\circ, 90^\circ, 45^\circ, -45^\circ]_s$ layup significantly outperforms the other plaques in the study, as highlighted in Figure 26. Similarly the worst performing preforms' layup $[90^\circ, -45^\circ, 45^\circ, 0^\circ]_s$ offers significantly lower properties. The performance of the worst preform is about one third that of the best performing one.

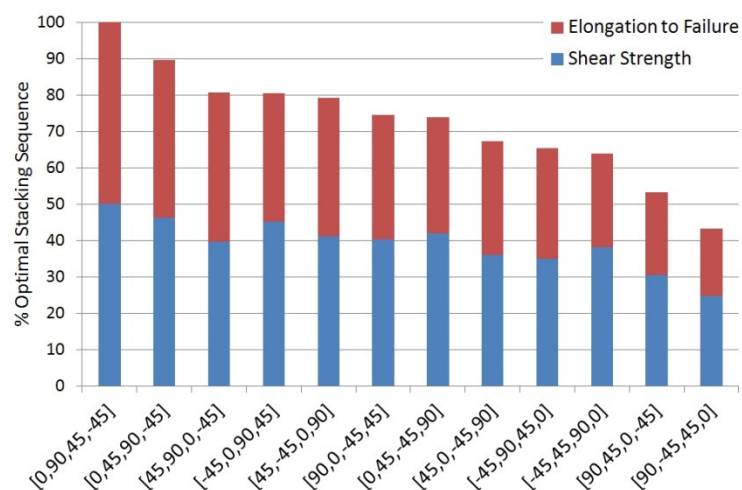


Figure 26 Comparison of Quasi-Isotropic SLS adhesive joints

4.4 Discussion

The study on the influence of surface fibre orientation and stacking sequence on the performance of composite SLS adhesive joints provided a good insight into the impact that the substrate material properties have on the resulting joint behaviour of SLS joints subject to tensile loading. It was possible to determine both the best and worst performing substrates as well as gain an understanding of how varying the fibre orientation can change the behaviour of a joint.

4.4.1 Effect of Fibre Orientation

The reasons for the large difference in failure loads and adhesive joint performance because of fibre orientation are relatively well established in the literature [1,40,43-45,74-76]. When 0° aligned fibres are located at the top surface of a fibre reinforced composite adhesive joint, the bulk of load transfer between the two substrates is carried through the reinforcing fibres of the material. When these fibres become aligned off-axis, the load transfer at the adhesive/substrate interface is carried by a combination of the reinforcing fibres and the matrix. Finally, with the fibres are aligned perpendicular to the load path, the load transfer becomes almost entirely dependent on the material properties of the matrix of the substrate. The fibres can act as a stress discontinuity thereby leading to stress concentrations within the substrate material. This in turn affects the failure characteristics of the different adhesive joints.

The substrates with a 0° fibre orientation outperformed the other SLS joints tested, unless this was followed by 2 layers of +/- 45° layers. There was a 31% spread in performance between the best and worst substrates with a 0° orientated surface layer. With the 0° surface fibre alignments the bulk of the failures occur as a cohesive failure, indicating a good bond having been created. There were cases of substrate failures; these were caused by a number of different factors. Primarily, the removal of the matrix from the fibres at the surface gave rise to a number of near surface substrate failures. This indicates the adhesive performance was higher than that of the epoxy matrix. By changing the sizing agents used to promote adhesion between the substrate matrix and fibres this failure mode may be reduced. Failure also occurred in the layers below the 0° oriented surface layer. Again this would be caused by the stress discontinuities that occur as the load is transferred between the two fibre layers. Finally, failure may occur as a result of fibre pullout of the 0° aligned fibres. In this case partial tows were removed from the substrate indicating either insufficient wetting of the fibre bundle during the RTM process or some other damage having been imparted on the fibre reinforcement.

The worst performing surface fibre orientation was the 90° aligned fibres. The lowest performing substrate (NCF 7 90°) had a 65% reduction in performance compared to the best performing substrate (NCF 5 9 0°). When there is a 0° second layer the

performance of the adhesive joint improves with the specimens being ranked 7th in overall performance. Between the best and worst stacking sequences with a 90° surface layer, [90°, 0°, -45°, 45°] and [90°, -45°, 45°, 0°] respectively, there was a 50% difference in overall performance. The joints exhibited a substrate failure for all of the 90° specimens. The fibre bundles close to the adhesive joint overlap ends were broken from the remaining substrate leading to failure at much lower loads than for the other substrates. Failure of the matrix over the adhesive indicates that the adhesive bonds well to the substrate; however, the joint performance is being limited by the matrix material properties.

Those composite SLS adhesive joints tested with a 45° surface fibre orientation provided the samples with the lowest overall spread in performance as a result of changes in the stacking sequence. In total there was a 28% difference when the best and worst performing substrates with a 45° surface layer were studied. When the surface fibres of the substrate are aligned at 45° the off-axis fibre alignment resulted in substrate failure near the surface of the material. Generally, delamination of the top layer was observed near the adhesive joint overlap ends. As the joint overlap ends are the point of highest stress, the off-axis fibre alignment means that the adhesive joint tends to fail at this point with a corner of the substrate lifting from the remaining substrate.

Of interest was the change in performance for the 45° and 90° layers when they were placed below the surface layers. Whilst at the surface the 45° fibre orientation is preferable to using a 90° layer, below the surface the 90° fibre orientation outperforms the 45° layers. This may be the result of the abrupt change in fibre orientation forcing shear loading to occur with each bundle restricting specimen movement. With the 45° the fibres can slip within the matrix up to eventual failure as a result the 45° specimens will cause longer elongation to failure.

4.4.2 Effect of Changing Stiffness on performance of NCF SLS joints

Previous studies [33,45,74,76] that varied the stacking sequence and fibre orientation of bonded SLS joints generally varied the entire stacking sequence, thus the overall substrate strength and bending stiffness was changed. The use of a quasi-isotropic

lamine sought to maintain a constant substrate strength and global stiffness. Although it was acknowledged that the stiffness close to the bond surface would vary with the change in fibre orientation this was a compromise that was accepted.

In an attempt to limit the rotation of the specimens observed and as a result reduce the peel stresses, reinforced SLS adhesive joints were manufactured. It was anticipated that the amount of bending observed in SLS testing should be reduced thereby causing a more consistent failure mode by reducing the contribution of the peel forces and placing the joints into pure shear. This in turn should have resulted in higher mechanical properties. The joints were the same SLS joints manufactured for the NCF study however a 6mm steel backing plate was bonded to the specimens prior to testing. The results have been included in Appendix D.

The use of the steel reinforcement had the effect of reducing the overall performance of the SLS joints whilst also diminishing the spread of results between the best and worst performing samples in the study for all of the responses studied. The 0° surface layer was still the optimal orientation; however there was no significant difference between the 45° and 90° fibre orientations. This may indicate either the experiments sample population was too small or there increase in stiffness makes the specimens less sensitive to fibre orientation.

The conclusions that could be drawn from the study were that the stiffness of the substrate evidently played a more important role in defining the behaviour of the specimens than the fibre orientation or stacking sequence did. There were no significant changes to the failure mode behaviour, with a slight increase in substrate and mixed failures. It was therefore decided that the addition of reinforcement offered no significant benefits to outweigh the additional time and costs of reinforcing composite SLS adhesive joints.

4.4.3 Design of Experiment

Owing to the design of the experiment, it was not possible to properly investigate the interactions that occurred with changing stacking sequence. The changing orientations in the layers below the surface will affect the load transfer of the adhesive joint so a future experimental investigation may be desirable as this may explain some of the

failure modes observed where layers below the surface failed prior to the surface layer. There have been attempts to model this with the work by Mortensen [40,75].

4.5 Conclusions

The aim of the investigation was to understand the effect of fibre orientation and stacking sequence on the performance of composite SLS adhesive joints using a non-crimp fabric preform. The study used 16 different stacking sequences in order to better understand the effect of changing fibre orientations on the shear strength and elongation to failure of the NCF SLS adhesive joints. A quasi-isotropic stacking sequence was used to reduce the difference in stiffness and strength between the different laminates. A separate study investigated the use of steel reinforcements bonded to the back face of the substrate so as to reduce the rotation and consequently peel stresses present within the SLS joints; however, this was unsuccessful.

The chapter aimed to provide a link between the DCFP joints studied in Chapter 5 and the Oriented DCFP adhesive joints studied in Chapter 6. If a better understanding of the influence of the stacking sequence and fibre orientation is achieved using a conventional laminar composite, it is anticipated that the trends may also be observed in DCFP substrates. This may allow aspects of both the oriented and random fibre architectures to be merged in future studies.

One observation that was made through the testing was the extent to which the NCF SLS adhesive joints were subject to rotation during the tensile testing. This rotation indicated that considerable peel stresses were present and would affect the measured shear strengths of the NCF SLS adhesive joints. Attempts to limit this and put the joints into pure shear through the use of steel reinforcement made the results more difficult to interpret. It demonstrated that the stiffness of the substrate exerts a much greater influence on the joint behaviour of composite SLS joints compared to the fibre orientation and stacking sequence.

The interpretation of the results both identified an optimum fibre orientation and stacking sequence for bonding NCF SLS adhesive joints as well as identifying the extent of the influence of fibre orientation and stacking sequence on the joint performance. The most important fibre orientation for maximising the joint

Chapter 4 – Effect of Fibre Orientation on Bonded SLS Joints

performance was the surface fibre orientation. When this was not the 0° fibre orientation, it was possible to increase the performance by including a 0° layer immediately below the surface. Overall, the 90° surface fibre orientation provided the worst performing preforms. The difference between the best and worst performing preforms equated to a 65% reduction in performance. This indicates that the stacking sequence and fibre orientation play a vital role in defining the overall joint behaviour of Fibre Reinforced Composite SLS adhesive joints.

Chapter 5. Optimisation of Bond Parameters for DCFP Single Lap Shear Joints

5.1 Introduction

The objective of the first study using a DCFP substrate was to study the effect of varying the substrate properties and bond dimensions on the tensile performance of SLS adhesive joints. A review of the literature identified a number of factors that significantly influence the mechanical performance of the bulk material. To date there has been no conclusive study on how varying these factors influence the performance of a bonded DCFP substrate.

Harper [73] identified eight different manufacturing factors that influence the mechanical properties of DCFP preforms. These are:

- Areal density consistency
- Fibre Length
- Fibre orientation
- Tool centre point height
- Robot speed
- Chopper gun speed
- Lay-down strategy
- Number of tows processed

The variables that are relevant to this study are: the areal density consistency, fibre bundle length effects and tow size. The effect of fibre orientation and tool centre point height are investigated separately in Chapter 6. The robot speed was maintained

constant throughout the investigation whilst the chopper gun speed was maintained to as close to 6m/s as possible. The lay-down strategy was maintained as an orthogonal spray pattern composed of an east/west pass followed by a north/south pass with each sweep being offset by 50mm. The number of tows processed was limited by the robot and was maintained at 4 tows for the 3k and 6k tow sizes and a single tow for the 24k fibre bundles.

The mechanical properties of the substrate are dependent on the substrate thickness as this ensures an areal density consistency. The manufacture of thin parts can result in poor fibre coverage. Harper [73] measured an 18.8% strength reduction when the areal density was reduced from 2.25kg/m^2 to 0.75kg/m^2 (4mm to 1.5mm laminate thickness). From a manufacturers perspective, when a demonstrator B-Pillar was manufactured using the P4 process, maintaining an even fibre coverage as the part thickness changed from 1.5mm to 8mm proved the biggest challenge [14].

In the studies by Harper [73,87], a shorter fibre length was used to enhance the tensile strength of the DCFP laminate. The shorter fibres improved the tensile strength of the laminates as a result of improved preform fibre coverage, aided by the natural filamentisation of the fibre bundles, which reduced the overall fibre bundle filament count. From a manufacturing point of view the shorter fibre lengths can be a challenge to process as the overall preform integrity is reduced and there is a risk of fibre washing during the injection phase of the DCFP plaque manufacture. As such the aim was to identify an optimum fibre length that enabled trouble free manufacture whilst maintaining a high mechanical performance.

The tow size used to manufacture the DCFP preforms will have an effect on both the fibre coverage of the preform and the level of filamentisation observed. As a consequence this has a large influence on the mechanical properties of the substrate. Throughout the experimental investigations three different tow sizes were used to investigate this relationship with the smaller tow sizes expected to improve the overall performance of the SLS joints owing to the improved homogeneity and reduction in the number of critical flaws.

The effect of varying bond dimensions was also investigated in the study. The effect of bond overlap, bond width and bondline thickness have all been well documented in

literature. As such a brief review of the literature is provided. The aim of varying these parameters was to validate whether the trends identified in conventional composite materials still applies to the bonding of DCFP substrates.

The influence of bond overlap has been well documented in literature. However, the degree to which this influences the overall joint strength is inconclusive. Hart-Smith discussed the important influence of adhesive bond overlap in his 1973 paper *Adhesive-Bonded Single-Lap Joints* [23]. Song et al conducted a study into the effect of bond overlap in single-lap shear joints when studying the effect of various manufacturing methods on the shear strength of composite SLS bonded joints. The investigation studied 4 different overlap lengths ranging from 12.7mm to 50.8mm. The findings confirm that there is a relationship between adhesive joint strength and the overlap length; however, the relationship is not linear. There appears to be a maximum effective length beyond which the joint strengths begin to decrease. The authors acknowledge the existence of a relationship between joint strength and overlap length; however, owing to the number of factors involved in defining the joint strength, no relationship is proposed [43]. The presence of a maximum effective overlap length was also identified by Ferreira et al when two different overlap lengths were studied, one of 30mm and the other of 60mm. The samples were subject both to static and fatigue tests with the 30mm overlap length outperforming the 60mm samples in both of these tests [44].

The effect of bondline thickness was investigated by Lee et al. Four different adhesive thicknesses were used in the study ranging from 0.2mm to 2mm. The authors found that reducing the adhesive bondline thickness from 2mm to 0.2mm resulted in a 22% increase in joint strength. Lee concluded that the most appropriate bondline thickness falls somewhere between 0.2mm and 0.5mm [47].

Davies et al investigated the influence of bondline thickness on the joint strength of adhesive joints. In the study 5 different factors regarding the bondline thickness were identified as having a potential impact on the adhesive joint strength. The nature or size of defects was identified as having an insignificant effect on bond strength with increasing bondline thickness. The adhesive polymer microstructure was investigated however no significant changes in the structure were observed with changes in bondline thickness from 0.2mm to 1.3mm. The interface properties between the

adhesive and substrate were observed to be near constant with a similar extent as the surface roughness of the substrate. In tensile testing there was a significant decrease in yield stress and failure strain for specimens with thicker bondlines. Using numerical analysis this was shown to be the result of higher stress concentrations occurring with larger bondline thickness. Finally, the authors propose an upper limit of 0.6mm bondline thickness for samples tested in tension. The use of smaller bond gaps can also reduce the influence of test imperfections such as specimen misalignment [49].

The study sets out to provide an optimum set of parameters for the optimal bonding of DCFP substrates. In the future this should simplify adhesive screening programs as well as provide a reference when designing adhesively bonded components using the DCFP manufacturing process.

5.2 Methodology

The six factors selected for the investigations were divided into 2 categories; substrate properties and bond dimensions. The properties that were investigated are listed in Table 12. Using a full factorial experiment the use of 6 factors at 3 levels would have been unfeasible; a total of 729 specimens would need manufacturing and including 5 replicates would equate to 3645 specimens.

Table 12 Factors investigated in DCFP optimisation study

Substrate Properties	Bond Dimensions
Tow Size	Bond Width
Fibre Length	Bond Overlap
Substrate Thickness	Bond Gap

An L27 (3**6) Taguchi orthogonal array was designed to identify both the most optimal solutions for the manufacture of the DCFP substrates as well as the bond dimensions. Three different levels were chosen for each of the factors studied. In total 27 different iterations were studied with the results being analysed using Minitab16 [88] statistical analysis software with 5 replicates for each iteration. A total of 135 samples were manufactured and tested.

The results were analysed to identify both the best performing joint configuration whilst also taking into consideration the variability of the adhesive performance. By

identifying those substrates with the best overall performance and the least variation, the optimal joint parameters should be identified for use in further studies.

5.2.1 Manufacturing of DCFP Substrate

Nine different DCFP preforms were manufactured to compare the strength and elongation to failure of the different DCFP substrates. The different levels for the tow size, fibre length and substrate thickness are summarised in Table 13.

Table 13 Level Settings for manufacturing DCFP substrate

Preform ID	Tow Size (k)	Fibre Length (mm)	Thickness (mm)
1	3	30	2
2	3	60	3
3	3	90	6
4	6	30	3
5	6	60	6
6	6	90	2
7	24	30	6
8	24	60	2
9	24	90	3

The tow sizes studied were selected owing to the common use of these filament counts within industry. The 3k tow size is more commonly used in structural applications and within aerospace. The 6k tow size has been used as a reference filament count throughout previous studies using the DCFP manufacturing process [17,73]; whilst, the 24k filament count is the most cost-effective fibre because of its wide use within the composites industry [89].

The fibre lengths were defined by the feed roller dimensions. The 30mm fibre length was the smallest length that would allow for the effective manufacture of DCFP preforms owing to the problems associated with handling short fibre preforms and the injection of the preforms. Again, the 60mm fibre length was used as a reference length in earlier studies whilst the 90mm length was at the upper limit of usable fibre lengths. Above this length there were problems associated with the deposition of the fibres, such as clogging of the chopper gun, highly aligned preforms and uneven fibre coverage.

The thicknesses studied were selected to encompass the different material thicknesses that have been studied in the past. The 2mm thickness was chosen as this was the lower limit of thickness before the problems associated with poor fibre coverage became apparent. The 3mm substrate thickness was the standard part thickness for characterising adhesives for bonding to composite materials at AML whilst the 6mm thickness was the thickest possible substrate that could be tested in the mechanical testing machines with the available equipment.

5.2.2 Resin Transfer Moulding

The injection procedure was carried out using a stainless steel mould assembled using a number of different picture frames depending on the desired part thickness. A CiJect One™ resin injection machine manufactured by Composite Integration was used to inject the preforms.

Release agent was applied to the moulding tool parts and allowed to thoroughly dry. The preform was then placed in the tool and loaded into a heated press with a 50ton clamping force. The press and tool were pre-heated to 50°C prior to injection whilst the resin was preheated to 80°C to maintain a low viscosity. An initial injection pressure of 0.5bar ensured the preforms were fully wet out. A vacuum pump attached to the exhaust port via a catch pot provided assistance in infusing the parts. The vacuum was removed once resin began to flow into the catch pot. When the resin ran clear in the exhaust port the injection was stopped and the temperature of the press ramped to 120°C for 1 hour. The tool was cooled and the manufactured plaque removed. A post-cure of 75°C was carried out for 4 hours to ensure the plaques were fully cured.

5.2.3 Cutting of Substrate

The specimens were extracted from the moulded preforms using a Diamant Boart diamond cut-off saw. The dimensions of the specimens were changed throughout the investigation; however, the dimensional tolerances were set at +/- 0.5mm for the specimen widths and +/-1mm for the specimen lengths. If a specimen fell outside of these dimensions it was deemed flawed and another specimen extracted.

5.2.4 Manufacture of DCFP SLS adhesive joints

In the study, the dimensions of the bond width, bond overlap and bond gap were varied, with 3 different levels being chosen for each of the factors studied. The bondline properties used in the study are summarised in Table 14.

The bond width of the specimens was only varied between the preforms and not within the 3 different bond areas studied for each preform. The 25mm bond width is the standard test dimension for the testing of SLS adhesive joints [90]. The other dimensions then studied were half and double the standard width respectively. This was done to verify whether the DCFP SLS joints are sensitive to a changing width owing to the heterogeneous nature of the material.

The bond overlaps were determined in a similar manner as for the bond width. Throughout characterisation programs at AML the standard adhesive overlap used is 10mm. To test the effect of varying this value it was both halved and doubled.

The standard adhesive bond gap of 0.2mm was determined by the characterisation specification [91] used internally at AML to characterise adhesives. The smallest practical bondline thickness available was 0.1mm whilst the 0.5mm dimension was used as above this thickness there was evidence in literature of an upper limit whereupon there was a significant drop in joint performance [47,51].

Following the extraction of the substrate, the specimens were cleaned in water to remove the majority of the contaminants that arose from the cutting process. The bond area was abraded using 500 grit abrasive papers followed by a ScotchBrite 7496 pad soaked in acetone. This ensured any remaining mould release; cutting fluid and loose debris were removed from the bond area. Finally, the specimens were wiped with a clean cloth soaked in acetone before the specimens were allowed to dry prior to bonding.

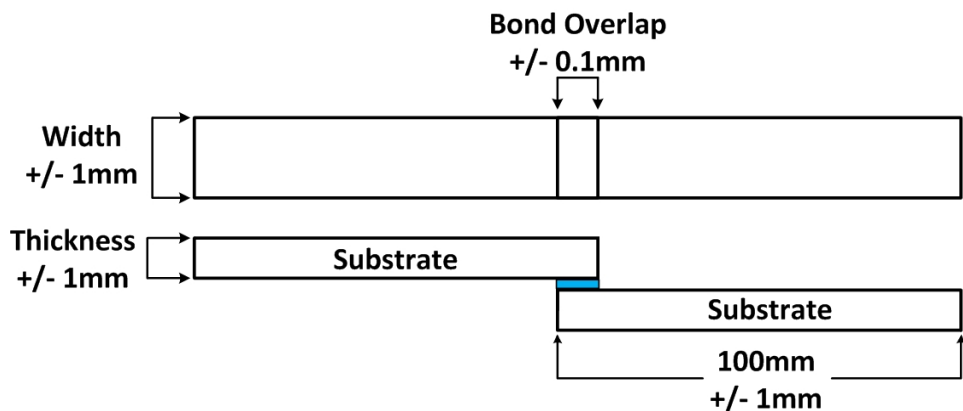


Figure 27 SLS Joint Configuration

The specimens (Figure 27) were mounted into the bonding jig (Figure 28) and a bead of adhesive was dispensed onto the substrate. The adhesive was spread across the bond area and 2 wire spacers were placed within the bond. The bond was then closed and the bond overlap dimensions checked. Once the desired overlap length was achieved any excess adhesive was removed using a sterile blade. This ensured a constant spew geometry as the adhesive joints had no fillet radii. The bonded joint was secured with bull clips and allowed to cure at room temperature for a 24 hour period before being cured using the AMLC cure cycle described in Appendix B.

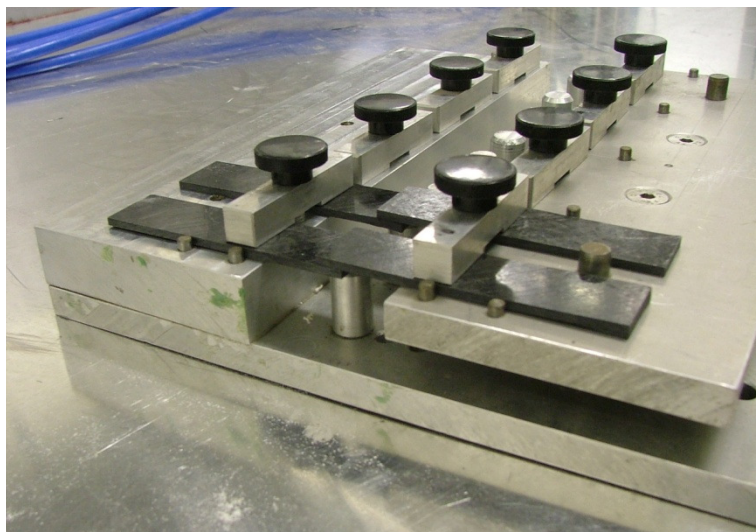


Figure 28 SLS adhesive joint bonding rig

5.2.5 Mechanical Testing

The tensile testing was carried out using an Instron mechanical testing machine. The test speed was set to 2mm/min. The load was measured using a 50kN load cell whilst

the extension was measured from the cross-head displacement. Although the cross-head displacement is not the most accurate form of measuring strain and displacement, owing to the SLS joint configuration it was not possible to use a conventional extensometer effectively.

In order to minimize the peel forces present in SLS tests, spacers the thickness of the substrate being tested were used in the jaw faces. This ensured that the load path passed centrally through the adhesive bondline. A 96mm gauge length was set to maintain a constant distance between the two jaw faces. A schematic of the tensile test setup is included in Figure 29.

The results from the mechanical testing of the DCFP SLS adhesive joints are presented in Table 14. Owing to the design of the experiment, interpretation is not feasible without the use of statistical analysis; this is presented in more detail in Appendix D.

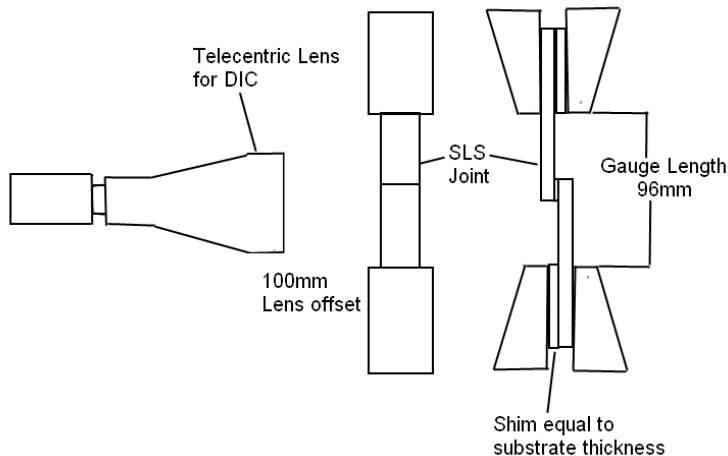


Figure 29 Schematic of SLS mechanical testing setup

Table 14 Level Settings and Mechanical Performance of DCFP SLS Joints

Preform Number	Sample ID	Bond Width (mm)	Bond Overlap (mm)	Bond Gap (mm)	Shear Strength (MPa)	StDev (MPa)	Elongation to Failure (mm)	StDev (mm)
Preform 1	1.1	12.5	5	0.1	29.58	5.34	1.69	0.94
	1.2	12.5	10	0.2	28.37	4.81	2.08	0.96
	1.3	12.5	20	0.5	17.62	1.95	3.24	1.24
Preform 2	2.1	25	5	0.1	26.90	5.28	0.68	0.22
	2.2	25	10	0.2	32.69	0.87	1.74	0.13
	2.3	25	20	0.5	19.70	1.11	2.14	0.15
Preform 3	3.1	50	5	0.1	23.56	0.99	1.18	0.29
	3.2	50	10	0.2	24.16	0.74	2.59	0.10
	3.3	50	20	0.5	18.42	1.82	4.35	0.22
Preform 4	4.1	50	5	0.2	19.31	3.18	1.15	0.18
	4.2	50	10	0.5	20.09	1.26	2.31	0.06
	4.3	50	20	0.1	17.46	0.29	3.62	0.95
Preform 5	5.1	12.5	5	0.2	22.84	1.85	0.67	0.08
	5.2	12.5	10	0.5	18.19	3.03	1.17	0.21
	5.3	12.5	20	0.1	15.07	1.88	2.80	0.40
Preform 6	6.1	25	5	0.2	25.63	1.36	1.15	0.11
	6.2	25	10	0.5	26.19	0.75	2.29	0.17
	6.3	25	20	0.1	21.90	1.90	3.98	0.30
Preform 7	7.1	25	5	0.5	23.06	0.65	1.04	0.07
	7.2	25	10	0.1	22.30	1.10	1.54	0.08
	7.3	25	20	0.2	16.03	2.99	3.24	0.50
Preform 8	8.1	50	5	0.5	24.01	2.93	1.46	0.22
	8.2	50	10	0.1	23.60	2.62	2.94	0.38
	8.3	50	20	0.2	17.92	1.63	4.27	0.58
Preform 9	9.1	12.5	5	0.5	24.52	3.26	0.53	0.09
	9.2	12.5	10	0.1	29.33	2.50	1.33	0.29
	9.3	12.5	20	0.2	24.88	2.81	2.58	0.55

5.3 Analysis of Joint Failure Modes

The manner in which the adhesive joints failed was studied by considering each of the factors in isolation. Although this neglects to study any higher order interactions that may influence the failure mode, it still serves as a good indicator as to how each factor can influence the failure behaviour of the DCFP SLS adhesive joints. An example of some of the observed failure modes is presented in Figure 30 below.

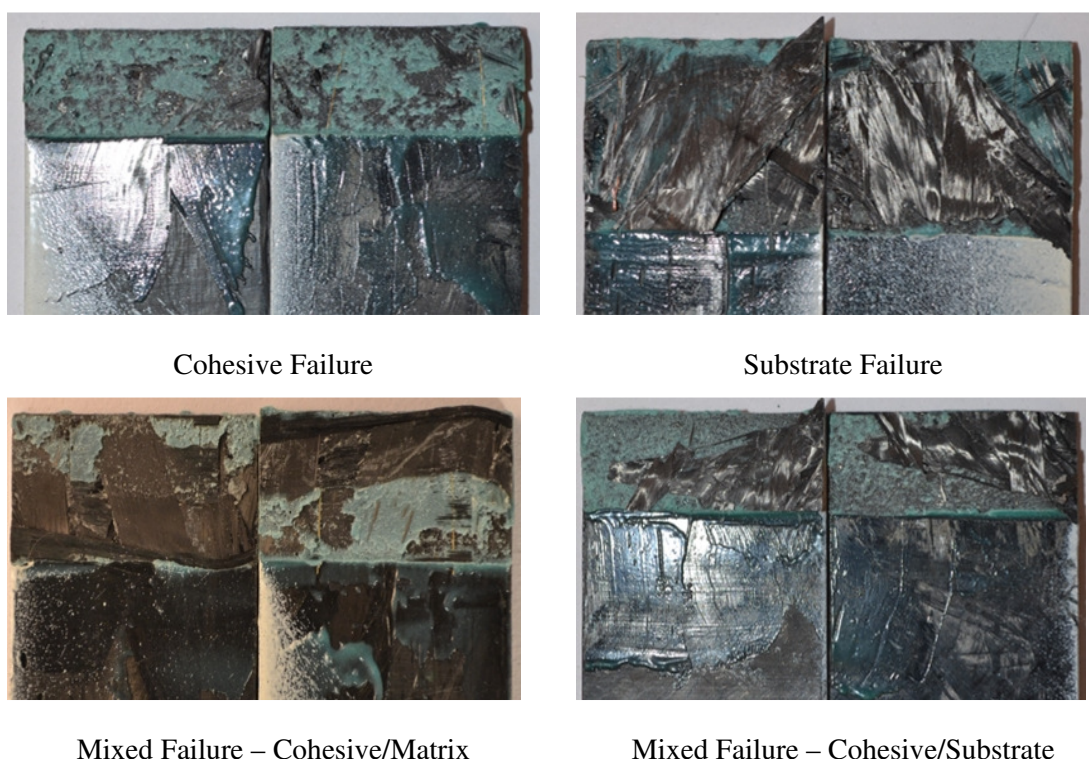


Figure 30 Example of Common Specimen Failure Modes in DCFP SLS Joints

When studying the distribution of failure modes across the entire specimen population just under 3% of the failures observed were adhesive failures, 36% were cohesive failure, 21% substrate failure and a further 41% were mixed (cohesive and substrate) failures. Adhesive failure appeared to be the result of poor specimen preparation. As only 36% of the failures were cohesive, it is hoped that by identifying the influential factors on failure mode the distribution of cohesive failures can be considerably improved in the future. It is desirable to try and identify the factors that would improve the structural integrity of the DCFP substrate as 62% of the failures are related to failure in the composite substrate.

The distribution of failure modes with varying tow size is presented in Table 15. The frequency of cohesive failures was the highest (40%) for the 3k tow size. In all 3 cases the majority of specimen failures were located within the substrate. The tow size appears to not exert as much influence on the failure mode as expected as there is little to distinguish between the three different tow sizes with regards to joint failure.

Table 15 Distribution of failure modes (%) for varying Tow Size

	3k	6k	24k
Adhesive	2%	2%	4%
Cohesive	40%	33%	33%
Substrate	18%	11%	33%
Mixed	40%	53%	29%

The effect of varying the substrate fibre length on the DCFP SLS adhesive joint's failure mode is presented in Table 16. The 30mm fibre length provided the highest distribution of cohesive failures (47%) whilst there was a clear decrease in cohesive failures with increasing fibre length. The incidence of combined substrate and mixed failure also increased with 71 % of the specimens demonstrating this failure mode at the 90mm fibre length compared to 53% for the 30mm fibre length. This may be the result of an increase in variability as a result of the decrease in fibres deposited for an equivalent areal mass.

Table 16 Distribution of failure modes (%) for varying fibre length

	30mm	60mm	90mm
Adhesive	-	4%	4%
Cohesive	47%	36%	24%
Substrate	24%	11%	27%
Mixed	29%	49%	44%

The 3mm substrate thickness provided the joints with the highest distribution of cohesive failures (51%) when studying the distribution of failure modes with changing substrate thickness as presented in Table 17; above this thickness the cohesive failures were limited to 20%. This is most likely the result of the low through thickness strength of the DCFP substrate. The increase in strength that would normally be observed for a larger substrate thickness is limited to somewhere between 3mm and 6mm as the adhesive strength beyond this point surpasses the strength of the substrate. Below the 3mm laminate thickness the fibre coverage would appear to be insufficient

to provide a robust surface to bond to with a high occurrence of mixed and substrate failure modes.

Table 17 Distribution of failure modes (%) for varying substrate thickness

	2mm	3mm	6mm
Adhesive	-	7%	2%
Cohesive	36%	51%	20%
Substrate	20%	9%	33%
Mixed	44%	33%	44%

The distribution of failure modes for varying specimen width is presented in Table 18. The frequency of cohesive failure was maximised when the specimen width was 25mm. A total of 47% of 25mm width specimens failed cohesively, compared to the 38% for the 12.5mm and 22% for the 50mm wide specimens. This validates the recommended 25mm specimen width; below this value it would seem the peak stresses at the specimen edges promote failure within the composite specimen [91]. There is also an increase in incidents of adhesive failure at the 12.5mm specimen width, a highly undesirable failure mode. The 50mm overlap would appear to be too wide for the adhesive strength to allow the specimen to fail cohesively and as such the substrate yields in a mix of substrate and cohesive failure.

Table 18 Distribution of failure modes (%) for varying specimen width

	12.5mm	25mm	50mm
Adhesive	7%	2%	-
Cohesive	38%	47%	22%
Substrate	13%	31%	18%
Mixed	42%	20%	60%

There appears to be a constant decrease in cohesive failure as the bond overlap was increased, as presented in Table 19. A total of 53% of the 5mm overlap specimens demonstrated cohesive failure whilst only 36% and 18 % of the 10mm and 20mm overlap specimens displayed a similar failure mode. This would indicate that the adhesive's strength was being achieved with these shorter overlap lengths whilst for the longer overlaps the increase in bond area resulted in a higher occurrence of substrate or mixed failure modes. Of concern is the 9% of adhesive failures occurring at the 5mm bond overlap, this is most likely owing to the challenge of manufacturing

such a short overlap length effectively and as a consequence, the number of flaws increased at this overlap length.

Table 19 Distribution of failure modes (%) for varying bond overlap

	5mm	10mm	20mm
Adhesive	9%	-	-
Cohesive	53%	36%	18%
Substrate	7%	11%	44%
Mixed	31%	53%	38%

Out of all of the factors studied, the number of observed cohesive failures was the most evenly distributed when the adhesive bond gap was studied. This is presented in Table 20. For the 0.1mm bond gap 22% of the failures were cohesive, at the 0.2mm bond gap 16% were cohesive whilst at a 0.5mm bond gap the distribution of cohesive failures was 24%. This would indicate that within the bond gap range tested the failure modes were relatively insensitive to the change in bond gap. If the bond gap were increased considerably (to approx 2-3mm) it would be expected that the majority of the failures would be cohesive as this would decrease the joints fracture resistance thereby promoting crack propagation through the adhesive [45].

Table 20 Distribution of failure modes (%) for varying adhesive bond gap

	0.1mm	0.2mm	0.5mm
Adhesive	2%	2%	4%
Cohesive	22%	16%	24%
Substrate	42%	33%	47%
Mixed	33%	49%	24%

5.3.1 Settings for Optimising Adhesive joint failure mode

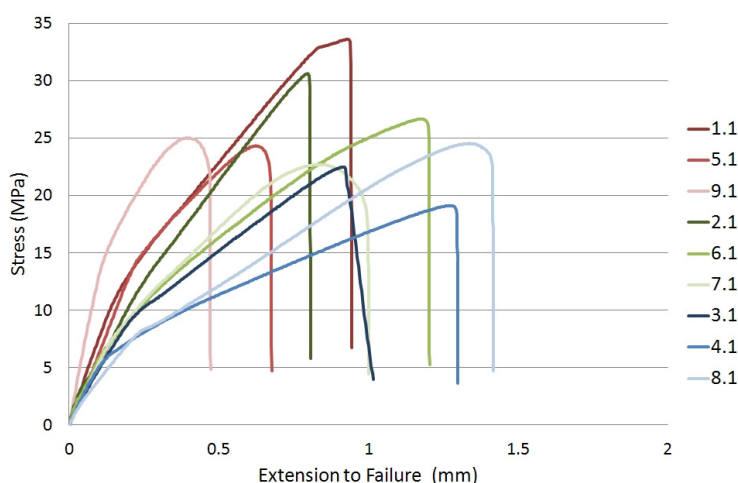
Having analysed the different observed failure modes and the contribution the different level settings have on the resulting joint failure, an optimal SLS joint configuration was identified that would maximise the occurrence of cohesive failures in the testing of DCFP SLS adhesive joints. The values are presented in Table 21. The recommended settings involve constructing a 3mm thick DCFP substrate constructed using 3k carbon fibre tows using a 30mm fibre length. The optimal bond dimensions identified were a bond width of 25mm, bond overlap of 5mm and an adhesive bond gap of 0.5mm. By using these settings the occurrence of cohesive failures should be maximised.

Table 21 Recommended Level Setting for DCFP SLS adhesive joints optimised for cohesive failure

	Tow Size	Fibre Length	Thickness	Bond Width	Bond Overlap	Bond Gap
Maximizing Cohesive Failure	3k	30mm	3mm	25mm	5mm	0.5mm

5.4 Representative Stress-Elongation Plots of Results

A set of stress-elongation plots were produced to demonstrate the variability of the SLS joint performance with variations in fibre architecture and bond areas. These are presented in Figure 31, Figure 32 and Figure 33. To reduce the number of plots on each of the graphs presented below the specimens were separated by the overlap length. This was chosen as it was the most influential factor with regards to joint performance and is discussed in the statistical analysis in Section 5.5. The plots are then further divided by colour according to the specimen bond width. Those plots using a shade of red were the 12.5mm specimen widths, the green corresponded to the 25mm width and the blue, 50mm specimen widths. Even so, it is hard to draw conclusions using these plots alone. The more general behaviour that was observed throughout the testing with regards to the bond dimensions was identified and these are briefly discussed; however, the effect of fibre architecture could not be studied using these plots.

**Figure 31 Stress-Elongation Plots for 5mm Overlap Specimens of DCFP SLS Joints**

The most evident observation was the effect of the bond overlap. Whilst the 5mm and 10mm overlap demonstrated similar shear strengths, there is a significant reduction when the 20mm overlap was used. This is understandable owing to the large reduction in cohesive failures that were observed with increasing fibre overlap lengths. Conversely, there was also a steady increase in elongation to failure of the specimens with increasing overlap.

When studying the specimen width effect, the 50mm specimen width resulted in the largest elongation to failure regardless of the overlap length. However, the 50mm specimens also tended to have the lowest shear strength. When comparing the 12.5mm and 25mm specimen widths, they were hard to differentiate due to variation in performance across bond overlaps and with changes in the fibre architecture.

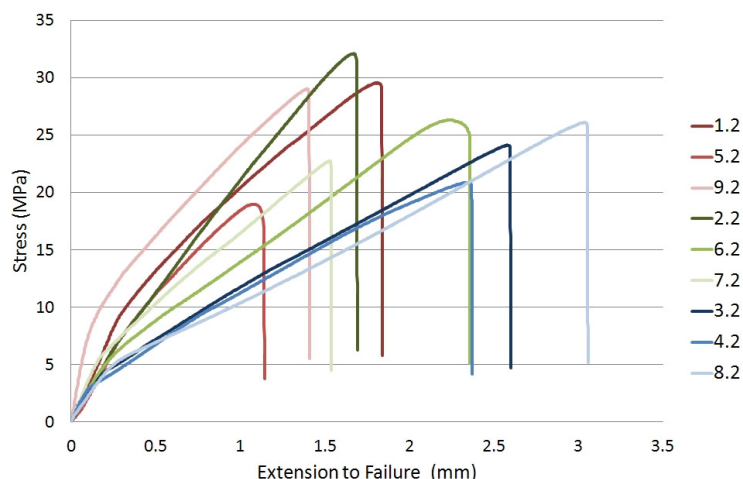


Figure 32 Stress-Elongation Plots for 10mm Overlap Specimens of DCFP SLS Joints

When the specimen substrate thickness was studied it was possible to observe that the 2mm thickness demonstrated the longest extension to failure; however, the difference between the 3mm and 6mm specimens was not evident. Similarly, it was not possible to identify any general effect on shear strength with changes in specimen thickness.

It was not possible to draw any conclusions simply studying the stress-elongation plots to understand the influence of the specimen fibre architecture between the specimens. This was the result of using a Taguchi orthogonal array when conducting the design of experiment. Overall, it was necessary to use statistical analysis to better understand the effect of all of the factors studied. The main results are presented in the following section.

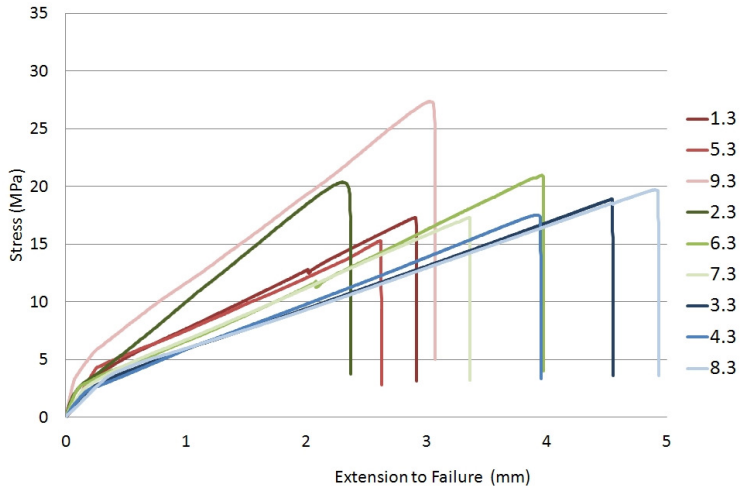


Figure 33 Stress-Elongation Plots for 20mm Overlap Specimens of DCFP SLS Joints

5.5 Results from Statistical Analysis

The statistical analysis included the 6 factors being studied along with 2 interactions that were of interest. These were the interactions of bond width-bond overlap and the bond width-bond gap. These were selected as these were the factors that were expected to exert the most influence over the bond area of the SLS joints studied. The shear strength and elongation to failure of the samples were input into the Design of Experiment (DOE) produced in Minitab 16 [88].

The signal-to-noise (S/N) ratio of the experiment is used to determine the effect each factor level has on the response variables being investigated. This is calculated as described in Equation 2. The S/N ratio is calculated for each level of each factor and is tabulated. By studying this, it is possible to select the best performing level for each factor which both minimizes the variability whilst maximizing the response variable being investigated. These response tables are included for reference in Appendix A.

$$\frac{S}{N} = \mu/\sigma \quad \text{Equation 2}$$

Where:

μ = mean of level response
 σ =standard deviation of level response

The aim of studying the standard deviations of the responses was to establish which levels of the factors provided the lowest variability. This coupled with the S/N ratio

results can then be used to help optimise the joint and substrate design to minimize the variation observed between samples.

The mean of the response variables investigated was studied to observe the actual influence the changing of the level of each factor had on the measured responses.

In order to calculate the optimal level settings for each factor, response tables were included in the analysis. The response tables show the average of the response characteristics (Signal/Noise ratio, means of data and standard deviations) for each level of the factors studied. These results are presented in main effects plots which allow for a more simple presentation of the results. The tables also include a ranking based on Delta statistics. The Delta value is determined by calculating the magnitude of the difference between levels for each factor. These values can then be ranked.

A linear model was fitted for the data means, signal to noise (S/N) ratios and the standard deviations of the data. This allowed for the analysis of variance (ANOVA) to be calculated. In order for a factor to be deemed statistically significant an α -level of 0.1 was used resulting in a confidence interval of 90%. The analysis was run separately for the shear strength and elongation to failure of the results. These are included in Appendix E.

The values in the response tables were then used to calculate the optimal substrate and bond area settings for the shear strength and elongation to failure using the factors deemed statistically significant in the analysis of variance. This data was tabulated and is presented in the following section.

5.5.1 Settings for Optimising Shear Strength of DCFP SLS joints

Studying the ANOVA for the shear strength results of the adhesive joints it was possible to identify the factors that significantly influence the strength. Referring to the response tables a set of optimal substrate fibre properties as well as recommended dimensions for the bond area could then be determined. The suggested level settings for maximising the shear strength are presented in Table 22.

When studying the S/N ratios the factors that were determined to be statistically significant were the bond overlap followed by substrate thickness, fibre tow size and

fibre length in descending order of influence. The recommended bond overlap was 10mm with the substrate properties being a 2mm substrate thickness manufactured using a 3k tow size and 90mm fibre length.

Considering the mean shear strengths, all of the factors studied, with the exception of bond gap, were deemed to be statistically significant. In this case the most influential factor was the overlap followed by the fibre tow size, substrate thickness, fibre length and finally the joint overlap. The optimal DCFP SLS adhesive joint for the highest overall shear strength was identified as being manufactured from a 2mm thick substrate using a 3k carbon fibre tow with a 90mm overall fibre length. The best bond area was a 25mm bond width with a 10mm adhesive bond overlap.

As there were no statistically significant results for the mean standard deviations for the factors studied, it is not possible to comment on the best level settings for minimizing the variability of results when considering the DCFP SLS adhesive shear strength.

Table 22 Recommended Level Settings for DCFP SLS Adhesive joints optimised for Shear Strength

	Tow Size	Fibre Length	Substrate Thickness	Bond Width	Bond Overlap	Bond Gap
S/N Ratios	3K	90mm	2mm	N/A	N/A	N/A
Data Means	3K	90mm	2mm	25mm	10mm	N/A
StDev				N/A		

5.5.2 Settings for Optimising Elongation to Failure of DCFP SLS joints

From the analysis of variance carried out on the elongation to failure of the DCFP SLS adhesive joints, the substrate thickness, bond width and bond overlap were identified as being statistically significant for all of the response characteristics studied. The fibre properties were only deemed to be statistically significant for minimizing the standard deviation of the elongation to failure. The recommended level settings for maximising the elongation to failure are presented in Table 23.

For both the S/N ratios and the data means the bond overlap, bond width and substrate thickness were the factors determined to be statistically significant in descending order of influence. The optimal settings for achieving a maximised response were

using a 2mm substrate thickness with a bond width of 50mm and a bond overlap of 20mm.

The only factor not to be statistically significant when studying the standard deviation was the adhesive bond gap. In descending order of significance; the bond width, substrate thickness, fibre length, adhesive overlap and tow size were all deemed to influence the elongation to failure. To obtain the most consistent testing results for elongation to failure the optimal substrate properties are a 6mm thick substrate made using a carbon tow with a 6k filament count and a 90mm fibre length. The best settings for the bond area were a 25mm bond width with a 5mm adhesive bond overlap.

Table 23 Recommended Level Setting for DCFP SLS Adhesive joints optimised for Elongation to Failure

	Tow Size	Fibre Length	Thickness	Bond Width	Bond Overlap	Bond Gap
S/N Ratios	N/A	N/A	2mm	50mm	20mm	N/A
Data Means	N/A	N/A	2mm	50mm	20mm	N/A
StDev	6k	90mm	6mm	25mm	5mm	N/A

5.5.3 Recommended Settings for Manufacture of DCFP Substrate

The results from the experimental investigation and practical manufacturing considerations were taken into account when deciding on a final set of factor levels that would provide the best solution for future experimental investigations of SLS adhesive joints manufactured using a DCFP substrate. There are 3 different level settings listed in Table 24. The first column was the recommended level settings purely decided by the statistical analysis of the results from the investigation, the second column are the recommended level settings for maximising the desired cohesive failure mode, whilst the final recommended level settings take into account additional manufacturing considerations.

The level settings that are presented for the optimal DCFP SLS joints as determined by the statistical analysis were identified by combining the recommended levels for the shear strength and elongation to failure. The results from the S/N ratios, mean values and standard deviations were all compared. With the exception of the tow size

and overlap length the optimal level settings were evident once the data was tabulated. For the tow size the recommended levels were split evenly between the 3k and 6k sizes. The 3k tow size is known to outperform the 6k preforms and as such the decision was taken to adopt this as the recommended level. The recommended overlap length was set to 10mm as this would optimize the shear strength of the SLS joints

For the manufacture of the optimal DCFP substrate for SLS adhesive tests, the recommended properties are a 3k filament count carbon tow with a 90mm fibre length using a 3mm target thickness. The reasoning for changing the substrate thickness to 3mm was the result of the analysis of the failure modes where the 2mm substrates had a much higher occurrence of substrate failures. By increasing the substrate thickness there would be a small decrease in performance; however this is offset by the fact that the increase would ensure the joint failure would occur more commonly within the bondline.

The adhesive bond area dimensions recommended are a sample width of 25mm with a 10mm bond overlap and a bond gap of 0.2mm. The statistical analysis indicated that a 50mm bond width would provide the optimal results but from a manufacturing perspective, this would result in double the volume of a 25mm samples' substrate being used. This would double the cost of manufacturing the DCFP SLS adhesive samples without any considerable performance gain. The analysis of the failure mode also contributed to selecting this dimension. The use of a 10mm bond overlap was chosen as this optimised the mechanical performance. The use of a 0.2mm adhesive bond gap was chosen as this is the traditional bond gap used when screening adhesives at AML and as there were no significant changes in performance with varying adhesive bondline thickness, changing this would offer no discernible advantage.

Table 24 Final Recommended Level Settings for DCFP SLS Adhesive joint Manufacture

Factor	Level Setting from Statistical Analysis	Level Setting from Failure Analysis	Final recommended Level Settings
Tow Size	3k	3k	3k
Fibre Length	90mm	30mm	90mm
Substrate Thickness	2mm	3mm	3mm
Bond Width	50mm	25mm	25mm
Bond Overlap	10mm	5mm	10mm
Bond Gap	N/A	0.5mm	0.2mm

5.6 Discussion

The use of the Taguchi method for optimising bonding of DCFP SLS adhesive joints and the analysis of variance carried out on the results from the experimental investigation provided the foundation work for understanding the role of both the substrate material properties and bond dimensions on defining the overall joint behaviour of DCFP SLS adhesive joints. The effect of varying these different parameters are all summarised and discussed. Owing to the design of the experiment, it was not possible to understand the complex interactions that may be present between different factors included in this investigation.

5.6.1 The use of the Taguchi Method

The Taguchi method was adopted for the experimental investigation of the adhesive bonding of DCFP SLS joints owing to the large number of factors under investigation. As there is very little literature available that discusses the challenges of bonding to discontinuous fibre reinforced composite materials, a broad study was required to gain an understanding of the most important factors that affect adhesive joint performance. The six factors that were chosen were three factors relating to the substrate properties and three that related to bond dimensions. The three substrate factors were the fibre filament count (tow size), the fibre length and the substrate thickness. The three factors affecting the bond dimensions were the specimen width (bond width), the adhesive bond overlap and the adhesive bond gap. Each of these factors was investigated using three different levels. If a conventional full factorial experiment had been carried out on these factors a total of 3645 samples would have been required for testing owing to the necessity of having repeat specimens. Using a

Taguchi orthogonal array for the design this was reduced to 135 samples, making a study involving all of these factors feasible.

There are however, certain deficiencies in the use of Taguchi methods for the design of experiments that must be acknowledged. The rigorous planning required to successfully implement a Taguchi designed experiment can make it unappealing. Even so, with a good understanding of the methodology and its deficiencies, it is possible to design and execute a successful experimental investigation.

The largest single deficiency of using a Taguchi design of experiment relates to its inability to identify interactions present between the factors being investigated. Although in this experiment the inclusion of the interactions yielded no statistically significant data, the accuracy of the model coefficients were significantly improved by the inclusion of these interactions.

Overall, the Taguchi method provided a good insight into the behaviour of adhesively bonded DCFP SLS joints; however certain considerations must be made. If running a complex investigation with many factors, the Taguchi method provides a good overview of the adhesive behaviour; however, it may be more desirable to carry out a full factorial experiment when there is already an established understanding of how the different factors affect joint performance. In this scenario, it would be more advisable to control as many factors as possible in order to gain a more detailed analysis of the interactions present between the factors under investigation.

5.6.2 Effect of Bond Overlap

The effect of changing the adhesive bond overlap was the most influential factor when studying the DCFP SLS adhesive joints. Three different bond overlaps were used which were 5mm, 10mm and 20mm.

When changing the bond overlap length there was a 41% contribution to defining the shear strength of the DCFP SLS adhesive joints. Whilst there was a small increase in shear strength when the overlap increased from 5mm to 10mm there was a 22% decrease when the overlap was increased to 20mm. This would indicate that the existence of an upper limit to an effective overlap length as described in literature is present when using the DCFP substrate; however, with the adhesive currently in use it

is at a significantly lower limit than for either metallic or conventional laminar composites [43,44]. From the analysis it is presumed the upper limit of an effective overlap length using the candidate adhesive lies somewhere between the 10mm and 20mm overlaps.

The analysis of failure modes with respect to the adhesive bond overlap demonstrated the number of cohesive failures decreased considerably as the overlap length was increased from 10mm to 20mm. As a result the substrate failure mode quadrupled with the increase in overlap length. This contributed to the theory that there exists a maximum overlap length and is similar to the behaviour Neto [46] observed when using a brittle epoxy adhesive. Neto found that by using a more ductile adhesive it was possible to increase the maximum effective overlap length which allowed the full strength of the adhesive to be achieved.

The elongation to failure of the DCFP SLS adhesive joints was greatly influenced by the adhesive bond overlap. The relationship can be described as almost linear with the 20mm overlap length having an elongation to failure more than 3 times higher than that of the 5mm overlap length. Of concern was the fact the mean standard deviation more than doubled when the overlap was increased to 20mm which is assumed to be the result of the considerable increase in substrate failures that were recorded.

5.6.3 Effect of Bond Width

The bond width was the second most influential factor in defining the behaviour of the DCFP SLS adhesive joints. Three different specimen widths were tested to study this effect; they were, 12.5mm, 25mm and 50mm.

When the effect of bond width on the shear strength was studied it was found that the 25mm specimens had the highest mean shear strength and while the 12.5mm specimens exhibited similar mean strength, when the specimen width was increased to 50mm there was a 12% reduction in shear strength. This was most likely, similar to the longer overlap lengths, the result of the significant reduction in the occurrence of cohesive failure in the joints and the resulting increase in failures within the DCFP substrate.

The analysis of the adhesive joint failure modes identified the 25mm bond width as the most effective width to ensure cohesive failure, 47% of the samples demonstrated this failure mode. Meanwhile the 50mm specimen width was the least effective bond width for promoting cohesive failure with only 22% of the specimens failing in this manner probably the result of an increase in stress raisers or defects within the DCFP substrate.

The elongation to failure of the specimens increased with specimen bond width. However, the variability was minimised at the 25mm specimen width. The small specimen width had a standard deviation twice that of the 25mm specimen width. This will have been caused in part by the presence of adhesive failures in the testing.

From the experimental investigations the optimum bond width recommended in testing standards for conventional metallic adherends is also the most suitable for testing SLS joints manufactured using a DCFP substrate [90,91]. The optimum strength as well as frequency of cohesive failure occurred at the 25mm specimen width, indicating it is the most suitable bond width from the dimensions studied.

5.6.4 Effect of Substrate Thickness

Three different substrate thicknesses were used in the experimental investigations to identify the optimum bond settings for DCFP SLS adhesive joints. The thicknesses used were 2mm, 3mm and 6mm. The change in substrate thickness had a large influence on all of the substrate properties.

There was a negligible difference in shear strength for the 2mm and 3mm specimens; however, when the substrate thickness was increased to 6mm there was more than a 15% reduction in shear strength. This is contrary to the suggestion by Song [43] that the shear strength increases with substrate thickness. Although this may have been observed when testing metallic substrates by Pereira [42], it has been suggested by Kelly[1] that the increase in shear strength will only occur up to the point at which the shear stress near the substrate surface surpasses the inter-laminar strength of the composite substrate. At this point failure of the joint will occur. The limit suggested by Kelly [1] appears to have been reached for the DCFP substrate somewhere between the 3mm and 6mm substrate thickness. When the effect of substrate thickness on the

failure modes was studied, 51% of the 3mm specimens exhibited cohesive failure compared to 20% for the 6mm thick specimens.

The 2mm substrate thickness had the highest mean elongation to failure owing to the lower stiffness of the substrate allowing greater deformation of the adhesive joints. The resulting deformations increased the incidences of substrate and mixed failure modes and as a result the 2mm substrate thickness had the highest standard deviation of the specimens studied. The 3mm and 6mm had a mean standard deviation less than half that of the 2mm specimens with only a small reduction in the mean elongation to failure.

The analysis demonstrates that the 3mm substrate is the optimum thickness for testing SLS joints manufactured with DCFP substrates. This thickness optimised the occurrence of cohesive failures whilst maximizing the overall shear strength and maintaining the least variability for the thicknesses studied.

5.6.5 Effect of Tow Size

The choice of carbon fibre tow size was influential in defining the apparent shear strength of the DCFP SLS adhesive joints manufactured in this experimental investigation, whilst its influence on the elongation to failure was limited to defining the variability of the results. A choice of 3k, 6k and 24k tow size was used in the investigation.

Whilst the 3k tow size provided the highest observed shear strengths, the relationship between tow size and shear strength would appear to be non linear. The 6k filament count specimens demonstrated the lowest performing properties with regards to shear strength. When the 24k tow size was used, although the performance did not match that of the 3k specimens, it considerably outperformed those manufactured with a 6k tow size. The 3k tow size was expected to be the best performing filament count owing to the improved fibre coverage that is observed when using smaller filament counts; however, it was unexpected that the 24k tow size would outperform the 6k[87]. When the standard deviations of the specimens were analysed there was no apparent relationship between this and the choice of carbon fibre tow size.

The analysis of the failure modes with respect to the specimen tow size demonstrated that the use of the 3k tow size resulted in approximately 40% of the specimens failing cohesively. Although this is above the 33% of cohesive failures for both the 6k and 24k tow sizes, 60% of the specimens demonstrated undesirable failure characteristics. The lack of any distinctive trends with regards to failure mode would indicate that the tow size does not necessarily control the failure behaviour of DCFP SLS joints.

When the elongation to failure of the specimens' was examined, there was no statistically significant relationship identified with regards to the substrate tow size. The choice of filament count did influence the standard deviations of the specimens with the 3k tow size having the highest variability. The standard deviation nearly halved when the 6k tow size was used whilst for the 24k specimens the variability was approximately half way between the 3k and 6k tow sizes.

Overall, the investigation demonstrated that the biggest influence of the fibre tow size was on determining the shear strength of the SLS joints as well as the variability of the shear strength and elongation to failure of the samples. The results confirmed that the tow size, which previous research into the bulk substrate properties had identified as being influential in determining the homogeneity of the substrate, plays a role in defining both the eventual mechanical properties and their variability [73,87].

5.6.6 Effect of Fibre Length

The effect of fibre length on the performance of DCFP SLS adhesive joints related to defining the shear strength of the adhesive joints as well as the variability of the elongation to failure. To test the effect of fibre length, fibres measuring 30mm, 60mm and 90mm were used to manufacture the DCFP substrates.

There was an almost linear increase in shear strength as the fibre length was increased from 30mm to 90mm with the 90mm fibres providing the best performing substrates for DCFP adhesive joints. There was no statistically significant influence of fibre length on the standard deviations for the shear strength of the adhesive joints tested. When studying the failure modes of the specimens, the shorter fibre length had the most consistent cohesive failure mode. A total of 47% of the specimens manufactured with a 30mm fibre length demonstrated this desirable failure mode as supposed to the

24% observed for the 90mm fibre length. This would indicate that despite the longer fibre length having the highest shear strengths, the shorter lengths provided the highest incidence of cohesive failure.

There have been conflicting studies with regards to the effect of fibre length on the mechanical performance of discontinuous fibre reinforced composites. Harper [73,87] argues the shorter fibre lengths improve the mechanical performance of DCFP substrates by reducing the number of critical flaws and by improving the overall fibre coverage, whilst Feraboli [52] observed a linear increase in the ultimate tensile strength of a pre-preg based discontinuous carbon fibre composite laminate. It would appear that in the case of the mainly shear based load transfer observed in SLS adhesive joint, the increase in fibre length helps to improve the load carrying ability of the substrate; however, there exists a trade-off owing to the high incidence of substrate based failures.

With respect to the elongation to failure, there was no easily identifiable relationship between substrate fibre length and the resulting elongation to failure of the specimens. There was however a strong relationship for the standard deviation of the elongation to failure. The standard deviation of the 30mm fibre length specimens was more than twice that of the 60mm and 90mm specimens with very little difference observed for the 60mm and 90mm fibre length specimens.

From the experimental investigations it would appear that both the tow size and fibre length are more important in defining the overall variability of the DCFP SLS joints than the influence on the overall mechanical performance. Owing to the design of the experiment it has not been possible to study how these two factors interact.

5.6.7 Effect of Bond Gap

To study the effect of adhesive bond gap on the performance of DCFP SLS adhesive joints, three different bondline thicknesses were used. These were: 0.1mm, 0.2mm and 0.5mm. When the effect of adhesive bond gap was investigated, the results were deemed to be not statistically significant. As such, there were no observations made with regards to the optimum bond gap. Similarly when the failure modes were studied there were no clear relationships identified with a low frequency of cohesive failures

being observed across the three adhesive bond gaps studied. It is likely that the range in bondline thicknesses was too narrow and as such any of the trends identified from literature were not observed. It is also possible that the large range in results owing to the stochastic nature of the DCFP substrate masked any subtle changes in performance that were related to the adhesive bondline.

5.7 Conclusions

The aim of the investigation was to identify the optimum bond parameters for the effective bonding of DCFP SLS adhesive joints. The use of a novel substrate material requiring a large study covering aspects of both substrate properties and bondline dimensions meant a Taguchi method was adopted for the design of experiment. A set of recommendations for experimental investigations involving the adhesive bonding of DCFP was presented and discussed. The implications of the findings are analysed along with potential areas of interest that may require further attention.

Having carried out the experimental investigations and the subsequent statistical analysis the results that were compiled provided a good initial understanding of how varying the 6 different factors affected the shear strength and elongation to failure of the DCFP SLS joints. The factors that exerted the most influence on the shear strength of the DCFP SLS samples were the bond overlap, followed by the bond width, adherend thickness, fibre tow size, and fibre length. This indicated that if the adhesive joint was being optimised for the highest achievable shear strength, these are the factors that would be of most interest for further investigations.

When considering the elongation to failure of the specimens, the variation in the bond dimensions had a much larger effect than changing the adherend properties. The adhesive bonds' overlap and bond widths were the two factors that had the most influence over the elongation to failure of the DCFP SLS joints. This was followed by the substrate thickness. When the variability was analysed the substrate properties were of importance, indicating it is possible to change the tow size and fibre length in order to minimize the inter-specimen variability of results in the future.

Although it was not possible to carry out an in depth statistical analysis of the influence of changing the factor levels on the resulting failure modes, a good

understanding of what can be done to maximise the occurrence of cohesive failures has been achieved. With the exception of the adhesive bond thickness, the changing of factor levels excerpted a large change in the distribution of failure modes of the DCFP SLS adhesive joints.

By analysing the best settings for optimising the bond performance of DCFP SLS joints it has been possible to identify a single set of recommended parameters for any adhesive screening programs in the future as well as provide an insight into other areas that may be of interest for future experimental investigations.

The results of the experiments in this chapter led to further investigations into the role of fibre alignment on the joint strength of DCFP materials manufactured using aligned fibres. A review of literature yielded inconclusive information about the influence of fibre orientation on the joint behaviour of adhesively bonded discontinuous fibre based composite materials. As a result, a full factorial experiment was conducted for oriented DCFP at 3 different fibre orientations. These investigations are detailed in Chapter 6.

Chapter 6. Effect of Fibre Alignment on the SLS Joint Performance of Oriented DCFP Substrates

6.1 Introduction

The investigation into surface fibre orientation and stacking sequence in Chapter 4 highlighted the sensitivity of SLS joints to fibre orientation variations when using a composite substrate. The development of a method to create highly aligned substrates using the DCFP process allowed an investigation to be carried out to identify the optimum parameters for bonding this substrate by building on the knowledge gained from both Chapter 4 and Chapter 5.

The fibre orientation was modified using 2 different approaches. The first was testing substrates extracted at 0°, 45° and 90° to the primary fibre alignment axis; whilst, the second method used the height of the chopper gun as a variable. By increasing the tool centre point (TCP) the homogeneity of the preforms increases as the effect of the fibre orientation diminishes. The fibre architecture of the manufactured DCFP substrates was modified by changing both the fibre tow size and fibre length using 2 levels for each of these factors. This allowed a full factorial experiment to be designed.

The substrate thickness and the bond geometry were controlled, using the recommended settings from Chapter 5. The robot and chopper gun speeds, as well as the lay down strategies were maintained constant. This was done so as to control the number of factors known to affect substrate performance.

The aims of the experimental investigation were divided into two parts. These were: to determine how the fibre orientation can affect the joint performance of SLS

adhesive joints manufactured using an Oriented DCFP (ODCFP) substrate; and, to identify an optimal set of parameters for future screening programs using ODCFP.

6.2 Methodology

A general full factorial design of experiment was adopted focussing on 4 different factors known to exert a degree of influence over the bond performance of an oriented DCFP adhesive joint. The factors studied are intended to provide a set of design recommendations with regards to the optimisation of bonding to Oriented DCFP (ODCFP). The factors that were modified throughout the experiment were: fibre tow size, fibre length, chopper gun height and the fibre orientation. Although many other factors can also influence the bond strength of an adhesive joint, so as to reduce the overall size of the experimental investigation, a number of factors were controlled as previously described in Chapter 5.

Using Minitab 16 [88] a Design of Experiment (DoE) was carried out prior to the manufacture of the specimens. In total twelve different ODCFP preforms were manufactured to compare the shear strength and elongation to failure of the SLS adhesive joints manufactured from the substrates. The final substrate factor levels are presented in Table 25.

The tow sizes selected were chosen as they represent the two extremes of fibre bundle counts investigated using the DCFP manufacturing process detailed in Chapter 5. These were the 3K and 24K fibre tow sizes.

The two fibre lengths were limited by the feed roller design. Whilst the 30mm fibre length was the smallest fibre length that allowed for the effective manufacture of DCFP preforms, the 90mm fibre length was the upper limit of the fibre length available using current manufacturing methods. Above this, fibre length problems associated with uneven fibre coverage and manufacturing problems such as fibre bundles clogging in the chopper gun become an issue.

The chopper heights studied were chosen as an initial estimate of the crossover point at which the preforms would begin to behave like conventional randomly aligned DCFP substrates. The 0mm chopper gun height was the lowest possible setting that allowed for deposition of fibres onto the perforated tool without the chopper gun

coming into contact with the fibres that had already been deposited; whilst, the 75mm and 150mm settings were displacements that were programmed into the robot control software prior to preform manufacture.

Table 25 Design Matrix for analysis of ODCFP SLS adhesive joints

Plaque #	Tow Size(K)	Fibre Length (mm)	Chopper Height (mm)
1	3	30	0
2	3	90	0
3	24	90	0
4	24	30	0
5	24	30	75
6	24	90	75
7	3	90	75
8	3	30	75
9	3	30	150
10	24	30	150
11	24	90	150
12	3	90	150

6.2.1 Manufacture of ODCFP Substrate

The preforms were manufactured using the process described in Section 1.4 to produce preforms measuring 600mm x 400mm constructed with a 5%wt binder to facilitate the handling of the preforms prior to the infusion of the resin.

6.2.2 Resin Transfer Moulding

The resin transfer moulding was carried out using a stainless steel mould assembled using a 3mm picture frame. A CiJect One™ resin injection machine manufactured by Composite Integration was used to inject the preforms.

Release agent was applied to the moulding tool parts and allowed to thoroughly dry. The preform was then placed in the tool and loaded into a heated press with a 50ton clamping force. The press and tool were pre-heated to 50°C prior to injection whilst the resin was preheated to 80°C, to maintain a low viscosity. An initial injection pressure of 0.5bar ensured the preforms were fully wet out. A vacuum pump attached to the exhaust port via a catch pot provided assistance. The vacuum was removed once resin began to flow into the catch pot. When the resin ran clear in the exhaust port the

injection was stopped and the temperature of the press ramped to 120°C for 1 hour. The tool was cooled and the manufactured plaque removed. A post-cure of 75°C was carried out for 4 hours to ensure the plaques were fully cured.

6.2.3 Cutting of Substrate

The samples were extracted from the moulded preforms using a Diamant Boart diamond cut-off saw. To test the effect of fibre orientation on the SLS joint performance of the ODCFP substrates, specimens were extracted at 0°, 45° and 90° to the principal fibre orientation. In total 10 specimens measuring 100mm x 25mm x 3mm were extracted at each orientation. The dimensional tolerances were +/- 0.5mm for the specimen widths and +/-1mm for the specimen lengths. If a specimen fell outside of these dimensions it was deemed flawed and another specimen extracted.

6.2.4 Assembly of Single Lap Shear Joints

Following the extraction of the substrate, the specimens were cleaned in water to remove the majority of the contaminants that arose from the cutting process. The bond area was abraded using 500 grit abrasive papers followed by a ScotchBrite 7496 pad soaked in acetone. This ensured any remaining mould release, cutting fluid and loose debris were removed from the bond area. Finally, the specimens were wiped with a clean cloth soaked in acetone before the specimens were allowed to dry prior to bonding.

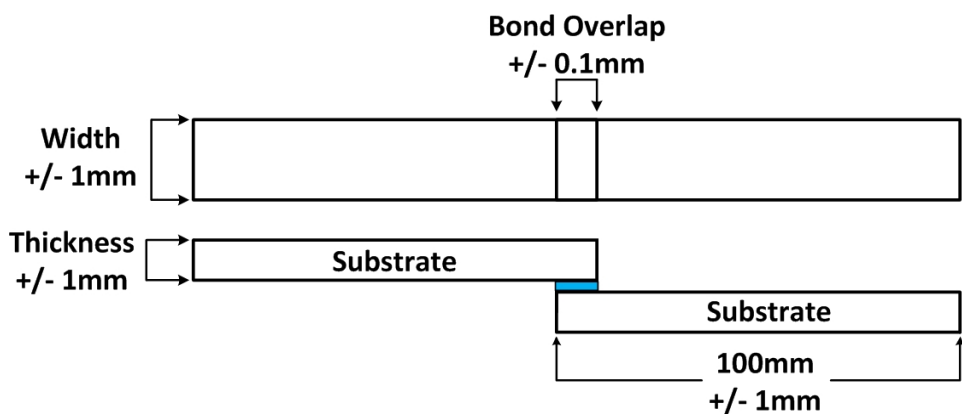


Figure 34 SLS Joint Configuration

The specimens (Figure 34) were then mounted into the bonding jig and a bead of adhesive was dispensed onto the substrate. The bond area dimensions used in the

study were: 25mm x 10mm x 0.2mm. The adhesive was spread across the bond area and 2 wire spacers were placed within the bond. The bond was then closed and the bond overlap dimensions checked. Once the desired overlap length was achieved any excess adhesive was removed using a sterile blade. This ensured a constant spew geometry as the adhesive joints had no fillet radii. The bonded joint was secured with bull clips and allowed to cure at room temperature for a 24 hour period before being cured using the AMLC cure cycle described in Appendix B.

6.2.5 Mechanical Testing

The tensile testing was carried out using an Instron mechanical testing machine. The test speed was set to 2mm/min, as a means of ensuring the capture of good images intended for use with Digital Image Correlation (DIC). The load was measured using a 50kN load cell whilst the extension was measured from the cross-head displacement. Although the cross-head displacement is not the most accurate form of measuring strain and displacement, owing to the SLS joint configuration it was not possible to use a conventional extensometer effectively.

In order to minimize the peel forces present in SLS tests spacers were used in the jaw faces, this ensured that the load path passed centrally through the adhesive bondline. A 96mm gauge length was set to maintain a constant distance between the two jaw faces. A schematic of the tensile test setup is included in Figure 35.

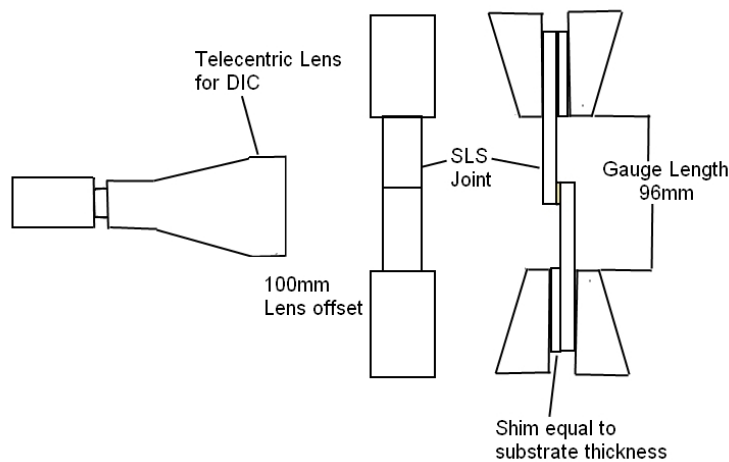


Figure 35 Schematic of SLS mechanical testing setup

6.3 Test Results for ODCFP SLS Samples

The results were input into Minitab 16 statistical analysis software and a full factorial analysis was run with model terms up to the 4th order being analysed. The main findings from the analysis of variance (ANOVA) for the shear strength and elongation to failure of the ODCFP adhesive samples are presented along with a study of the adhesive joint failure locations.

The analysis of the experimental results gives the relative importance of the variables included in the investigation. The main effects plots of the investigation along with all of the major interactions were studied in order to identify the best combination of factors for optimizing joint performance. The interaction plots were produced in order to gain an understanding of the complex relationship the different factor levels have on the overall performance of the ODCFP SLS adhesive joints. An interaction is considered to potentially exist when the 2 line plots are non parallel. The more the plots deviate from one another, the stronger the interaction is assumed to be.

The means at each level for the factors investigated are presented in Table 26. This provides an insight into the optimum level settings for the factors investigated. The data is presented graphically in main effects plots and interaction plots for the shear strength and elongation to failure. By studying the main effects plots it is easy to deduce whether the factors investigated represent a statistically significant variation.

Table 26 Mean response values for level settings

	Tensile Strength (MPa)	Standard Error (95%CI)	Elongation to Failure (mm)	Standard Error (95%CI)
Tow Size				
3K	21.72	0.34	1.46	0.03
24K	18.01	0.37	1.26	0.03
Fibre Length				
30 mm	21.09	0.36	1.43	0.03
90 mm	18.64	0.35	1.29	0.03
Chopper Height				
0 mm	18.83	0.44	1.32	0.04
75 mm	19.72	0.43	1.42	0.04
150 mm	21.05	0.44	1.34	0.04
Fibre Orientation				
0°	27.64	0.41	1.51	0.04
45°	18.78	0.45	1.41	0.04
90°	13.17	0.44	1.16	0.04

The study of the failure modes of the ODCFP SLS adhesive joints was separated into 4 sections. The failure modes were separated according to the substrate fibre orientation. Then only using the 0° aligned specimens the influence of tow size, fibre length and chopper gun height on failure mode are discussed. It is important to note that throughout the entire experimental investigation there were no cases of adhesive failure recorded. This indicated that the adhesive used and current ODCFP substrate offers a good compatibility and the surface preparation technique offers a good solution. The main challenge remains finding a way to constrain the failure to within the adhesive joint.

6.3.1 Stress-Elongation Plots

The stress-elongation plots of four different plaques are presented in Figure 36. They were chosen to demonstrate the effect that changes in both the fibre orientation and fibre architecture can have on the joint performance of ODCFP SLS joints. The specimens that were chosen are all from the 0mm chopper gun height.

Plaque 1 was manufactured using a 3k tow size and a 30mm fibre length, it is plotted in the three shades of red according to the fibre orientation. Plaque 2 is plotted in blue

and was manufactured using the 3k tow size and 90mm fibre length. Plaque 3, in green, made used of the 24k tow size and 30mm fibre length configuration whilst Plaque 4, in purple, used the 24k tow size and 90mm fibre length.

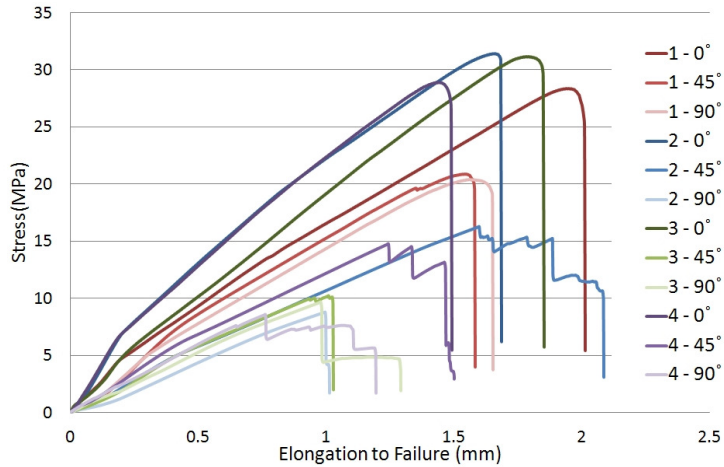


Figure 36 Examples of Stress-Elongation Plots of ODCFP SLS joints

Without the use of statistical analysis it is hard to derive any conclusive observations; however, a number of general trends were apparent from studying the graph. In general, the plaques aligned in the 0° orientation demonstrated little difference in strength with the elongation to failure being more affected by the fibre architecture. The 45° fibre orientation had the largest spread in performance with approximately a 10MPa difference in strength and 1mm in elongation to failure. For the 90° fibre orientation the joints failed at approximately 10MPa and 1mm extension with the exception of Plaque 1 which considerably outperformed the other plaques.

When studying the Plaques considering the effect of fibre length and tow size there appears to be little difference when the fibres were aligned at 0°. However, when the specimens became oriented off-axis the specimens all demonstrated different behaviour. There is a definite ability to tailor the bond performance of a discontinuous composite material structure by changing the properties of the underlying substrate. This is discussed in greater detail through the use of statistical analysis. Main effects plots describing the effect each factor has on the bond performance are detailed as well as the failure behaviour of the joints as the factors were varied.

6.3.2 Effect of Fibre Orientation

Unsurprisingly, the most influential factor on adhesive joint performance was the substrate fibre orientation. This was the first factor that was studied with the distribution of the failure modes at the 3 fibre orientations presented in Table 27 and the effect of the different fibre orientations presented in Figure 37.

Table 27 Distribution of Failure modes (%) for the three fibre orientations

	0°	45°	90°
Adhesive	-	-	-
Cohesive	63%	7%	2%
Substrate	7%	50%	80%
Mixed	30%	43%	18%

At the 0° fibre orientation 63% of the specimens exhibited a cohesive failure mode; with a further 30% exhibiting a mixed mode of failure. This generally was a combination of cohesive failure and failure of the ODCFP substrate matrix close to the joint surface. The final 7% of the failures were substrate failures. In this situation a combination of the substrate matrix and fibre bundles were removed prior to any yielding of the adhesive. With additional work to toughen the composite matrix the occurrence of mixed failures may be further reduced.

With both of the off-axis fibre orientations, the substrate failure was dominant highlighting the poor performance achieved when using these orientations in a bonded application. Having determined that the best way to ensure cohesive failure of the adhesive joint was to orient the fibres parallel to the load path, the specimens tested at 0° were isolated by the specimen tow size, fibre length and chopper gun height to try and gain a better understanding of how these factors influence the joint failure. These failure modes are presented in the relevant sections.

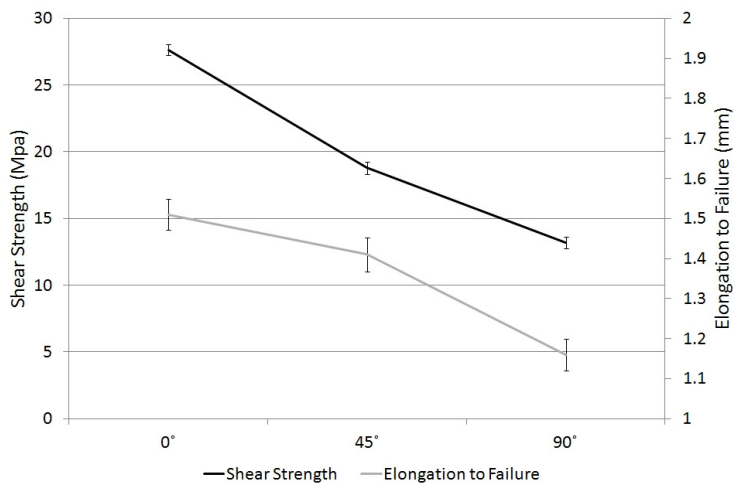


Figure 37 Effect of Fibre Orientation on performance of ODCFP SLS joints with 95% CI error bars

The plot of the mechanical performance in Figure 37 emphasizes the influence fibre orientation has on the behaviour of the SLS adhesive joints. When studying the shear strength of the SLS joints, the samples with a 0° fibre orientation had a mean shear strength of 27.64 MPa, on average 32% higher than those specimens with a 45° fibre orientation and 52% higher than those with 90° fibre orientations. With the elongation to failure of the samples, the average extension to failure for the 0° aligned samples was 1.51mm. At the 45° fibre orientation there was a 7% decrease and at the 90° fibre orientation, a 23% reduction in mean elongation to failure.

6.3.3 Effect Chopper Gun Height

The change in induced alignment achieved by varying the chopper gun height was investigated separately. The distribution of the failure modes separated by the chopper height used to manufacture the DCFP preforms is presented in Table 28 whilst the effect on the mechanical performance is plotted in Figure 38.

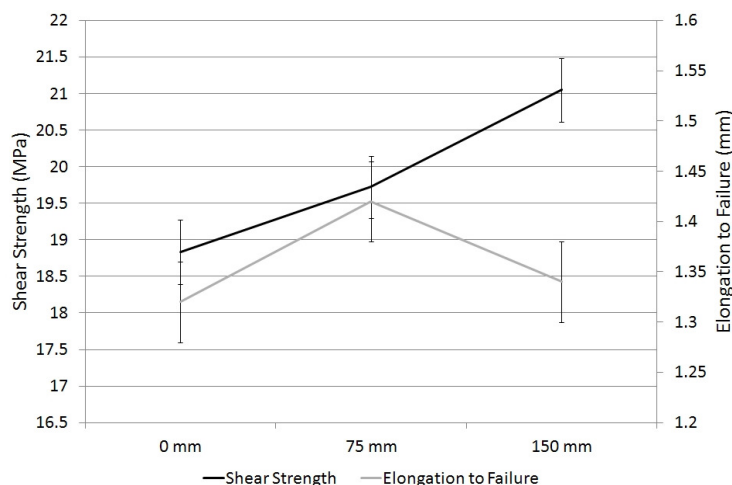
The role of the chopper gun height as a means of influencing the failure mode of the adhesive joints tested is not entirely clear. At the 0mm chopper gun height 70% of the failures occurred as cohesive fracture and similarly at the 150mm chopper gun height 75% of the failures were recorded as cohesive whilst at the 75mm height only 45% of the specimens demonstrated this failure. This may indicate that the chopper height does not exert as much influence on the failure mode as the tow size and fibre length, or may signal that the range of the experimental investigation was too limited.

Table 28 Distribution of Failure modes (%) for the variation in chopper gun height

	0mm	75mm	150mm
Adhesive	-	-	-
Cohesive	70%	45%	75%
Substrate	5%	-	15%
Mixed	25%	55%	10%

By studying the means of the shear strength of the ODCFP SLS samples tested at different chopper heights, a 150mm chopper gun height resulted in the highest mean shear strength with an average of 21.05 MPa. This is approximately 10% higher than the 0mm chopper gun height and 6% higher than the 75mm chopper gun height.

The effect of chopper height on the elongation to failure of the SLS joints was identified as exerting no significant influence over the elongation to failure of the samples. Studying the mean values, the elongation to failure was highest at the 75mm chopper gun height with an average elongation to failure of 1.42mm. This was approximately 7% higher than for the 0mm chopper gun height and 5.6% higher than for the 150mm chopper gun height; however studying the error bars at a 95% CI this is very close to being within the limits of the errors.

**Figure 38 Effect of Chopper Gun Height on mechanical performance of ODCFP SLS adhesive joints with 95% CI error bars**

6.3.4 Effect of Tow Size

The effect of tow size on the failure mode and mechanical performance of the ODCFP SLS adhesive joints is detailed in Table 29 and Figure 39 respectively. This large difference in the failure behaviour of the SLS specimens indicates the 3k tow size

greatly enhances the performance of Oriented DCFP SLS joints when compared to the larger tow sizes. Although there was some evidence of this in Chapter 5, the difference was not significant enough to be confirmed. The cause is most likely the result of more even fibre coverage across the substrate surface.

Table 29 Distribution of Failure modes (%) for variation in tow size

	3K	24K
Adhesive	-	-
Cohesive	83%	43%
Substrate	3%	10%
Mixed	14%	47%

When analysing the plot for the fibre tow size, the 3k carbon fibre tows outperformed the 24k tow size for all of the measures of performance. With an average of 21.72 MPa for the shear strength, this equated to an average shear strength gain of 17% compared to using the 24k tow size. When considering the average elongation to failure of the ODCFP SLS samples, the average elongation for the 3k samples was 1.46mm, some 14% higher than that of the specimens manufactured with a 24k tow size.

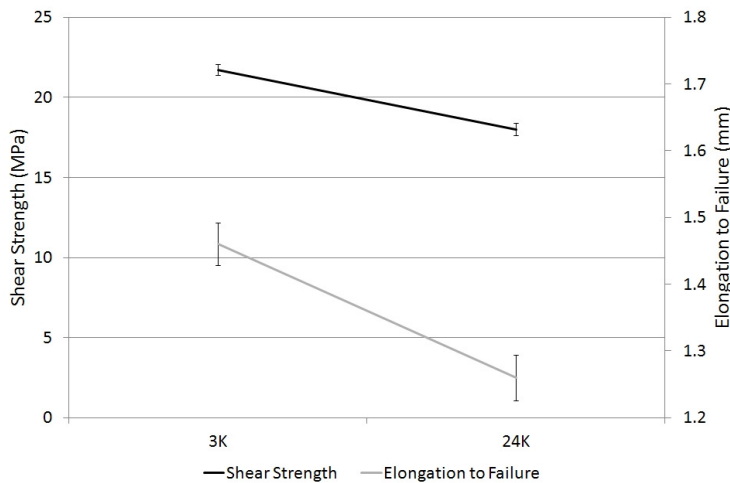


Figure 39 Effect of Tow Size on mechanical performance of ODCFP SLS adhesive joints with 95% CI error bars

6.3.5 Effect of Fibre Length

The effect of fibre length has been difficult to understand owing to the conflicting results in literature [52,73,84]. The distribution of failure modes is detailed in Table 30 whilst the mechanical performance is detailed in Figure 40.

When the effect of the substrate fibre length was compared, the 90mm fibre length demonstrated failure characteristics that were much more favourable to those of the 30mm fibre lengths as shown in Table 30.

Table 30 Distribution of Failure modes (%) for the variation in fibre length

	30mm	90mm
Adhesive	-	-
Cohesive	43%	83%
Substrate	13%	-
Mixed	43%	17%

The average shear strength for the 30mm fibre length was 21.09 MPa, which is approximately 12% higher than for those samples tested with a 90mm fibre length. It is important to note that the interaction between fibre length and fibre orientation was not considered in this analysis but is discussed in Section 6.3.6.

The effect of changing the fibre length indicated that the elongation to failure of the 30mm fibre length specimens failed at an average of 1.43mm, on average 10% higher for the 30mm fibre length compared to the 90mm fibre length.

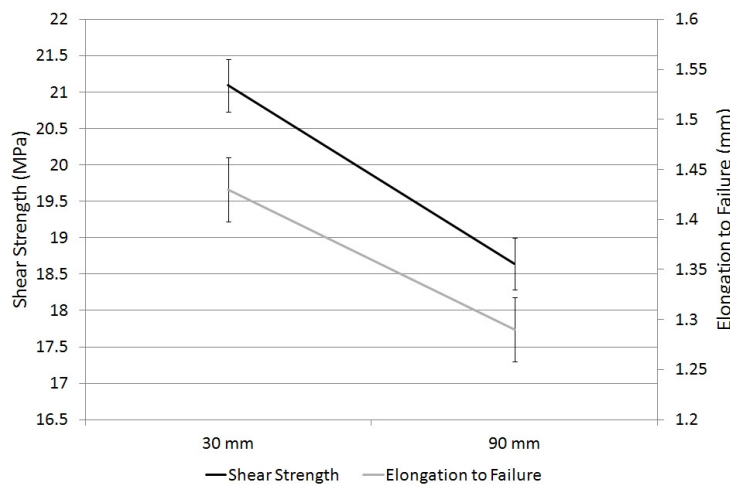


Figure 40 Effect of Fibre Length on mechanical performance of ODCFP SLS adhesive joints with 95% CI error bars

6.3.6 Interactions of Note

The tables of the analysis of variance presented in Appendix F identified three 2-way interactions that were of interest to the investigation. These were related to the fibre orientation interacting with: the tow size, fibre length and chopper height. There appears to be other significant interactions relating to the tow size and fibre length and

the tow size and chopper height; however, owing to the large influence the fibre orientation has on the results, these interactions cannot be accurately studied in isolation. The higher order 3-way and 4-way interactions are also deemed to be statistically significant, highlighting the complex behaviour of the ODCFP substrate fibre architecture when used in bonded applications.

- **Tow Size and Fibre Orientation**

Studying the interaction of the tow size against the fibre orientation in Figure 41 the influence of tow size only becomes apparent at the off axis fibre orientations. When the fibres are aligned at 0° to the load path there is a negligible difference in joint performance; however, when the loading is off axis the 3K tow size considerably outperforms the larger 24K tow size. There appears to be very little change in elongation to failure of the 3k tow size samples tested at the 0° and 45° fibre orientations; however, for the 24k tow size there was a constant decrease in elongation to failure as the fibre orientation changed from 0° to 90° indicating the sensitivity of tow size on the ODCFP SLS joints' elongation to failure.

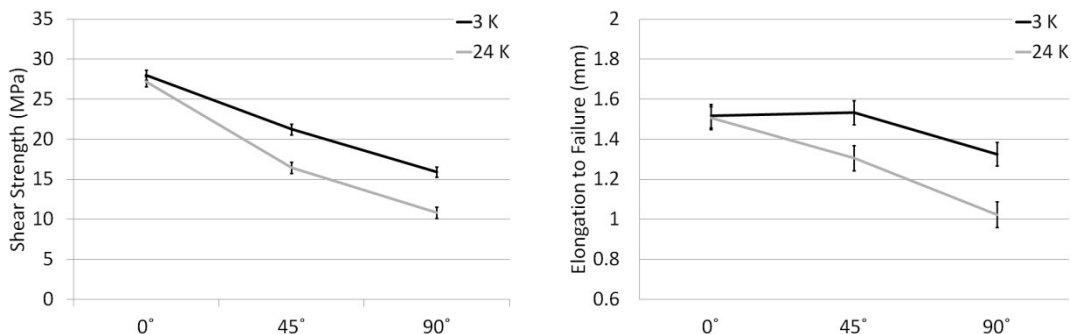


Figure 41 Interaction Plots of Tow Size vs. Fibre Orientation of ODCFP SLS joints

Fibre Length and Fibre Orientation

The interaction between the fibre length and fibre orientation is one that would be expected as the longer fibre lengths should retain the intended fibre orientation better, and thereby improve on-axis load transfer. This interaction was only considered to be statistically significant for the shear strength of the ODCFP SLS joints. The interaction plot of the shear strength in Figure 42 shows the 90mm fibre length produced the highest strength ODCFP SLS joints at the 0° fibre orientation; however, the difference is not very large. When the fibre orientation was aligned off-axis, the

30mm fibres considerably outperformed those specimens with a 90mm fibre length. This is most likely the result of the shorter fibre lengths creating a more homogeneous laminate. This is highlighted when the fibre orientations move off-axis.

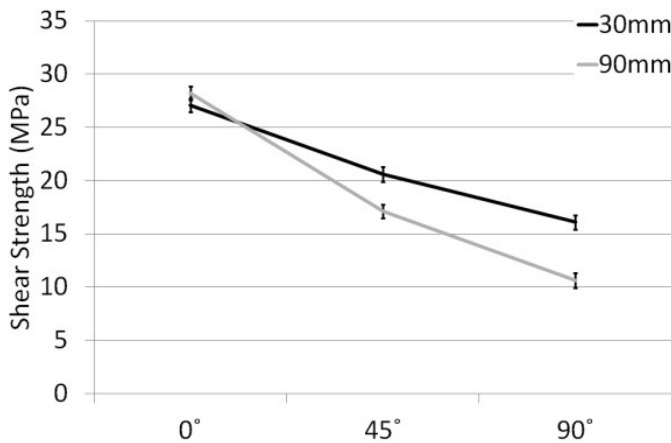


Figure 42 Interaction Plots of Fibre Length vs. Fibre Orientation of ODCFP SLS joints

Chopper Height and Fibre Orientation

The final interaction that was studied was the chopper height and fibre orientation. This was of interest as it was related to the 2 different methods of controlling the fibre orientation. It was anticipated that whilst the 0mm chopper gun height would provide the best performance at the 0° fibre orientation, the 2 higher chopper heights would outperform the 0mm chopper height when the fibres were loaded off-axis. Studying the interactions in Figure 43, this has been confirmed.

At the 0° fibre orientation the substrates with a 0mm chopper gun height were the best performing samples for both of the measures of performance; however, as the fibre orientation moved to 45° and 90° the larger chopper heights provided better performance. For the shear strength, the 75mm chopper gun height only outperformed the 0mm chopper height at the 90° fibre orientation. The 0mm chopper gun height meanwhile demonstrated a constant decrease in elongation to failure with the changing fibre orientation; whilst, for the 75mm and 150mm chopper gun heights the decrease in elongation to failure only became apparent at the 90° fibre orientation. This indicated that the level of heterogeneity in the preforms increases with increasing chopper gun height, as would be anticipated.

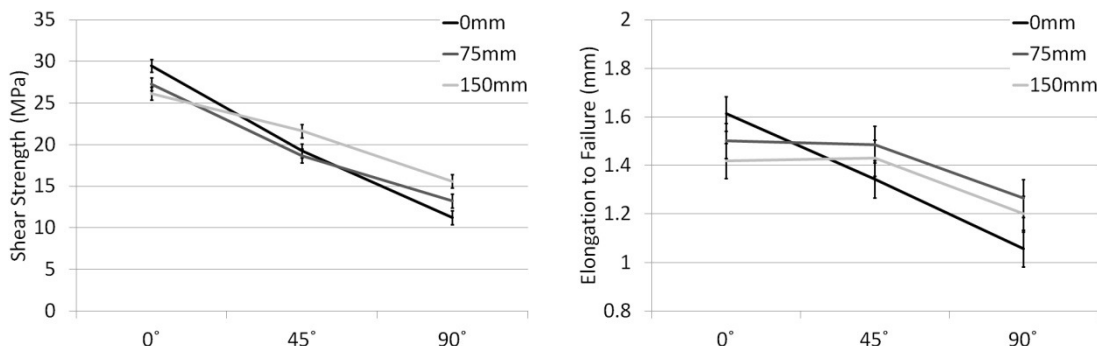


Figure 43 Interaction Plots of Chopper Gun Height vs. Fibre Orientation for ODCFP SLS joints

6.4 Optimal Level Settings for ODCFP SLS adhesive joints

Two different substrate rankings are proposed for use in future adhesive screening programs. The first is a ranking of the most effective substrate fibre properties for testing the ODCFP plaques disregarding the fibre direction at the bond surface and the joint failure characteristics. The second was the best substrate for maximizing the performance of the ODCFP substrate for bonding, taking into account the substrate performance as well as the failure modes and orientation of the substrates. The tabulated results are included in Appendix F. The recommended level settings are presented in Table 31.

The 3k tow size is recommended for the two different preforms, whilst the differences in the fibre length and chopper gun height come about as a result of changing the principal fibre orientation and considerations made with regards to the desirable failure modes. For the optimal oriented preform it is anticipated that this material would be used with the fibres aligned along the principal load path whilst the general preform disregards fibre orientation.

The shorter fibre length will not be as highly aligned as the longer fibre length and as such, a more random fibre arrangement is produced making the 30mm fibre length favourable for manufacturing the optimised general preform. The 90mm fibre lengths would appear to behave more like a conventional uni-directional composite laminate and as such are better when the load path is aligned along the principal fibre direction.

With regards to the settings of the chopper gun height, when the specimens are to be tested at the 0° fibre orientation the best recommended setting is at 0mm. This is because this chopper height produces the most highly aligned fibres and as such will

improve the load carrying capability of the fibres. Conversely, as the chopper gun height is raised, the process becomes inherently more heterogeneous. As such, when the fibres are aligned away from the principal fibre direction, the more random distribution of fibre orientations helps to increase the overall load bearing capability of the composite adhesive joints.

Table 31 Recommended Level settings for optimal manufacture of ODCFP SLS adhesive joints

	Tow Size	Fibre Length	Chopper Gun Height
Optimal General Preform	3k	30mm	150mm
Optimal Oriented Preform	3k	90mm	0mm

6.5 Discussion

The statistical analysis of the results from the ODCFP SLS study identified the interactions between the different factors as being statistically significant up until the 4th order. This highlights the fact that bonding to ODCFP substrates is a complex system where joint performance is not defined by just a number of separate factors but also the interactions that occur between a number of different factors. Even so, to gain a better understanding of the joint behaviour each of the factors was studied to determine which factors exert the most influence on the joint behaviour and which levels provide the best ODCFP SLS adhesive joint performance. The fibre orientation, tow size, fibre length and the level of induced alignment are all discussed separately along with observations about some of the more influential interactions.

6.5.1 Interaction Effects

The full factorial design of experiment allowed a more detailed examination of the effect of varying the fibre architecture in an ODCFP adhesive joint. The smaller number of levels and factors was a compromise made to allow for more complex interactions between the factors to be studied, unlike the Taguchi design used previously. When studying the interactions, the effect of fibre orientation combined with: tow size, fibre length and chopper gun height all displayed characteristics indicating a strong interaction between the factors.

The fibre architecture (including tow size and fibre length) interaction with the fibre orientation was interesting as this demonstrated that the choice of tow size and fibre

length only become significant if the loading of the adhesive joint is away from the principal fibre direction. At the 0° fibre orientation the difference in performance for the different levels is almost negligible; however, when considering the tow size, the 3k tow size improved the off-axis performance considerably. This is most likely the result of improved fibre coverage across the substrate as a result of the increase in fibre misalignment. A similar effect was also observed for the fibre length with the 90mm fibre length being the best choice at the 0° alignment; however, off-axis the 30mm length considerably improved performance.

When studying the chopper gun height in isolation the effect of varying the chopper gun height was not immediately apparent. Initial assumptions were that the range at which this was studied was too limited but when combined with the fibre orientation the differences were clear. By increasing the chopper gun height the heterogeneity of the fibres in the substrate was increased, thereby improving the performance of the adhesive joints when the load path was aligned off the principal fibre direction. This was something that had been anticipated but which had not been observed when studying these factors in isolation.

The 3-way and 4-way interactions were also deemed to be statistically significant; highlighting the complex behaviour of adhesive joints manufactured using an oriented discontinuous composite.

6.5.2 Fibre Orientation

The fibre orientation was the factor that had the most influence over the ODCFP SLS joint performance. The poor off-axis structural integrity of the substrate meant that the strength and elongation to failure were severely degraded when the load path was aligned away from the 0° fibre alignment.

Studying the modes of failure of the adhesive specimens, the importance of fibre orientation was emphasized. The aim of studying the modes of failure was to determine which factors maximised the occurrence of cohesive failures. With regards to fibre orientation this was achieved using the 0° fibre alignment. With the fibres aligned at 0°, 63% of the specimens demonstrated cohesive failure in comparison to less than 7% and 2% for the 45° and 90° fibre orientations respectively. This

highlights that the most efficient load transfer across the bondline occurs between the fibres aligned along the load path with the efficiency reducing the further off-axis the fibres become.

Analysis of the results with the fibre orientation isolated demonstrated that the performance was maximised with a 0° fibre orientation. The shear strength decreased by 32% for the 45° fibre orientation and 52% for those specimens aligned at 90° to the load path. Meanwhile the elongation to failure observed decreases; however not as significant as for the shear strength. At the 0° fibre orientation elongation was measured at 1.51mm whilst for the 45° fibre orientation there was a 6.6% decrease and at the 90° fibre orientation there was a 23.2% reduction in elongation to failure.

6.5.3 Induced Alignment

By increasing the chopper gun height the levels of alignment of the ODCFP plaques are reduced thereby making the substrate inherently more stochastic in nature. The effect of this was not immediately clear; however, when coupled with the fibre orientation interaction the effect was significant.

Studying the statistical analysis for the chopper gun height in isolation, the 150mm chopper gun height had the highest mean shear strength. At this chopper height the shear strength increased by approximately 11% compared to the 0mm height. For the elongation to failure the 75mm chopper gun height produced the highest means, some 5% higher than the 0mm chopper gun height; however, there was a high degree of variability within these results obscuring any significant trends. However, without taking into account the interaction between the induced alignment and the chopper gun height the results can be misleading.

At the 0° fibre alignment the 0mm chopper height produced the best performing substrates. This was because using a low chopper height allowed the substrate to be more highly aligned thereby increasing the efficient load transfer across the bondline. It was when the substrate fibre orientation was changed to 45° or 90° that the increase in chopper height became beneficial. The increased heterogeneity that results from having a less aligned plaque allowed for increased joint integrity.

Having analysed the results for the influence of induced alignment, a reduced degree of alignment has been shown to improve the properties of adhesively bonded ODCFP SLS joints. Disregarding the original sample fibre orientation, the 150mm chopper gun height maximised the shear strength of the specimens, whilst the 75mm maximised the response of the elongation to failure. Owing to the complex loading of structural DCFP parts, a degree of fibre tow misalignment may serve to increase the overall performance of bonded ODCFP components.

6.5.4 Tow Size

The effect of tow size was studied to determine the influence on the performance of ODCFP SLS adhesive joints. Studying the failure modes of the samples aligned at 0° to the load path the 3k tow size had an 83% occurrence of cohesive failure, compared to the 43% of the 24k specimens. This large disparity demonstrates that whilst there are mechanical performance benefits of using the smaller tow sizes, the failure characteristics are also heavily influenced by the fibre architecture of the substrate. This is most likely related to the increased fibre coverage that occurs when using a smaller tow size.

The statistical analysis indicated that the 3k tow size considerably outperforms the 24k tow size regardless of any interaction effects. The mean shear strength of the 3k tow size SLS samples was 21.72MPa whilst for the 24k there was a 16% reduction in shear strength. Similarly, the elongation to failure was some 12% higher for the 3k tow size. This indicates that increasing the tow size to 24k is detrimental to the performance of ODCFP SLS adhesive joints. The benefits of using a 24k are financial, and as such, the economic benefits versus the loss in performance would have to be assessed independently from this study.

6.5.5 Fibre Length

Two different fibre lengths were investigated when the ODCFP study was conducted. The lengths used were the high and low values of the fibre lengths studied in Chapter 5. To understand how the fibre length affects the performance of ODCFP SLS adhesive joints the results were studied in isolation with the interaction effects then considered independently.

The fibre length was observed to exert a large influence on the failure behaviour of the SLS joints. When the failure modes were studied at the 0° fibre orientation; perhaps unsurprisingly the 90mm fibre length outperforms the 30mm length. It is assumed this is the result of there being a lower probability of fibre ends being present within the bondline area.

When studying the statistical analysis there is a significant difference between the means of the 30mm and 90mm fibre length ODCFP SLS adhesive samples. The 30mm fibre length had a mean shear strength of 21.09 MPa. This reduced by 12% when the fibre length was increased to 90mm. For the elongation to failure the decrease as a result of the increased fibre length equated to an 11% reduction. The results from the study indicate that a 30mm fibre length produces the best overall performance of ODCFP SLS adhesive specimens. However, considering the interaction between fibre length and fibre orientation, when the fibres were aligned along the load path the 90mm fibre length performed better than the samples manufactured with a 30mm fibre length; in all other circumstances the shorter length was better.

6.6 Conclusions

This initial investigation into the factors affecting adhesive joint behaviour when using an aligned discontinuous composite substrate provides a foundation for more advanced investigations into specific phenomena observed in this experiment. Suggestions of future investigations are discussed in Section 7.3. The study of the influence of fibre alignment on the performance of ODCFP SLS adhesive joints was able to identify a strong relationship between the performance of the ODCFP SLS samples and the fibre architecture of the substrate. The effect of fibre orientation, induced alignment, tow size and fibre length were considered using a full factorial design of experiment,

By checking the confidence levels of the statistical analysis, it was determined that the factors influencing the overall joint behaviour all interacted with each other highlighting the complexity of the adhesive system produced when bonding DCFP substrates. A set of optimised parameters were determined for the substrate to allow further adhesive characterisation trials to be carried out in the future.

Chapter 6 – Effect of Fibre Alignment on the SLS Joint Performance of ODCFP

An ODCFP preform manufactured using a 3k tow size, 30mm fibre length and a 150mm chopper gun height would produce the optimal substrate for maximising the performance of ODCFP joints regardless of the fibre orientation. In practice the fibres should be aligned parallel to the predominant load path so as to gain optimal performance; in this case a 3k substrate using a 90mm fibre length and 0mm chopper height should be used. In this way the strength of the ODCFP joints can be maximised.

Overall, the experimental investigation yielded important information on the behaviour of ODCFP SLS adhesive joints subjected to tensile testing. An optimal substrate design was identified, whilst areas of interest for future investigations were identified.

Chapter 7. Discussion and Conclusions

This chapter reviews the work that has been presented in the main body of this thesis. It attempts to tie together the results of the bonding studies using DCFP, Non-Crimp Fabric (NCF) and ODCFP substrates. The wider implications of the research are then discussed along with recommendations for the design, implementation and execution of future experiments and the potential modifications that could be made to the DCFP preforming process so as to improve the bond performance of these materials.

7.1 General Discussion

The findings and detailed discussions for each of the experimental investigations have been detailed in the corresponding chapters whilst there is a brief summary discussing the main findings in this section. The data for the shear strength and elongation to failure were amalgamated and are presented in Figure 44. The elongation to failure was normalised using the bond overlap length. Each of the substrates investigated was studied and a rough estimate of their corresponding performance envelope was created. For the NCF and ODCFP substrates, linear fits were performed at the 0°, 45° and 90° fibre orientations to compare the performance of a conventional laminar composite to the ODCFP material.

The testing carried out using a DCFP substrate provided the results with the broadest range in joint performance. These results were achieved through a combination of dimensional changes in the bond area as well as to the fibre architecture of the material. The DCFP adhesive joint results ranged in shear strength from 15 MPa up to just below 33 MPa with the elongation to failure ranging from 4.35mm down to 0.53mm. This highlighted just how sensitive adhesive joint performance can be to changes in the substrate fibre architecture and the bond area of an SLS adhesive joint.

The unpredictable nature of the adhesive joints was further highlighted when the failure modes of the specimens were studied. Considering the entire test population,

Chapter 7 – Discussion and Conclusions

only 36% of the joints exhibited a cohesive failure mode whilst 21% failed in the substrate and 41% exhibited a combination of substrate and cohesive failure. The remaining 3% were adhesive failures, the result of imperfections caused during manufacture of the specimens. The challenge of ensuring good joint strengths is highlighted by the fact that the majority of DCFP specimens had a lower mean shear strength than those of the NCF specimens with a 45° surface fibre orientation. This emphasizes the need to engineer the bond surfaces to promote better structural integrity.

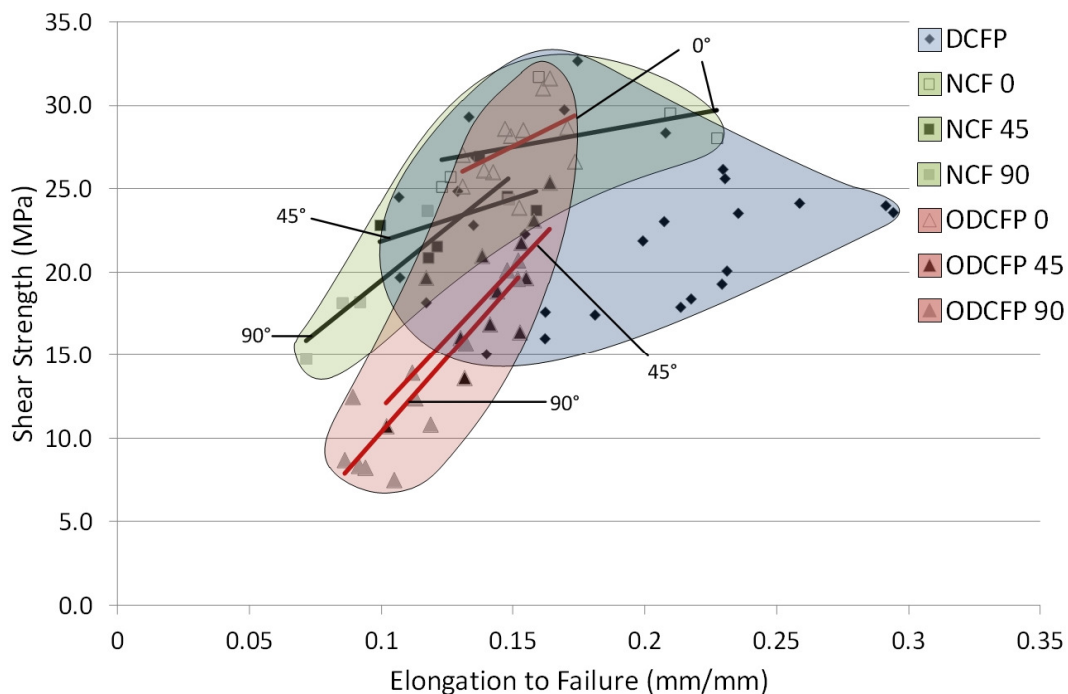


Figure 44 Estimated Performance Envelope of the SLS adhesive joints studied in this body of work.

Non-Crimp Fabric (NCF) substrates manufactured using a quasi-isotropic stacking sequence were tested to develop an understanding of how the surface fibre orientation and stacking sequence of the composite substrate affected the joint performance of adhesive joints. The bond dimensions were kept constant to ensure the only changes were the fibre orientations of the different layers. Overall the strength and elongation to failure increased the closer the substrate fibres got to being aligned along the load path.

At the 90° surface fibre orientation the shear strength ranged from 15 MPa to 25 MPa and the elongation to failure ranged from 0.7mm to approx 1.5mm. The testing

Chapter 7 – Discussion and Conclusions

demonstrated that it was possible to nearly double both the shear strength and elongation to failure of the lap shear joints by modifying the layers below the surface of the substrate. For the 45° surface fibre orientation, the mean performance was slightly higher than for the 90° orientation with a more narrow performance envelope ranging from 21 MPa to 27 MPa for the shear strength and 1mm to 1.6mm for the elongation to failure. There appears to be a transition point at approximately 22 MPa shear strength and 1.2 mm elongation to failure where the 90° surface orientation performs better than the 45° fibre orientation. The study of failure modes highlighted that whilst there was a significant improvement in performance, only 10% of the failures were cohesive failures with 77% manifesting substrate failure characteristics and 13% being a mixed failure mode. This indicated that at this fibre orientation the substrate integrity was the most limiting factor.

As would be anticipated, the 0° fibre orientation was the best regardless of where it was positioned in the laminate. At the surface the shear strength of the SLS joints was no lower than 25 MPa and increased up to 32 MPa with the elongation to failure ranging from 1.2mm to 2.5mm. The most significant development was with regards to the failure characteristics of the joints. In total, 64% of the specimens demonstrated a cohesive failure which highlights the fact that the fibre orientation exerts a large influence on failure mode.

The final section of the thesis dealt with the highly oriented DCFP substrate material. An experimental study was carried out to optimise the aligned substrate for use in bonded applications. The results of the testing had the narrowest range in performance with respect to the elongation to failure of the samples whilst also having the largest spread in strength, ranging from 7.5 MPa up to 32 MPa. At its optimal design configuration the ODCFP had almost the same peak performance as that of the highest strength NCF laminate.

The 90° fibre orientation was the lowest performing with a range from 7.5 MPa up to approx 20MPa depending on the chosen fibre architecture and chopper gun height configuration. The elongation to failure ranged from 0.75mm to 1.6 mm. Studying the failure modes only 2% were cohesive with 80% being substrate failures and the remaining 18% being a mixed failure. For the SLS samples tested at 45°, the shear

strength ranged from 11MPa to 25MPa and 1mm to 1.6mm for the elongation to failure. The substrate integrity was again the limiting factor with only 7% cohesive failures.

The 0° fibre orientation was the best performing substrate configuration with shear strength ranging from approximately 24MPa to 32MPa and the elongation to failure ranging from 1.3mm to 1.7mm with 63% of the specimens demonstrating cohesive failure. The performance is comparable with the NCF results demonstrating that the ODCFP process has the potential to compete with conventional laminar composites in bonded applications.

7.2 Major Conclusions

The work undertaken set out to investigate how the fibre architecture of a discontinuous carbon fibre reinforced composite affects the joint behaviour of these adhesively bonded components. An extensive set of testing using single-lap shear specimen geometry has allowed for both the specimen geometry and fibre architecture of a bonded fibre reinforced substrate to be examined. The specimen geometry was studied to validate previously established test methods using a novel substrate as the modification of aspects of the fibre architecture has not been previously studied for bonded SLS joints. An understanding of how this affected joint performance and variability was obtained which will allow for more effective control of adhesive bonding techniques when using a discontinuous fibre reinforced composite substrate in the future. The major findings of the research are detailed below.

- Initial Adhesive Screening

The characterisation of the 5 candidate adhesives resulted in the BM 2098 adhesive being selected for the substrate trials contained within this thesis. This adhesive was chosen as it offered the best overall performance with very little surface treatment required to ensure a good degree of adhesion. Additionally, the adhesive supplier was able to reformulate the adhesive to improve the thermal resistance of the adhesive. Having completed the investigations there are a number of issues which have been identified that may be of interest to future investigations. To aid with future adhesive

characterisation work using a discontinuous carbon fibre substrate, an adhesive specification was written for use by Aston Martin Lagonda.

- Influence of Specimen Geometry

The characterisation of an SLS adhesive joint manufactured using a DCFP substrate involved understanding how changing the joint geometry could affect the overall joint performance. As the DCFP substrate had not previously been used in a bonded application, it was important to validate whether conventional bonding approaches could be used to carry out adhesive characterisation trials. The effects of the bond overlap, bond width, bond gap and substrate thickness were all tested to develop an optimised specimen. This is shown in Table 32.

Table 32 Optimised Specimen Geometry for DCFP Single Lap Shear Joints

	Bond Overlap	Bond Width	Bond Gap	Substrate Thickness
DCFP	10mm	25mm	0.2mm	3mm

- Effect of Overlap

The adhesive bond overlap had the biggest influence on defining the joint strength of the SLS joint; although, there exists an upper limit at which the overlap length does not continue to increase joint strength. This has been alluded to in previous literature [43,44,46] but at longer overlap lengths than for the limit observed when using DCFP. The maximum overlap length lies somewhere between 10mm and 20mm. It may be possible to increase the effective joint overlap length; however, this would most likely involve changing both the adhesive and further modifying the substrate properties.

- Effect of Bond Width

Although the bond width is not significant when considering a bonded structure, this was investigated to identify an optimum specimen dimension for future adhesive characterisation studies. The specimen bond width is generally maintained constant throughout adhesive characterisation studies. For the DCFP specimens the 25mm specimen width was recommended as this optimised the joint performance, minimised variability as well as maximising the occurrence of the cohesive failure mode. This validates the specimen widths traditionally recommended in both the ISO EN 1465

standard as well as the AMES 014 Standard [91] produced for characterising adhesives at AML.

- **Effect of Bond Gap**

The effect of the adhesive bond gap was not considered to be statistically significant in the range tested (0.1mm-0.5mm). There was very little change in either the joint performance or the failure modes that were studied regardless of the bondline thickness. This demonstrates that with regards to the bond gap, the behaviour of a bonded DCFP joint is similar to those manufactured with more traditional substrates. The bondline thickness will have an impact on the overall vehicle stiffness so increasing the bondline thickness beyond a limit is not desirable. By increasing the bondline thickness the torsional rigidity of a vehicle body would be reduced which could affect both the handling of the vehicle as well as the NVH [5].

- **Effect of Substrate Thickness**

The effect of substrate thickness was caused by a combination of factors, primarily, the increase in the strength and stiffness of the substrate and the improved fibre coverage.

There was a negligible difference in shear strength when the substrate thickness was increased from 2mm to 3mm; however, when the thickness was increased to 6mm there was a 15% reduction in shear strength. This confirmed the presence of an upper limit whereupon the stresses at the adhesive-substrate interface surpassed the interlaminar strength of the substrate. This limit had been suggested however; when Song [43] investigated the effect of increasing substrate thickness using conventional laminar composites this was not observed up to 7.62mm. For the DCFP substrate the optimum substrate thickness was 3mm which indicates the DCFP substrate has a lower limit compared to using a conventional laminar composite.

- **Influence of Fibre Architecture**

The emphasis of this work has been on understanding the influence of fibre architecture on the performance of adhesively bonded composite substrates. Over the studies, 3 different fibre architectures were identified to help optimise the

Chapter 7 – Discussion and Conclusions

performance of the discontinuous carbon fibre preforms. These are detailed in Table 33 for the random DCFP substrate, ODCFP substrate loaded in numerous directions and ODCFP to be tested along the principal fibre orientation. The main findings with regards to the tow size, fibre length and chopper gun height are described.

Table 33 Recommended Fibre Architectures for Optimised Joining of DCFP Substrates

	Tow Size	Fibre Length	Chopper Gun Height
DCF	3k	90mm	-
ODCFP General Preform	3k	30mm	150mm
ODCFP Oriented Preform	3k	90mm	0mm

- Effect of Tow Size

The tow size was a factor that has a large influence over the performance of the bonded SLS joints. The 3k tow size fibres were consistently the best performing fibres regardless of the substrate being manufactured. This confirmed what was expected from the literature; however, this has not been previously validated when bonding a discontinuous carbon fibre substrate.

When the random DCFP substrate was tested the shear strength was the most influenced by the tow size along with the variability of the elongation to failure of the adhesive joints. With regards to the failure modes, approximately 40% were cohesive when a 3k tow size was used and 33% for the 6k and 24k tow sizes.

By using the ODCFP oriented substrates it was possible to better understand the effect of tow size as the orientation of the fibres reduced the stochastic nature of the material. The 3k tow size demonstrated a gain of 17% in shear strength and 14% in elongation to failure compared to using a 24k tow size when disregarding the different fibre orientations. Using the ODCFP manufactured with a 3k tow size and the fibres aligned at 0°, over 80% of specimens demonstrated cohesive failure characteristics, compared to 43% for the 24k tow size. This emphasizes how it is possible to control DCFP adhesive joints' failure characteristics by changing the fibre bundle filament count.

- Effect of Fibre Length

For the DCFP substrate the most noticeable increase in performance was the shear strength. There was no large change in the mean elongation to failure of the specimens; however, the variability reduced by more than half when the fibre length was increased from 30mm to 60mm. There was a smaller reduction when the fibre length increased to 90mm indicating the presence of an upper limit to increasing the fibre length. When considering the failure modes of the specimens there was a reduction in cohesive failures with increasing fibre length.

The ODCFP substrate allowed for much more effective control of the performance and failure modes of the specimens. When aligned at 0°, the SLS samples observed an 83% occurrence of cohesive failure modes when a 90mm fibre length was used. This was compared to a 43% cohesive failure rate for the 30mm fibre length. This changed when the off-fibre-axis specimens were tested. In this case the 30mm fibre length had the highest mean shear strength and elongation to failure.

7.3 Future Work

The experimental investigations have developed an understanding of the behaviour of single lap-shear adhesive joints manufactured using a discontinuous composite substrate. By investigating both random and highly oriented fibre architectures it has been possible to develop a set of recommendations as well as developments for enhancing the bond strength of these materials. Two proposed substrate designs are proposed that would require validation work along with recommendations for investigations that would complement the current research.

From the initial outset of this project the focus of the research had been on using a 2-part epoxy adhesive as a substitute to the adhesive currently in use. In retrospect this may have been an oversight as the adhesive in its current configuration does not achieve its full potential. Previous research [25,30,46] has demonstrated the potential of using alternate adhesives, such as a modified Polyurethane, that despite the lower strength and stiffness are more effective at distributing stress peaks at the substrate surface. The effect this would have on joint stiffness would have to be assessed, as in production the vehicle handling as well as the Noise, Vibration and Harshness (NVH)

Chapter 7 – Discussion and Conclusions

characteristics could be affected; however, it may allow for better joint integrity and more consistent joint failures.

The first proposed substrate design uses a DCFP Sandwich concept which would incorporate outer skins manufactured using the highly oriented DCFP process manufactured with a 0mm chopper gun height with the core manufactured using a random DCFP fibre architecture deposited from a higher chopper gun height. Using the NCF study for reference, the optimal skin thickness should be in the region of ~1mm. The fibre architecture would most likely be optimised using a 3k tow size and a 90mm fibre length. A schematic of the proposed adhesive joint is included in Figure 45.

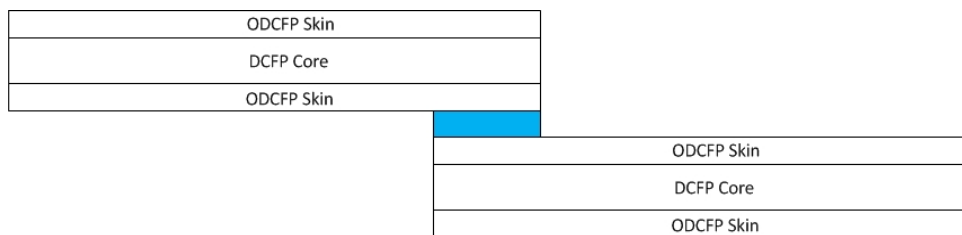


Figure 45 A proposed design for enhancing DCFP joint strength by depositing Oriented Fibres on the outer surface of the substrate material to create a 'sandwich' construction

A more complex approach could use a selectively oriented area of the substrate surface, close to the bond area. This would have to be studied to determine the best means of achieving good fibre coverage. In an industrial setting this technique would allow for there to be selectively oriented reinforcement at the bondline without necessarily influencing the overall substrate properties. A schematic of this proposal is shown in Figure 46.

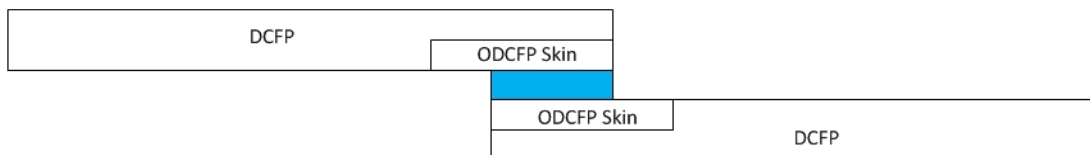


Figure 46 A proposed design for enhancing DCFP joint strength by selectively reinforcing the adhesive joint bond area with highly oriented fibres

The current discontinuous composite substrates have been limited by the low inter-laminar strength of the material. Research into modifying the polymer matrix to improve the toughness of the resin system or implementing a new resin system may help in increasing the inter-laminar strength of the DCFP substrates, thereby improving both the performance and failure characteristics of the adhesive joints. This

Chapter 7 – Discussion and Conclusions

has been successfully achieved by Feraboli using a chopped carbon fibre prepreg to reduce the variability and increase the shear transfer between the fibres and matrix of the material [92].

Owing to the hesitance to implement entirely adhesive solutions into structural applications, a method of hybrid bonding could provide an intermediate solution. Research has shown discontinuous carbon fibre/epoxy composite materials to be relatively notch insensitive [24]. These findings mean it may be possible to use a hybrid bonded joint with some form of mechanical fastening without compromising the substrate strength. These could provided additional confidence in the fixturing techniques as well as facilitate the handling of the composite bonded structures during assembly and cure.

Finally, an understanding of the dynamic behaviour of adhesively bonded DCFP substrates will require investigation. This would study both the impact performance and life-cycle testing to validate the adhesive system as a whole.

References

- ¹ Kelly, Gordon,*Joining of Carbon Fibre Reinforced Plastics for Automotive Applications*. PhD in Department of Aeronautical and Vehicle Engineering at Royal Institute of Technology Sweden, 2004.
- ² Lutsey, Nicholas,*Review of technical literature and trends related to automobile mass-reduction technology* for Technical Report for Institute of Transportation Studies, University of California, Davis, 2010.
- ³ Jacob, George C., Starbuck, J. Michael, Fellers, John F., and Simunovic, Srdan,*Effect of Fiber Volume Fraction, Fiber Length and Fiber Tow Size on the Energy Absorption of Chopped Carbon Fiber-Polymer Composites* for Oakridge National Laboratory & US Department of Energy, 2005.
- ⁴ Turner, Thomas A,*The Effects of Processing Variables on the Energy Absorption of Composite Crash Structures*. PhD in Division of Materials, Mechanics and Structures,at University of Nottingham, 2004.
- ⁵ Pujol, Sylvain,*Optimisation of Adhesive Bonding for Aluminium Automotive Structures*. PhD in Department of Mechanical, Materials and Manufacturing Engineering,at University of Nottingham, 2009.
- ⁶ Mortimer, John, *Adhesive bonding of car body parts by industrial robot*. Industrial Robot: An International Journal 31 (5), 423 (2004).
- ⁷ Manson, Jan-Anders, *HIVOCOMP: large-scale use of carbon composites in the automotive industry*. Reinforced Plastics 56 (6), 44 (2012).
- ⁸ *Technologies for Carbon fibre reinforced modular Automotive Body Structures (TECABS)*, Available at http://www.mtm.kuleuven.be/Onderzoek/Composites/projects/finished_projects/tecabs20publish20presentation.pdf, (2004).
- ⁹ Miel, Rhoda, *Group advances concept of composite car floor*, Available at <http://www.plasticsnews.com/toolbox/printer.html?id=24396>, (2012).
- ¹⁰ Brandt, M.R. and Reeve, S.R.,*Directed Fibre Preform Case Studies in Composites 2001 Convention and Trade Show* (Composite Fabricators Association, Tampa, FL, USA, 2001).
- ¹¹ Rondeau, Roger, Reeve, Scott, and Bond, Gary,*The Effect of Tows and Filament Groups on the Properties of Discontinuous Tow Fiber Composites*.

References

- Presented at the Proceedings of 44th International SAMPE Symposium and Exhibition, Long Beach, CA., 1999.
- ¹² Liakus, J., Wang, B., Cipra, R., and Siegmund, T., *Processing-microstructure-property predictions for short fiber reinforced composite structures based on a spray deposition process*. Composite Structures 61 (4), 363 (2003).
- ¹³ Johnson, Nancy et al., *Composite-Intensive Body Structure Development for Focal Project 3* for Department of Energy, 2003.
- ¹⁴ Dahl, J. S. et al., *Development of Manufacturing Methods for Fiber Preforms* for Department of Energy, 2003.
- ¹⁵ Warren, David, Chavka, Norman, Carpenter, Joseph, and Sklad, Philip, *P4 Carbon Fiber Preform Development* for Department of Energy, 2000; Chavka, Norman, Warren, David, Carpenter, Joseph, and Sklad, Philip, *Development of Manufacturing Methods for Fiber Preforms* for Department of Energy, 2001.
- ¹⁶ Dahl, Jeffrey, DeBolt, Michael, and Steenkamer, David, *Processing and Performance of Chopped Glass Fiber Reinforced RTM Composites*. Composites in Manufacturing (2004); Chavka, Norman, Dahl, J. S., and Kleven, Eric, *F3P Fiber Preforming for the Aston Martin V12 Vanquish* in *SAMPE Conference Europe* (Paris, France, 2001); Dahl, J. S., Smith, Glen, DeVries, James, and Houston, Daniel, *The Influence of Fiber Tow Size on the Performance of Chopped Carbon Fiber Reinforced Composites* in *37th ISTC Conference* (Seattle, USA, 2005).
- ¹⁷ Harper, L. T. et al., *Characterisation of random carbon fibre composites from a directed fibre preforming process: Analysis of microstructural parameters*. Composites Part A: Applied Science and Manufacturing 37 (11), 2136 (2006).
- ¹⁸ Stahl, Jan, *Development of a Methodology for Joining Technology Selection based on Cost Information in the Preliminary Automotive Body-in-White Product Development Process*. PhD in School Of Applied Sciences, at Cranfield University, 2008.
- ¹⁹ Bell, Samantha, *Structural adhesives deliver lighter structures with performance and costs benefits*. Reinforced Plastics 56 (1), 34 (2012).
- ²⁰ Davis, Maxwell and Bond, David, *Principles and practices of adhesive bonded structural joints and repairs*. International Journal of Adhesion and Adhesives 19 (2-3), 91 (1999).
- ²¹ Keller, Thomas and Vallee, Till, *Adhesively bonded lap joints from pultruded GFRP profiles. Part I: stress-strain analysis and failure modes*. Composites Part B: Engineering 36 (4), 331 (2005).
- ²² Baldan, A, *Adhesively-bonded joints in metallic alloys, polymers and composite materials: Mechanical and environmental durability performance* Journal of Materials Science 39 (15), 4729 (2004).

References

- ²³ Hart-Smith, L. J.,*Single-Lap Joints for NASA*, 1974.
- ²⁴ Qian, C., Harper, L. T., Turner, T. A., and Warrior, N. A., *Notched behaviour of discontinuous carbon fibre composites: Comparison with quasi-isotropic non-crimp fabric*. Composites Part A: Applied Science and Manufacturing 42 (3), 293 (2011).
- ²⁵ Banea, M D and da Silva, Lucas F. M., *Adhesively bonded joints in composite materials: an overview*. Proceedings of the Institution of Mechanical Engineers, Part L: Journal of Materials: Design and Applications 223 (1/2009) (2009).
- ²⁶ da Silva, Lucas F. M. and Öchsner, Andreas, *Special topic issue on structural adhesive joints*. International Journal of Adhesion and Adhesives 28 (8), 391 (2008).
- ²⁷ Duncan, Bruce and Dean, Greg, *Measurements and models for design with modern adhesives*. International Journal of Adhesion and Adhesives 23 (2), 141 (2003).
- ²⁸ Daggett, Susan, *A guide to selection of methacrylate, urethane and epoxy adhesives* in *Composites Technology* (Composites World 2004).
- ²⁹ Tierney, J. J. et al., *Joining of Composites* in *Comprehensive Composite Materials* (Pergamon, Oxford, 2000), pp. 1029.
- ³⁰ Sauer, Jochem, *High Performance adhesives for composite bonding*. Presented at the Joining Technologies for FRP Composite Materials, Chesterfield, UK 2012.
- ³¹ Boylan, Sarah and Castro, Jose M., *Effect of reinforcement type and length on physical properties, surface quality, and cycle time for sheet molding compound (SMC) compression molded parts*. Journal of Applied Polymer Science 90 (9), 2557 (2003).
- ³² Prolongo, Silvia G., del Rosario, Gilberto, and Ureña, Alejandro, *Comparative study on the adhesive properties of different epoxy resins*. International Journal of Adhesion and Adhesives 26 (3), 125 (2006).
- ³³ Taib, Abdelaziz A. et al., *Bonded joints with composite adherends. Part I. Effect of specimen configuration, adhesive thickness, spew fillet and adherend stiffness on fracture*. International Journal of Adhesion and Adhesives 26 (4), 226 (2006).
- ³⁴ Chalkley, Peter and Rose, Francis, *Stress analysis of double-strap bonded joints using a variational method*. International Journal of Adhesion and Adhesives 21 (3), 241 (2001).
- ³⁵ da Silva, Lucas F. M., das Neves, Paulo J. C., Adams, R. D., and Spelt, J. K., *Analytical models of adhesively bonded joints - Part I: Literature survey*. International Journal of Adhesion and Adhesives 29 (3), 319 (2009).

References

- ³⁶ da Silva, Lucas F. M., Lima, Ricardo F. T., Teixeira, Rui M. S., and Puga, A., *Closed-form solutions for adhesively bonded joints* (Universidade do Porto, Porto).
- ³⁷ W R Broughton, L E Crocker, J M Urquhart, *Strength of Adhesive Joints: A Parametric Study* for National Physical Laboratory, 2001.
- ³⁸ Tsai, M. Y., Oplinger, D. W., and Morton, J., *Improved theoretical solutions for adhesive lap joints*. International Journal of Solids and Structures 35 (12), 1163 (1998).
- ³⁹ Magalhaes, A. G., de Moura, M. F. S. F., and Goncalves, J. P. M., *Evaluation of stress concentration effects in single-lap bonded joints of laminate composite materials*. International Journal of Adhesion and Adhesives 25 (4), 313 (2005).
- ⁴⁰ Mortensen, F. and Thomsen, O. T., *Analysis of adhesive bonded joints: a unified approach*. Composites Science and Technology 62 (7-8), 1011 (2002).
- ⁴¹ da Silva, Lucas F. M. et al., *Effect of material, geometry, surface treatment and environment on the shear strength of single lap joints*. International Journal of Adhesion and Adhesives 29 (6), 621 (2009).
- ⁴² Pereira, A. M., Ferreira, J. M., Antunes, F. V., and Bartolo, P. J., *Analysis of manufacturing parameters on the shear strength of aluminium adhesive single-lap joints*. Journal of Materials Processing Technology 210 (4), 610 (2010).
- ⁴³ Song, Min-Gyu et al., *Effect of manufacturing methods on the shear strength of composite single-lap bonded joints*. Composite Structures In Press, Corrected Proof (2009).
- ⁴⁴ Ferreira, J. A. M., Reis, P. N., Costa, J. D. M., and Richardson, M. O. W., *Fatigue behaviour of composite adhesive lap joints*. Composites Science and Technology 62 (10-11), 1373 (2002).
- ⁴⁵ de Goeij, W. C., van Tooren, M. J. L., and Beukers, A., *Composite adhesive joints under cyclic loading*. Materials & Design 20 (5), 213 (1999).
- ⁴⁶ Neto, J. A. B. P., Campilho, R. D. S. G., and da Silva, L. F. M., *Parametric study of adhesive joints with composites*. International Journal of Adhesion and Adhesives 37 (0), 96 (2012).
- ⁴⁷ Lee, H. K., Pyo, S. H., and Kim, B. R., *On joint strengths, peel stresses and failure modes in adhesively bonded double-strap and supported single-lap GFRP joints*. Composite Structures 87 (1), 44 (2009).
- ⁴⁸ Grant, L. D. R., Adams, R. D., and da Silva, Lucas F. M., *Experimental and numerical analysis of single-lap joints for the automotive industry*. International Journal of Adhesion and Adhesives 29 (4), 405 (2009).

References

- ⁴⁹ Davies, P. et al., *Influence of adhesive bond line thickness on joint strength*. International Journal of Adhesion and Adhesives In Press, Accepted Manuscript (2009).
- ⁵⁰ Arenas, Jose M., Narbon, Julian J., and Alia, Cristina, *Optimum adhesive thickness in structural adhesives joints using statistical techniques based on Weibull distribution*. International Journal of Adhesion and Adhesives 30 (3), 160 (2010).
- ⁵¹ Cognard, J. Y., Davies, P., Sohier, L., and Créac'hcadec, R., *A study of the non-linear behaviour of adhesively-bonded composite assemblies*. Composite Structures 76 (1-2), 34 (2006).
- ⁵² Feraboli, Paolo et al., *Characterization of Prepreg-Based Discontinuous Carbon Fiber/Epoxy Systems*. Journal of Reinforced Plastics and Composites 28 (10), 1191 (2009).
- ⁵³ Hart-Smith, L. J., *Surface Preparations for Ensuring that the Glue Will Stick in Bonded Composite Structures* in *Handbook of Composites*, edited by S.T. Peters (Chapman & Hall, London, 1998), pp. 667.
- ⁵⁴ Ebnesajjad, Sina ed., *Adhesives Technology Handbook*, Second Edition ed. (William Andrew Inc., Norwich, N.Y., 2008).
- ⁵⁵ Comyn, John, *Adhesion Science*. (The Royal Society of Chemistry, Cambridge, 1997).
- ⁵⁶ Adams, R. D., *Structural Adhesive Joints in Engineering*. (Chapman & Hall, London, 1997).
- ⁵⁷ Pethrick, R. A., Anthony, Kelly, and Carl, Zweben, *Bond Inspection in Composite Structures* in *Comprehensive Composite Materials* (Pergamon, Oxford, 2000), pp. 359.
- ⁵⁸ Packham, D. E., *Surface energy, surface topography and adhesion*. International Journal of Adhesion and Adhesives 23 (6), 437 (2003).
- ⁵⁹ Shanahan, M. E. R. and Bourgès-Monnier, C., *Effects of plasma treatment on the adhesion of an epoxy composite*. International Journal of Adhesion and Adhesives 16 (2), 129 (1996).
- ⁶⁰ Sorrentino, L. and Carrino, L., *2024 aluminium alloy wettability and superficial cleaning improvement by air cold plasma treatment*. Journal of Materials Processing Technology 209 (3), 1400 (2009).
- ⁶¹ Rhee, K. Y., Lee, S. G., Choi, N. S., and Park, S. J., *Treatment of CFRP by IAR method and its effect on the fracture behavior of adhesive bonded CFRP/aluminum composites*. Materials Science and Engineering A 357 (1-2), 270 (2003).

References

- ⁶² Belingardi, Giovanni, Goglio, Luca, and Tarditi, Andrea, *Investigating the effect of spew and chamfer size on the stresses in metal/plastics adhesive joints.* International Journal of Adhesion and Adhesives 22 (4), 273 (2002).
- ⁶³ Wang, Z. Y. et al., *An investigation on strain/stress distribution around the overlap end of laminated composite single-lap joints.* Composite Structures 89 (4), 589 (2009).
- ⁶⁴ Lang, T. P. and Mallick, P. K., *Effect of spew geometry on stresses in single lap adhesive joints.* International Journal of Adhesion and Adhesives 18 (3), 167 (1998).
- ⁶⁵ Technomic Publishing, Company, Materials Sciences, Corporation, American Society for, Testing, and Materials, *The Composite Materials Handbook-Mil 17: Guidelines for Characterization of Structural Materials.* (Technomic Pub.Company, 1999).
- ⁶⁶ Zhang, Ye, Vassilopoulos, Anastasios P., and Keller, Thomas, *Effects of low and high temperatures on tensile behavior of adhesively-bonded GFRP joints.* Composite Structures 92 (7), 1631 (2009).
- ⁶⁷ da Silva, Lucas F. M. and Adams, R. D., *Joint strength predictions for adhesive joints to be used over a wide temperature range.* International Journal of Adhesion and Adhesives 27 (5), 362 (2007).
- ⁶⁸ Hart-Smith, L. J., *Adhesive-Bonded Double-Lap Joints* for Langley Research Center, 1973.
- ⁶⁹ Ashcroft, I. A. et al., *The effect of environment on the fatigue of bonded composite joints. Part 1: testing and fractography.* Composites Part A: Applied Science and Manufacturing 32 (1), 45 (2001).
- ⁷⁰ Heslehurst, R. B., *Observations in the structural response of adhesive bondline defects.* International Journal of Adhesion and Adhesives 19 (2-3), 133 (1999).
- ⁷¹ de Moura, M. F. S. F., Daniaud, R., and Magalhaes, A. G., *Simulation of mechanical behaviour of composite bonded joints containing strip defects.* International Journal of Adhesion and Adhesives 26 (6), 464 (2006).
- ⁷² Feraboli, Paolo et al., *Defect and damage analysis of advanced discontinuous carbon/epoxy composite materials.* Composites Part A: Applied Science and Manufacturing 41 (7), 888 (2010).
- ⁷³ Harper, L. T., *Discontinuous Carbon Fibre Composites for Automotive Applications.* PhD in Polymer Composites Group, at University of Nottingham, 2006.
- ⁷⁴ Mathews, F.L. and Tester, T.T., *The influence of stacking sequence on the strength of bonded CFRP single lap joints.* International Journal of Adhesion and Adhesives 5 (1) (1985).

References

- 75 Mortensen, Flemming and Thybo Thomsen, Ole, *Coupling effects in adhesive bonded joints*. Composite Structures 56 (2), 165 (2002).
- 76 Meneghetti, Giovanni, Quaresimin, Marino, and Ricotta, Mauro, *Influence of the interface ply orientation on the fatigue behaviour of bonded joints in composite materials*. International Journal of Fatigue In Press, Corrected Proof (2009).
- 77 Godara, A. and Raabe, D., *Influence of fiber orientation on global mechanical behavior and mesoscale strain localization in a short glass-fiber-reinforced epoxy polymer composite during tensile deformation investigated using digital image correlation*. Composites Science and Technology 67 (11-12), 2417 (2007).
- 78 Boss, J. N., Ganesh, V. K., and Lim, C. T., *Modulus grading versus geometrical grading of composite adherends in single-lap bonded joints*. Composite Structures 62 (1), 113 (2003).
- 79 Reeve, Scott, Rondeau, Roger, Bond, Gary, and Tervet, Fred *Mechanical Property Translation in Oriented, Discontinuous Carbon Fiber Composites*. Presented at the SAMPE International Symposium, 2000.
- 80 Dahl, Jeffrey and Hoseck, Thomas, *Investigation into the Light Transmission Characteristics of Random Chopped Carbon Fiber Preforms*. Presented at the 48th International SAMPE Symposium, Long Beach, CA, 2003.
- 81 Dahl, J. S., Warren, David, Carpenter, Joseph, and Sklad, Philip, *Development of Manufacturing Methods for Fiber Preforms* for, 2004.
- 82 Dockum, John and Schell, Philip L., *Fiber Directed Preform Reinforcement: Factors that May Influence Mechanical Properties in Liquid Composite Molding*. Presented at the 6th Annual ASM/ESD Advanced Composites Conference, Detroit, Michigan, 1990; Schell, Philip L. and DiMario, J.M., *Fiber Directed Preform Reinforcement: Factors that may Influence Mechanical Properties in Liquid Composite Molding* in *46th Annual Conference, Composites Institute* (The Society of the Plastics Industry, 1991).
- 83 Harper, L. T., Turner, T. A., Martin, J.R.B., and Warrior, N. A., *Fiber Alignment in directed carbon fiber preforms - A feasibility study*. Journal of Composite Materials 43 (1), 57 (2009).
- 84 Pan, Ning, Zhao, Shumin, and Hua, Tao, *Relationship between scale effect and structure levels in fibrous structures*. Polymer Composites 21 (2), 187 (2000).
- 85 Hitchen, S. A., Ogin, S. L., and Smith, P. A., *Effect of fibre length on fatigue of short carbon fibre/epoxy composite*. Composites 26 (4), 303 (1995).
- 86 Jander, M, *Industrial RTM - New Developments in Molding and Preforming Technologies* Presented at the Advanced Composite Materials: New Developments and Applications Detroit, Michigan, USA, 1991.

References

- ⁸⁷ Harper, L. T., Turner, T. A., Warrior, N. A., and Rudd, C. D., *Characterisation of random carbon fibre composites from a directed fibre preforming process: The effect of fibre length*. Composites Part A: Applied Science and Manufacturing 37 (11), 1863 (2006).
- ⁸⁸ *Minitab 16 Statistical Software* (Minitab Inc., State College, PA, 2010).
- ⁸⁹ Harper, L. T., Turner, T. A., Warrior, N. A., and Rudd, C. D., *Characterisation of random carbon fibre composites from a directed fibre preforming process: The effect of tow filamentisation*. Composites Part A: Applied Science and Manufacturing 38 (3), 755 (2007).
- ⁹⁰ *Adhesives-Determination of tensile lap-shear strength of rigid-to-rigid bonded assemblies* in *BS EN 1465:1995*, edited by BSi Group (1995); *Standard Test Method for Apparent Shear Strength of Single-Lap-Joint Adhesively Bonded Metal Specimens by Tension Loading (Metal-to-Metal)* in *D 1002- 05*, edited by ASTM (ASTM International, 2005).
- ⁹¹ Hill, John, *Specification for Structural Adhesives* in *AMES-014-STRUCTURAL ADHESIVE*, edited by Aston Martin Lagonda PLC (2007).
- ⁹² Feraboli, Paolo, Peitso, Elof, Cleveland, Tyler, and Stickler, Patrick, *Modulus Measurement for Prepreg-based Discontinuous Carbon Fiber/Epoxy Systems*. Journal of Composite Materials 43 (19), 1947 (2009).

Appendix A. Materials

A.1 Resin System

To ensure continuity with regards to the epoxy matrix used to manufacture the composite substrates a single resin formulation was used throughout the experimental investigations.

PrimeTM 20LV is manufactured by SP Gurit and is an epoxy resin infusion system designed for use in resin infusion processes. The system has a choice of 4 different hardeners, for the manufacture of specimens the hardener used was the fast hardener mixed using a 100:26 mix ratio by weight. The neat resin mechanical properties are displayed in Table 34.

Table 34 Material Properties of Gurit PRIME 20LV matrix resin

	Tensile Strength (MPa)	Tensile Modulus (GPa)	Strain to Failure (%)	Cured resin density (g/cc)
Gurit PRIME 20LV	68.6	2.97	4.9	1.089

Appendix A – Materials

A.2 Reinforcement Fibres and Fabrics

- Fibre Tow Specifications

When manufacturing the DCFP and Oriented DCFP substrates described in Chapter 4 and Chapter 6, three different carbon fibre tow sizes were used. Carbon Fibre was supplied on bobbins from Teijin Toho Tenax in 3k, 6k and 24k fibre bundles for use in the DCFP manufacturing process. The material properties are listed in Table 35.

Table 35 Properties of Carbon Fibre Tows

Designation	Tensile Strength (MPa)	Tensile Modulus (GPa)	Elongation at break (%)	Linear Density (tex)	Sizing Level (%)	Density (g/ccm)	Filament Diameter (µm)
3k E HTA40	4064	238	1.62	201	1.27	1.76	7
E13							
6k E HTA 5131	3784	238	1.51	398	1.27	1.76	7
24k E STS 5631	4447	240	1.74	1604	0.94	1.79	7

- Non-crimp Fabric Specifications

The Non-crimp fabric (NCF) composite substrates used to study the effect of fibre orientation in Chapter 4 was a unidirectional stitched non-crimp fabric manufactured by Sigmatex. The fabric properties are summarised in Table 36.

Table 36 Properties of NCF fabric

Manufacturer	ID Code	Fibre Type	Tow Size	Areal Weight
Sigmatex	PC2510600	T700s	12k	300gsm

Appendix A – Materials

A.3 Adhesives

A total of 5 different two-part epoxy adhesives were subjected to an adhesive characterisation program as described in Chapter 3. Each of the adhesives had been selected from a larger adhesive characterisation program being run concurrently at Aston Martin Lagonda. An overview of the material properties is highlighted in Table 37.

To ensure the appropriate dispensing of the different candidate adhesives a Newborn VR400 XSP hand held variable ratio manual adhesive applicator was purchased for the research. This allowed adhesives with different mixing ratios to be used with the same applicator. MIXPAC static mixing nozzles provided by the adhesive suppliers were used to dispense the adhesive. A minimum of 24 elements within the mixing nozzle ensured sufficient mixing of the two components of the adhesive.

Table 37 List of Candidate Adhesives

Adhesive	Tensile UTS (MPa)	Tensile Modulus (MPa)	Elongation to Failure (%)	Glass Transition Temperature (°C)
Desired Performance	50	3000	4.00	120
3M DP 490	32.1	1863	2.96	96
3M DP 460	44.5	2098	5.87	80
Hysol 9461	35.5	3220	3.75	82
Dow BM 2096	26.2	1664	3.50	79
Dow BM 2098	41.2	2456	6.35	84

After the initial adhesive characterisation described in Chapter 3, only the DOW BM 2098 adhesive was used to manufacture the adhesive specimens.

A.4 Ancillary Materials

- Cleansing Agents

Acetone was used to clean the substrates prior to bonding. The acetone was applied to a clean ScotchBrite7496 abrasive pad that was used to abrade and clean the surface of the substrates. After cleaning the substrate was wiped with a lint free clean cloth and allowed to dry for at least 1 hour prior to bonding.

Appendix A – Materials

- Release Agent

The release agent selected for the moulding operations was Chem-Trend Chemlease PMR-90. The release agent was applied prior to each moulding operation. The release agent was applied as a thin layer using a lint free cloth. The mould was left until the release agent began to bead and was then wiped again using a dry cloth before being left for 15 minutes before use. Following mould cleaning this process was repeated 5 times, whilst between mouldings the process was only carried out once.

- Powder Binder

A thermosetting epoxy powder binder was used for manufacturing the preforms at a 5% addition by weight. The binder used throughout the experimental investigations was Pretex® 110 manufactured by Reichhold. The addition of binder during the preforming stage allowed for easy handling of the preforms prior to the moulding operation. The binder was evenly distributed through the preforms by adding it between each preform layer.

- Dimensional Controls

Two different methods of controlling the adhesive bondline thickness were used in the experimental investigations. For the initial adhesive characterisation glass microspheres were added to the adhesive bondline whilst for the remaining investigations wire spacers were used as this meant the bondline thickness could be changed by varying the gauge of the wire.

The glass microspheres used in the initial investigations were 0.2mm in diameter. After the adhesive had been applied to the adherends a small amount of the glass beads were evenly spread over the bondline before the joint was closed.

In total three different wire gauges were used when varying the bondline thickness. The thicknesses studied were; 0.1mm, 0.2mm and 0.5mm, with a pair of wires being inserted to maintain a constant bond thickness across the width of the specimen.

Appendix B. Adhesive Cure Cycles

A SNOL Pro VUC programmable oven was used to cure the SLS samples. A cure cycle was designed alongside colleagues at AML that represented the minimum cure cycle an adhesive would be subjected to when a vehicle was assembled at the plant. To determine this, a vehicle tub was instrumented with thermocouples that captured the temperature profile as it passed through the paint ovens during assembly. The results were processed and the lowest recorded temperatures were used to build-up the cure cycle. This is shown in Figure 47.

After the curing stage, the adhesive specimens were left for a 7 day period at room temperature before being tested.

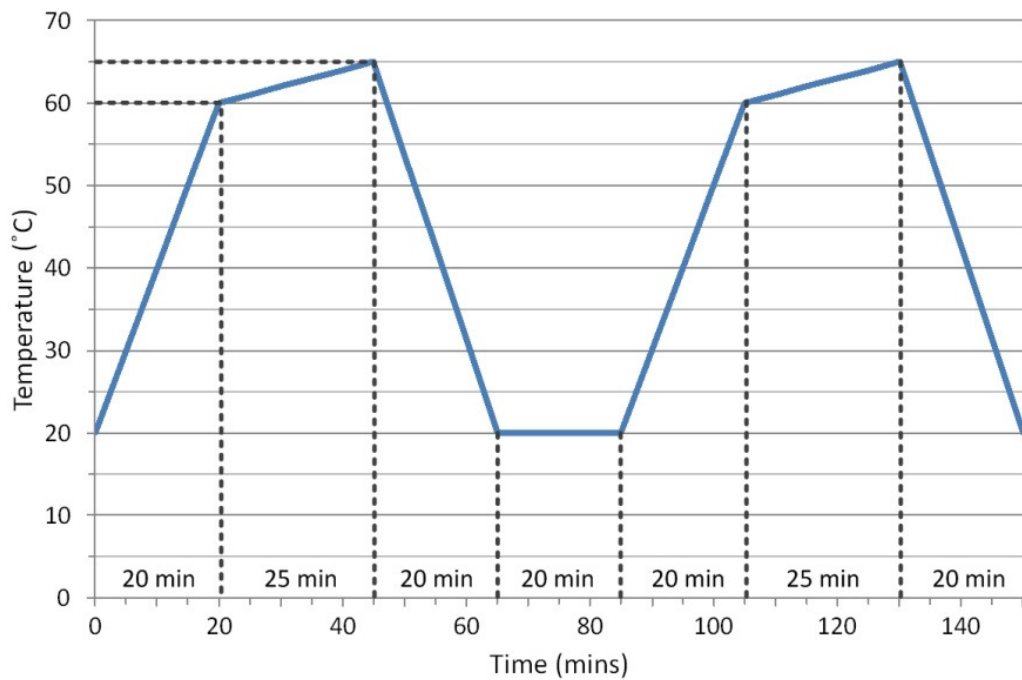


Figure 47 Temperature Profile of AMLC Cure Cycle

Appendix C. Analysis of adhesive joint failure loci

Whilst the mechanical performance of the adhesive joints tested is important, similarly the manner in which the adhesive joints fail is also of interest. Following the mechanical testing of the ODCFP SLS adhesive joints, the failure location of each of the tensile specimens was recorded. The failures were classified by the following types:

- Adhesive failure – The interfacial debonding of the adhesive from the joint substrate;
- Cohesive failure – Fracture of the adhesive;
- Substrate failure – Caused by the failure of the substrate matrix or fibres or a combination of the two;
- Mixed failure – A combination of both substrate failure and cohesive fracture of the adhesive.

By identifying the location of the failure it is possible to identify the weakest part of the adhesive joint. The failure modes were recorded as a percentage of the failures observed following the testing.

Most quality standards require that an adhesive joint fail cohesively with the adhesive. This failure mode indicates that there is a good compatibility between the substrate material, surface preparation and the adhesive in use. As such, the aim is to try and ensure cohesive failure is induced in the adhesive specimens.

Appendix D. Non-Crimp Fabric

D.1 Anomalous Results

There were 4 plaques that attracted interest owing to their similarity in stacking sequence but with a different performance with regards to the elongation to failure of the SLS specimens. Plaques NCF 1 [0°,45°,90°,-45°]s and NCF 6 [90°,45°,0°,-45°]s had a stacking sequence that was 90° offset with the exception of the 45° layers being inverted. Similarly, NCF 3 [0°,90°,45°,-45°]s and NCF 5 [90°,0°,45°,-45°]s had the same 90° offset with inverted 45° layers. The performance differences were considered to be significant enough to be subject to further investigation.

Whilst NCF 1 0° provided the second highest overall performance, NCF 6 90° was the 8th highest performer despite a similar stacking sequence. NCF 1 0° had a stacking sequence of [0°, 45°, 90°, -45°] and NCF 6 90° had the same stacking sequence with the directions of 45° fibres switched. Interestingly, with this change in signs the later plaque had a 32% lower performance than NCF 1 0°. The difference in overall performance for the NCF 1 90° and NCF 6 0° samples was only 5% between the 2 different plaques.

Discrepancies were also observed for NCF 3 0° and NCF 5 90° which had a stacking sequence of [0°, 90°, 45°, -45°] for NCF 3 0° whilst the signs of the 45° layers were switched for NCF 5 90°. The difference in overall performance equated to a drop of approximately 11%. The difference in the samples extracted at 0° and 90° of the original substrate was also checked with the performance between NCF 3 90° and NCF 5 0° calculated to be 14% different., similar to the 11% of the perpendicular samples. Despite the difference in overall performance, the 2 plaques significantly outperformed all of the other SLS joints with the exception of NCF 1 0°.

When considering the NCF 3 and NCF 5 data, both the 0° and 90° data have similar differences in performance. This would indicate a possible manufacturing fault or problem as the error is observed in both sets of data. In contrast, for NCF 1 and NCF 6 the 0° and 90° data are considerably different indicating a different problem; possibly from specimen extraction or during bonding. The possibility of fibre misalignment

Appendix D – Non-Crimp Fabric

was investigated; however, no problems were identified. At present there are no suitable explanations for the behaviour of these plaques.

The specimens were studied for discrepancies in the failure modes of the samples; however, there were no significant differences noted. It would appear that the difference as a result of the change of direction of the 45° layers had a larger impact on the results the closer the layers were to the substrate surface.

D.2 Study of Reinforced NCF SLS Joints

- Manufacture of Reinforced SLS joints

A side study was carried out to try and reduce the variability observed when testing the NCF preforms by reinforcing the NCF substrates with an additional 6mm steel substrate as illustrated in Figure 48. It was anticipated that the amount of bending observed in SLS testing should be reduced thereby causing a more consistent failure mode by reducing the contribution of the peel forces to the final failure. The effect of the reinforcement was studied as well as its viability as a means of improving SLS joint performance.

The Reinforced NCF SLS joints were manufactured as in Section 4.2.4 and after the joints had been completed a 6mm thick steel reinforcement was bonded to the back face of the SLS joints using the BM2098 candidate epoxy adhesive. After a 7 day period the samples were subject to the same tensile testing as the standard NCF samples.

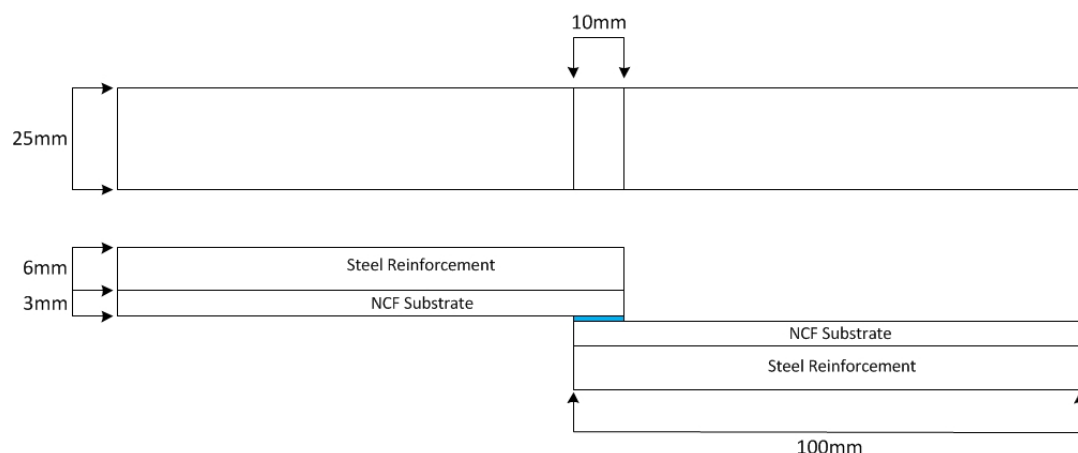


Figure 48 Schematic of Reinforced NCF SLS adhesive joint

- Results of Reinforced NCF SLS Results

The following section provides a comparison between the reinforced SLS and traditional SLS adhesive joints with a summary of the reinforced NCF joint data presented in Table 38. In theory, the reduction in joint rotation should result in more accurate measurements of the adhesive shear strength of the joint system. In practice, the benefits would have to outweigh the time and financial costs of adding the extra reinforcement to the adhesive joints.

Table 38 Summary of performance of Reinforced NCF SLS adhesive joints

	Stacking Sequence (0°)	Tensile Strength (MPa)	St Dev. (MPa)	Elongation to Failure (mm)	St Dev. (mm)
R-NCF 1	[0°,45°,90°,-45°]	21.9	1.55	1.26	0.18
R-NCF 2	[45°,90°,0°,-45°]	25.0	1.94	1.69	0.21
R-NCF 3	[0°,90°,45°,-45°]	25.6	1.20	1.71	0.15
R-NCF 4	[45°,-45°,0°,90°]	19.7	2.13	1.24	0.19
R-NCF 5	[90°,0°,45°,-45°]	22.2	1.98	1.17	0.15
R-NCF 7	[0°,45°,-45°,90°]	23.2	2.42	1.44	0.27
R-NCF 8	[45°,0°,-45°,90°]	24.6	0.99	1.52	0.12

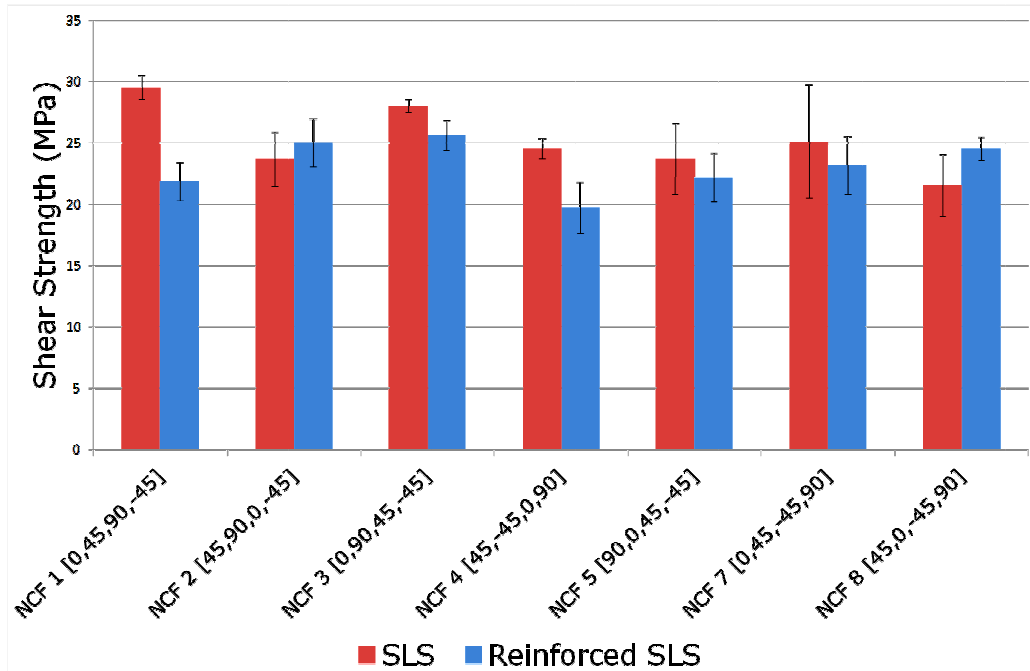
To verify whether the reinforced SLS adhesive joints provided any gains in performance or reductions in variability of the data, the means of the shear strength and elongation to failure of the samples were compared to the results from the testing of the traditional NCF SLS adhesive joints.

When the shear strength of the reinforced SLS joints were compared to those results collected previously there was a large spread of results as is demonstrated in Figure 49. The resulting reinforcement of the SLS joints affected all of the composite joints differently ranging from a 26% reduction in strength for NCF 1 to a 14% increase for NCF 8. There were no discernible patterns that could be identified from the results with the role of fibre orientation and stacking sequence being less clear than for the larger study of regular SLS joints.

It was postulated that the reduction in rotation would result in more consistent results from the testing. However, as with the results of the shear strength, the results were mixed. For NCF 8 there was a 61% drop in the standard deviation of shear strength; however, there was also a 137% increase in the standard deviation for NCF 3 which

Appendix D – Non-Crimp Fabric

indicates that the problem of variability has not been solved with the use of the additional reinforcement mechanism.



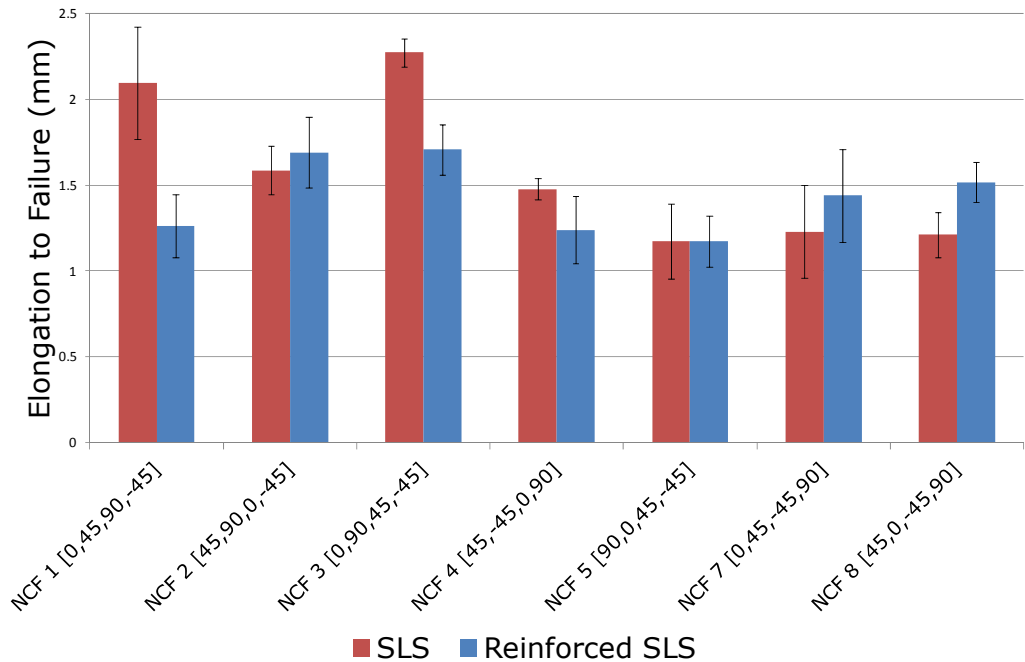
Plaque ID	SLS		Reinforced SLS		Comparison	
	Shear Strength (MPa)	St Dev. (MPa)	Shear Strength (MPa)	St Dev. (MPa)	Shear Strength (%)	St (% change)
NCF 1	29.6	0.96	21.9	1.55	74.1	163
NCF 2	23.7	2.20	25.0	1.94	105	88.2
NCF 3	28.1	0.51	25.6	1.20	91.4	237
NCF 4	24.6	0.81	19.7	2.13	80.4	263
NCF 5	23.7	2.93	22.2	1.98	93.7	67.7
NCF 7	25.1	4.61	23.2	2.42	92.24	52.4
NCF 8	21.6	2.51	24.6	0.99	114	39.4

Figure 49 Comparison in Shear Strength for NCF and Reinforced NCF SLS Joints

A comparison of the elongation to failure of the NCF and Reinforced NCF specimens is presented in Figure 50. There were mixed results with the reinforcement resulting in a 40% drop in elongation to failure for NCF 1 compared to a 25% increase for NCF 8. One observation that can be made for the elongation to failure is that the best (NCF 3) and worst (NCF 5) performing substrates were the same regardless of the use of reinforcement. The ordering of the rest of the results did differ depending on the use of the steel reinforcement.

Appendix D – Non-Crimp Fabric

When studying the variability in the results, 4 of the 7 preforms studied exhibited greater inter-specimen variability. There were some reductions in the standard deviations of the results, such as NCF 1 which demonstrated a 45% reduction in variability; however, this was offset by other results such as for NCF 4 where there was a 220% increase in variability as a result of the use of steel reinforcements.



Plaque ID	SLS		Reinforced SLS		Comparison	
	Elongation to Failure (mm)	St Dev. (mm)	Elongation to Failure (mm)	St Dev. (mm)	Elongation to Failure (%)	St Dev. (% change)
NCF 1	2.09	0.33	1.26	0.18	60.3	55.9
NCF 2	1.59	0.14	1.69	0.21	106	144
NCF 3	2.27	0.08	1.71	0.15	75.1	175
NCF 4	1.48	0.06	1.24	0.19	83.9	320
NCF 5	1.17	0.22	1.17	0.15	99.7	68.2
NCF 7	1.23	0.27	1.44	0.27	117	100
NCF 8	1.21	0.13	1.52	0.12	125	86.9

Figure 50 Comparison in Elongation to Failure of NCF and Reinforced NCF SLS Joints

- Failure Modes Reinforced NCF SLS Adhesive Joints

The failure modes of the reinforced NCF SLS joints are described in Table 39. With the fibres aligned at 0° to the load path, 53% of the specimens exhibited cohesive

Appendix D – Non-Crimp Fabric

failure, 33% were mixed and the remaining 13% were failures within the substrate. The mixed failure generally was a mix of matrix failure and cohesive failure of the adhesive, similar to those observed for the non-reinforced NCF samples. Meanwhile, the substrate failure was also generally constrained to being failure at the matrix and fibre bundle interface.

In total, 47% of the specimens with a 45° surface layer had substrate failures, 40% were mixed failures and the remaining 13% were cohesive. The mixed failures were generally the result of the corners of the 45° surface laminate being separated from the remaining substrate and then a cohesive failure being present in the remainder of the adhesive joint.

At a 90° surface fibre orientation all of the specimens tested exhibited substrate failures with fibre bundles being pulled away from the underlying composite substrate in much same manner as for the un-reinforced NCF SLS adhesive joints.

Table 39 Distribution of failure modes (%) for the first layer fibre orientation of Reinforced NCF SLS adhesive joints

	0°	45°	90°
Adhesive	-	-	-
Cohesive	53%	13%	-
Substrate	13%	47%	100%
Mixed Failure	33%	40%	-

- Discussions and Conclusions from Reinforced NCF SLS Joint Study

The aim of the study using Reinforced NCF SLS adhesive joints was to try and reduce the variability in performance amongst NCF plaques manufactured with the same fibre orientations and stacking sequence. Using steel backed NCF substrates it was anticipated that the reduction in joint rotation and peel stresses should reduce the amount of variability observed during the previous study. The results indicated that this was achieved with mixed success. The increase in substrate stiffness resulted in the overall performance of the Reinforced NCF SLS joints being reduced whilst the variability between similar substrates demonstrated mixed results. The addition of the steel reinforcement reduced the spread in data across the entire study.

Appendix D – Non-Crimp Fabric

Overall, the use of steel reinforcements served to reduce the joint rotation of the NCF SLS samples. Undoubtedly, the effect of stacking sequence and fibre orientation also play a significant role in defining the performance of adhesively bonded NCF SLS joints; however, the benefits of using the additional reinforcement to reduce the joint rotation and increase specimen stiffness does not appear to be particularly beneficial to the investigation. The decrease in performance indicates that the fibre orientation and stacking sequence may also play a significant role in defining the joint strength of adhesive joints where peel forces are predominant.

Appendix E. Optimisation of DCFP Substrate

E.1 Effect on Shear Strength

- Signal-to-Noise Ratio

Studying the analysis of variance for the S/N ratios of the shear strength in Table 40 it is possible to identify 4 factors that have P values that are under the α -level. The factor with the lowest P value was the Bond Overlap ($P=0.002$). This is followed by the substrate thickness ($P=0.026$), tow size (0.051) and the fibre length (0.057). The main effects plot and response table for the S/N ratio is presented in Figure 51.

Table 40 Analysis of Variance for Shear Strength S/N Ratios

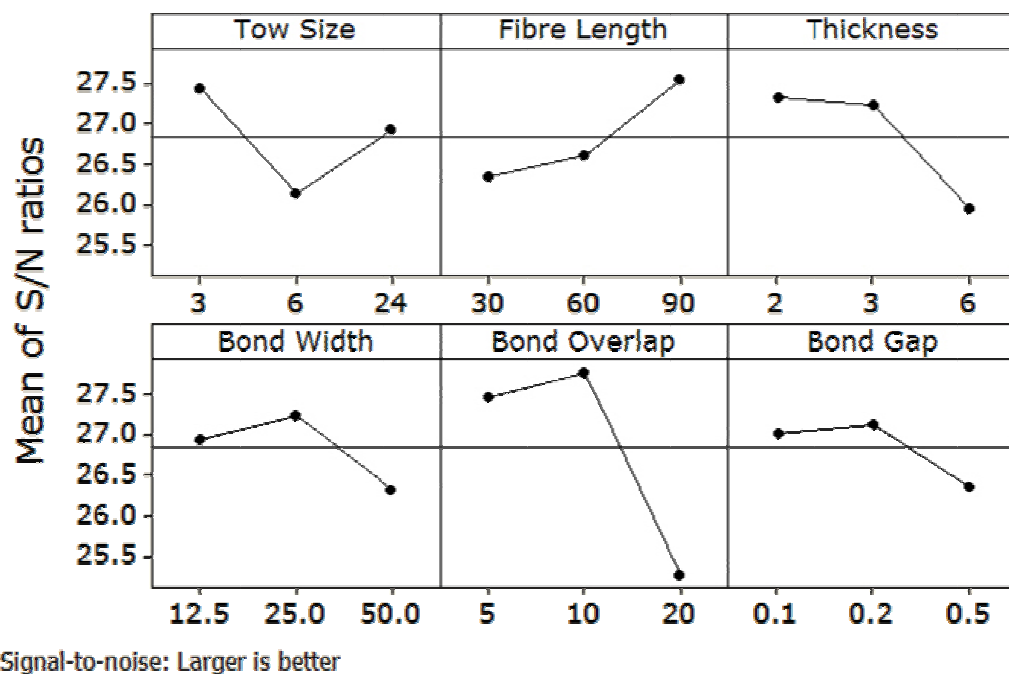
Source	DF	Seq SS	Adj MS	F	P	% Contribution
Tow Size	2	7.70	3.85	5.11	0.051	10.0
Fibre Length	2	7.19	3.60	4.77	0.057	9.3
Thickness	2	10.7	5.35	7.10	0.026	13.9
Bond Width	2	4.02	2.01	2.67	0.148	5.2
Bond Overlap	2	33.5	16.8	22.3	0.002	43.6
Bond Gap	2	3.04	1.52	2.02	0.214	3.9
Bond Width*Bond Overlap	4	1.44	0.36	0.48	0.751	1.9
Bond Width*Bond Gap	4	4.81	1.20	1.59	0.29	6.2
Residual Error	6	4.52	0.75			5.9
Total	26	76.96				

The most influential factor with respect to the S/N ratio was the bond overlap. Although there was a small increase in the S/N ratio when the bond overlap was changed from 5mm to 10mm there was an 8% reduction in performance as the overlap was increased to 20mm. The thickness was the second most influential factor. There was a small drop in performance as the thickness of the substrate increased in thickness from 2mm to 3mm; however, the decrease in the S/N ratio, as the substrate thickness doubled to 6mm, was more significant.

The influence of tow size on the shear strength S/N ratios of the experiment identified the 3k tow size as the best performing tow. There was a drop in S/N ratio when the 6k fibre was tested before increasing when the 24k tow size was used. The last factor with a statistically significant result for the shear strength S/N ratio was the fibre

Appendix E – Optimisation of DCFP Substrate

length. As can be seen from Figure 51, the S/N ratio increased with the fibre length resulting in the 90mm being the preferred length.



Level	Tow Size	Fibre Length	Substrate Thickness	Bond Width	Bond Overlap	Bond Gap
1	27.44	26.35	27.32	26.95	27.47	27.01
2	26.14	26.61	27.24	27.25	27.77	27.13
3	26.94	27.55	25.95	26.32	25.27	26.37
Delta	1.3	1.2	1.37	0.93	2.5	0.76
Rank	3	4	2	5	1	6

Figure 51 Main Effects Plot and Response Table for S/N Ratio of Shear Strength

- Mean Shear Strength

The analysis of variance for the data means of the shear strength in Table 41 yielded 5 factors that were statistically significant. The bond overlap ($P=0.002$) was the most influential factor followed by the substrate thickness ($P=0.025$) and the tow size ($P=0.038$). There was then a significant increase in the P values for the bond width ($P=0.08$) and fibre length (0.096) which were close to the α -level limit. As there was no statistically significant interaction, the factors were studied independently.

Appendix E – Optimisation of DCFP Substrate

Table 41 Analysis of Variance for Data Means of Shear Strength

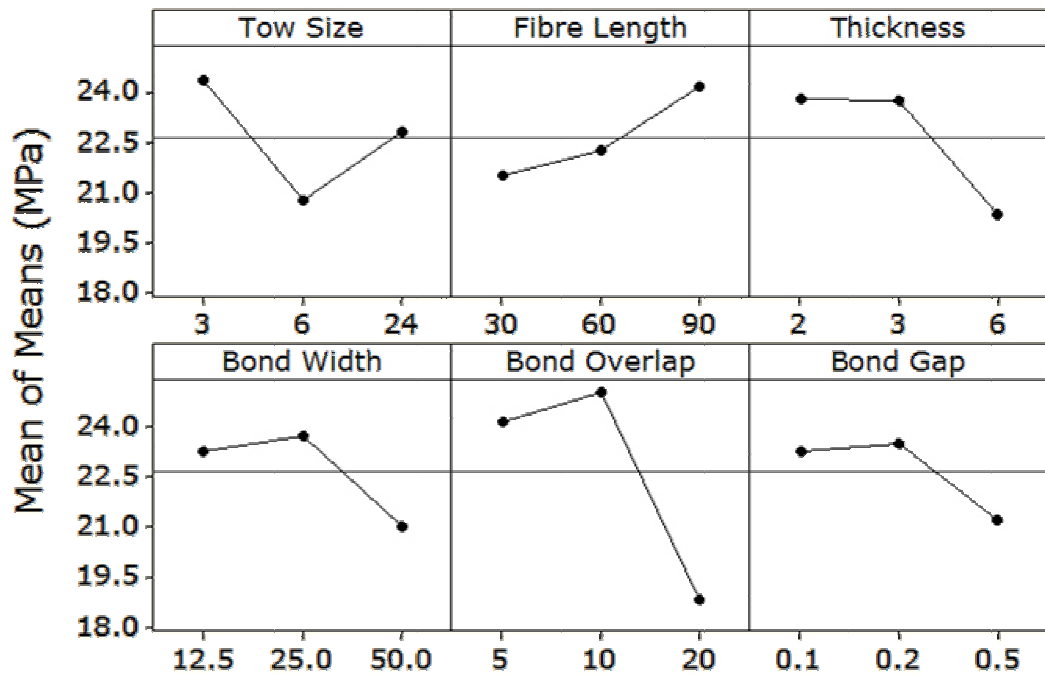
Source	DF	Seq SS	Adj MS	F	P	% Contribution
Tow Size	2	58.0	29.0	5.96	0.038	11.6
Fibre Length	2	34.5	17.3	3.55	0.096	6.9
Thickness	2	70.3	35.2	7.23	0.025	14.0
Bond Width	2	38.4	19.2	3.95	0.080	7.7
Bond Overlap	2	204	102	20.9	0.002	40.6
Bond Gap	2	28.5	14.3	2.93	0.129	5.7
Bond Width*Bond Overlap	4	10.3	2.58	0.53	0.719	2.1
Bond Width*Bond Gap	4	28.9	7.23	1.49	0.316	5.8
Residual Error	6	29.2	4.86			5.8
Total	26	501.7				

The shear strength means, plotted in Figure 52, show a small increase as the bond overlap increased from 5mm to 10mm followed by a 22% decrease in mean shear strength as the overlap was increased to 20mm. This would indicate an upper limit being reached for the bond overlap. The thickness of the substrate was the second most influential factor. While there was an almost negligible decrease as the substrate thickness changed from 2mm to 3mm, a 15% decrease in shear strength was observed when the thickness increased to 6mm compared to the 2mm substrate.

For the tow size, the shear strength followed a similar trend as those observed for the S/N ratios. The best performing tow size being 3k and the worst being the 6k. The 24k tow size improved the performance of the SLS joints compared to the 6k fibres; however, not to the extent of the 3k fibres. The influence of bond width identified the 25mm specimen width as the optimal level for maximizing the strength of the joint. Whilst there was only 0.5 MPa difference in mean shear strength between the 12.5mm and 25mm specimen widths, the mean shear strength of the 50mm bond width reduced by 12% compared to the 25mm samples. The influence of fibre length was again observed with the lowest performing fibre length being 30mm. An almost linear increase in shear strength was observed with increasing fibre length.

The analysis of variance of the standard deviations of the shear strength were not considered statistically significant meaning there was no clear effect on the standard deviations of the shear strength as the factor levels were changed.

Appendix E – Optimisation of DCFP Substrate



Level	Tow Size	Fibre Length	Substrate Thickness	Bond Width	Bond Overlap	Bond Gap
1	24.4	21.5	23.8	23.2	24.2	23.3
2	20.8	22.3	23.8	23.7	25.0	23.5
3	22.8	24.2	20.4	21.0	18.8	21.2
Delta	3.58	2.69	3.45	2.74	6.21	2.29
Rank	2	5	3	4	1	6

Figure 52 Main Effects Plot and Response Table for Mean Shear Strength

E.2 Effect on Elongation to Failure

- Signal-to-Noise Ratio

The analysis of variance for the signal/noise (S/N) ratios of the elongation to failure is presented in Table 42. Using the α -level of 0.1 there were 3 factors that were deemed to be statistically significant, these were the substrate thickness (0.002), bond width (0.000) and the bond overlap (0.000). Studying the main effects plot presented in Figure 53 the influence of each of the factors on the S/N response can be visualised.

Table 42 Analysis of Variance for S/N ratios of Elongation to Failure

Source	DF	Seq SS	Adj MS	F	P	% Contribution
Tow Size	2	0.596	0.298	0.23	0.802	0.1
Fibre Length	2	6.82	3.41	2.62	0.152	1.0
Thickness	2	53.2	26.6	20.4	0.002	7.4
Bond Width	2	98.1	49.0	37.7	0.000	13.7
Bond Overlap	2	532	266	204	0.000	74.2
Bond Gap	2	2.03	1.02	0.78	0.500	0.3
Bond Width*Bond Overlap	4	3.16	0.79	0.61	0.673	0.4
Bond Width*Bond Gap	4	13.1	3.28	2.52	0.150	1.8
Residual Error	6	7.81	1.30			1.1
Total	26	717				

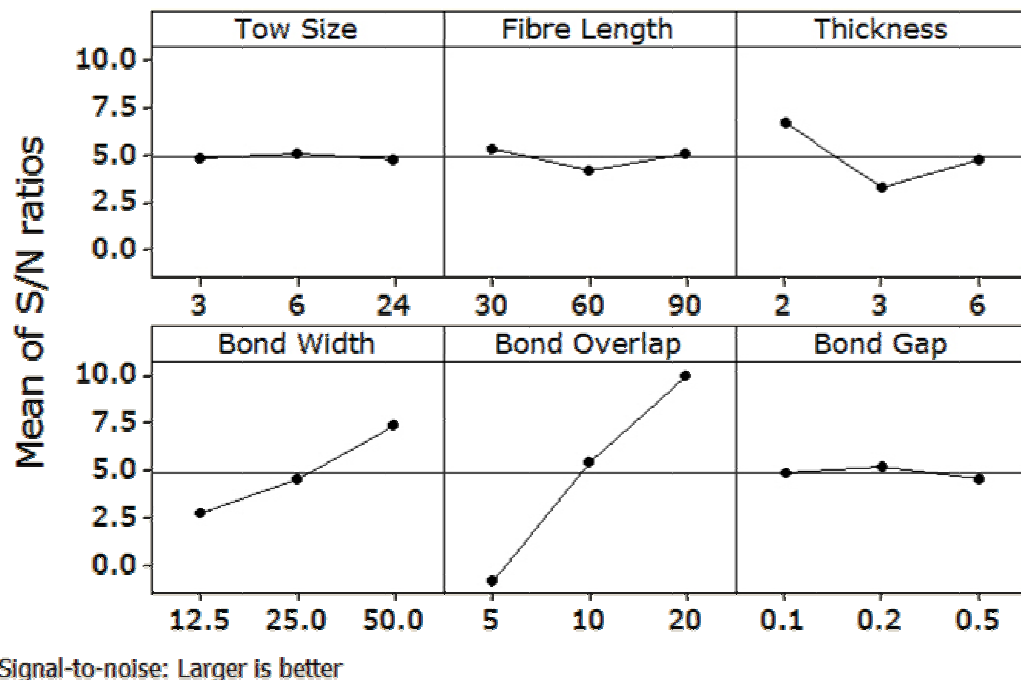
The adhesive bond overlap provided the biggest contribution to maximizing the S/N ratio for the elongation to failure of the DCFP SLS adhesive joints. There was an almost linear increase in the S/N ratio as the bond overlap increased. This shows that increasing the bond overlap to 20mm is the most effective way of maximizing the response.

The bond width also demonstrated an almost linear increase in the S/N ratio as the width increased. The 50mm bond width had a S/N ratio nearly 3 times higher than that of the 12.5mm width when considering the elongation to failure.

When considering the substrate thickness, the 2mm substrate thickness was the most effective way of maximising the S/N ratio whilst the 3mm substrate thickness had the lowest S/N ratio.

Appendix E – Optimisation of DCFP Substrate

The tow size, fibre length and bond gap factors display almost flat lines in the main effects plot indicating that the mean S/N ratio for the elongation to failure was pretty constant regardless of the levels chosen for these properties. This is confirmed by studying the values displayed in the response tables.



Level	Tow Size	Fibre Length	Substrate Thickness	Bond Width	Bond Overlap	Bond Gap
1	4.80	5.33	6.66	2.73	-0.821	4.90
2	5.07	4.17	3.24	4.51	5.41	5.18
3	4.73	5.10	4.70	7.36	10.0	4.51
Delta	0.345	1.16	3.43	4.63	10.8	0.670
Rank	6	4	3	2	1	5

Figure 53 Main Effects Plot and Response Table for S/N Ratio of Elongation to Failure

- Mean Elongation to Failure

The analysis of variance for the mean elongation to failure of the DCFP SLS samples in Table 43 indicates that the factors identified in the S/N ratios ANOVA were statistically significant. The thickness ($p=0.009$), bond width ($p=0.004$) and the bond overlap ($p=0.000$) have a strong influence on the mean elongation to failure of the DCFP SLS specimens. This is highlighted by the main effects plot and response tables in Figure 54.

Appendix E – Optimisation of DCFP Substrate

Table 43 Analysis of Variance for Data Means of Elongation to Failure

Source	DF	Seq SS	Adj MS	F	P	% Contributio n
Tow Size	2	0.023	0.011	0.09	0.914	0.1
Fibre Length	2	0.319	0.160	1.28	0.344	0.9
Thickness	2	2.80	1.40	11.2	0.009	8.3
Bond Width	2	3.97	1.98	15.9	0.004	11.7
Bond Overlap	2	24.7	12.4	99.4	0.000	73.3
Bond Gap	2	0.153	0.076	0.61	0.573	0.5
Bond Width*Bond Overlap	4	0.930	0.233	1.87	0.235	2.8
Bond Width*Bond Gap	4	0.089	0.022	0.18	0.942	0.3
Residual Error	6	0.747	0.125			2.2
Total	26	33.8				

The bond overlap again demonstrated a strong linear increase in mean elongation to failure as the bond lap increased with the 20mm overlap more than 3 times higher than those DCFP SLS adhesive joints manufactured with a 5mm lap joint. The bond width indicated the elongation to failure increased with specimen width with the 50mm width increasing the elongation to failure by approximately 50%. When studying the effect of substrate thickness, the 2mm substrate thickness achieved the highest mean elongation to failure of the samples tested, most likely a result of the decreased stiffness of the substrate allowing greater specimen movement. Whilst the 3mm specimen had the lowest extension to failure, the 6mm specimen thickness was only marginally better.

The main effects plot for tow size, fibre length and bond gap have very little change in mean elongation to failure. This indicates that similar to the main effects plot for S/N ratios, there was very little variation in the elongation to failure of the specimens when the levels of these factors were changed.

Appendix E – Optimisation of DCFP Substrate

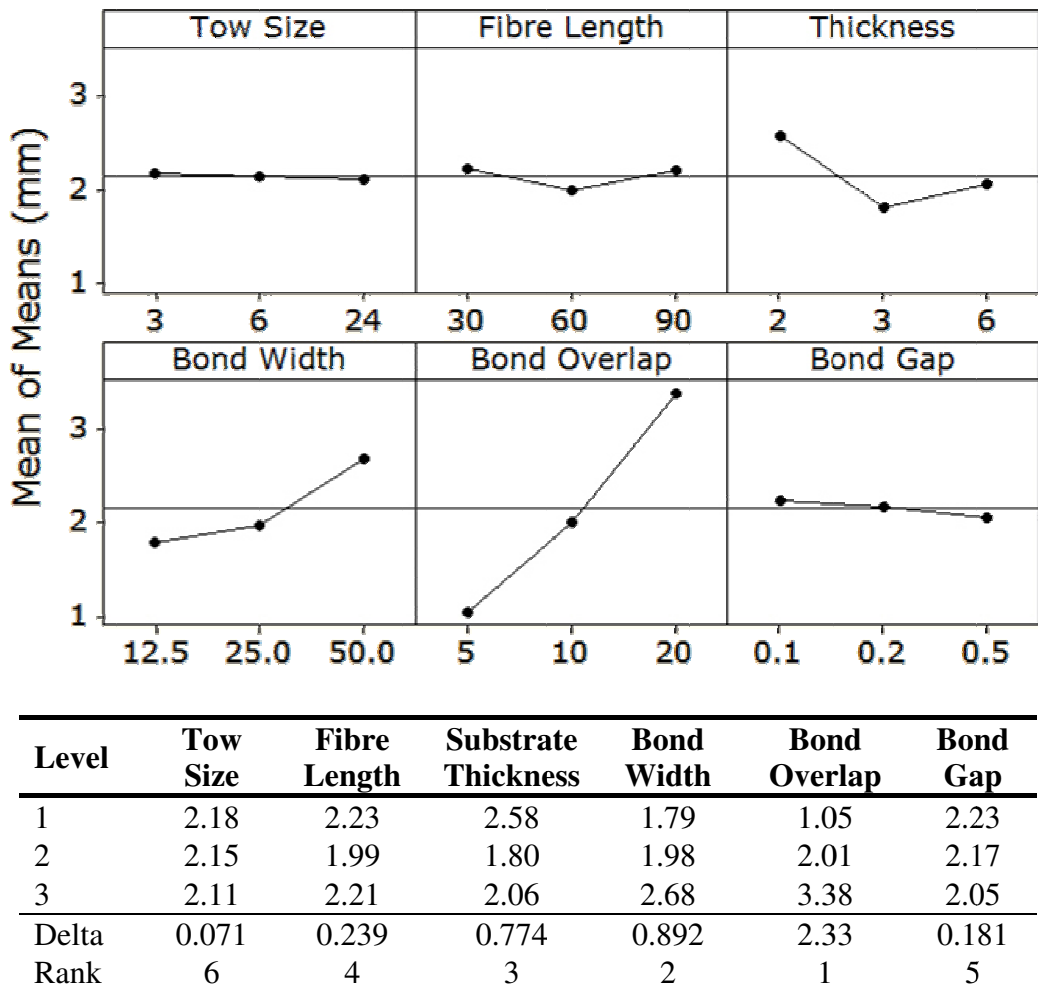


Figure 54 Main Effects Plot and Response Table for Mean Elongation to Failure

- Standard Deviation

The analysis of variance for the mean standard deviations of the elongation to failure of the DCFP SLS adhesive joints presented in Table 44 indicates that 5 different factors were statistically significant at an α -level of 0.1. The tow size ($P=0.019$), fibre length ($P=0.003$), substrate thickness ($P=0.003$), bond width ($P=0.002$) and bond overlap ($P=0.005$) had an influence on the standard deviations of the results for the elongation to failure. The main effects plot and response table is included in Figure 55.

Appendix E – Optimisation of DCFP Substrate

Table 44 Analysis of Variance for Standard Deviations of Elongation to Failure

Source	DF	Seq SS	Adj MS	F	P	% Contribution
Tow Size	2	0.234	0.117	8.17	0.019	9.2
Fibre Length	2	0.536	0.268	18.7	0.003	21.1
Thickness	2	0.503	0.251	17.6	0.003	19.8
Bond Width	2	0.577	0.288	20.1	0.002	22.8
Bond Overlap	2	0.412	0.206	14.4	0.005	16.3
Bond Gap	2	0.074	0.037	2.57	0.156	2.9
Bond Width*Bond Overlap	4	0.037	0.009	0.64	0.651	1.5
Bond Width*Bond Gap	4	0.077	0.019	1.34	0.355	3.0
Residual Error	6	0.086	0.014			3.4
Total	26	2.53				

For the tow size, the 3k fibres produced the highest average standard deviation, whilst the 6k and 24k tow size had very similar values. The main effects plot for the fibre length indicates that the 30mm fibre length had a mean standard deviation over twice that of the 60mm and 90mm fibre lengths with a small decrease in standard deviation as the fibre length increased from 60mm to 90mm.

Studying the substrate thickness, the 2mm substrates had the highest mean standard deviations with the increase in thickness to 3mm reducing the mean standard deviation by approximately half. The 6mm substrate thickness only reduced the variability slightly.

The 25mm bond width was the joint width with the lowest mean standard deviation, which was less than half that of the 12.5mm substrates. Meanwhile, the 50mm bond width showed a slight increase in standard deviation compared to the 25mm bond width.

The main effects plot for the bond overlap showed the 5mm bond overlap produced the samples with the lowest mean standard deviation. As the bond overlap increased the mean standard deviations also increased. There was a small increase as the overlap was changed from 5mm to 10mm; however, the increase to a 20mm overlap more than doubled the mean standard deviations of the samples tested.

Appendix E – Optimisation of DCFP Substrate

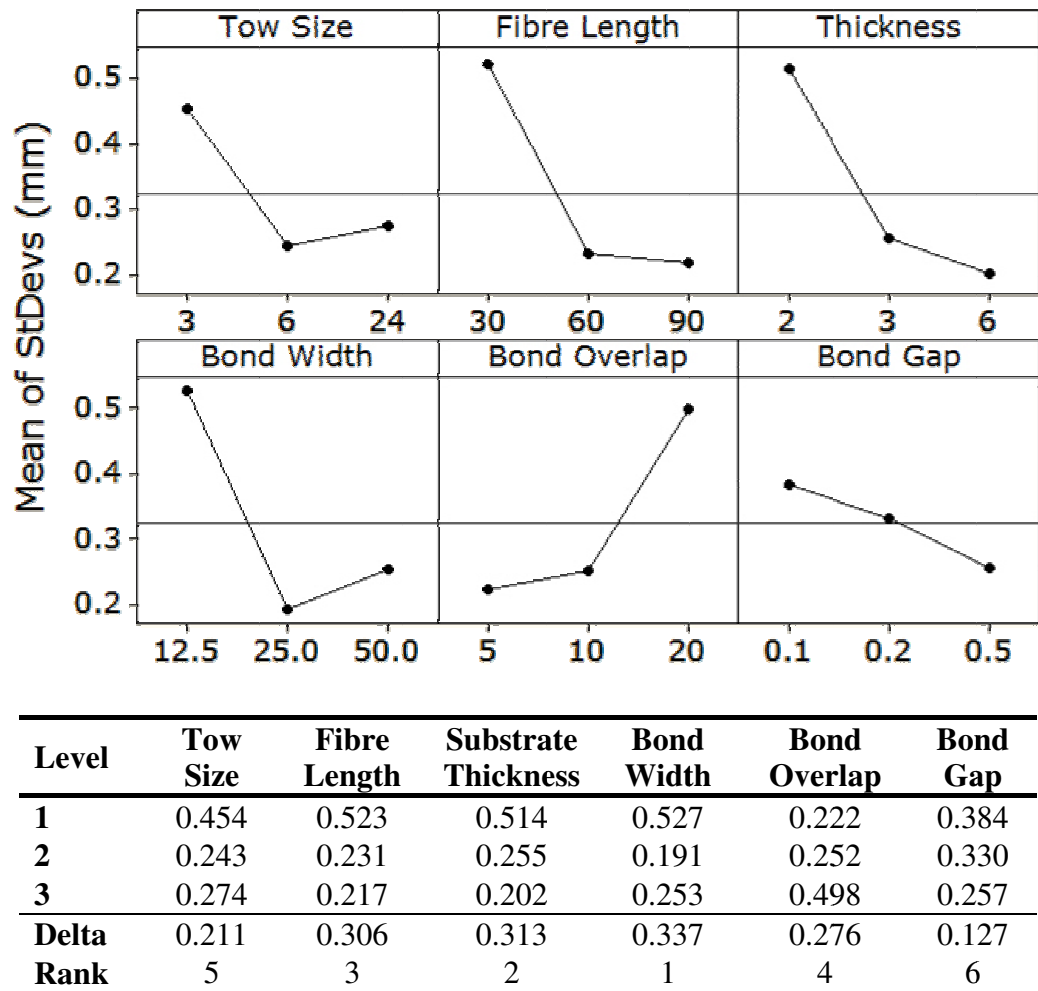


Figure 55 Main Effects Plot and Response Table for Standard Deviation of Elongation to Failure

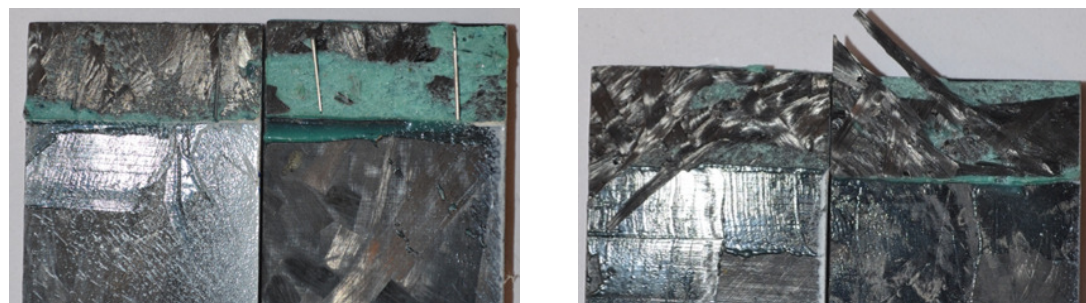
Appendix F. Investigation of SLS Joints manufactured using ODCFP Substrate

F.1 Commonly Occurring Failure Modes



Cohesive Failure

Substrate Failure



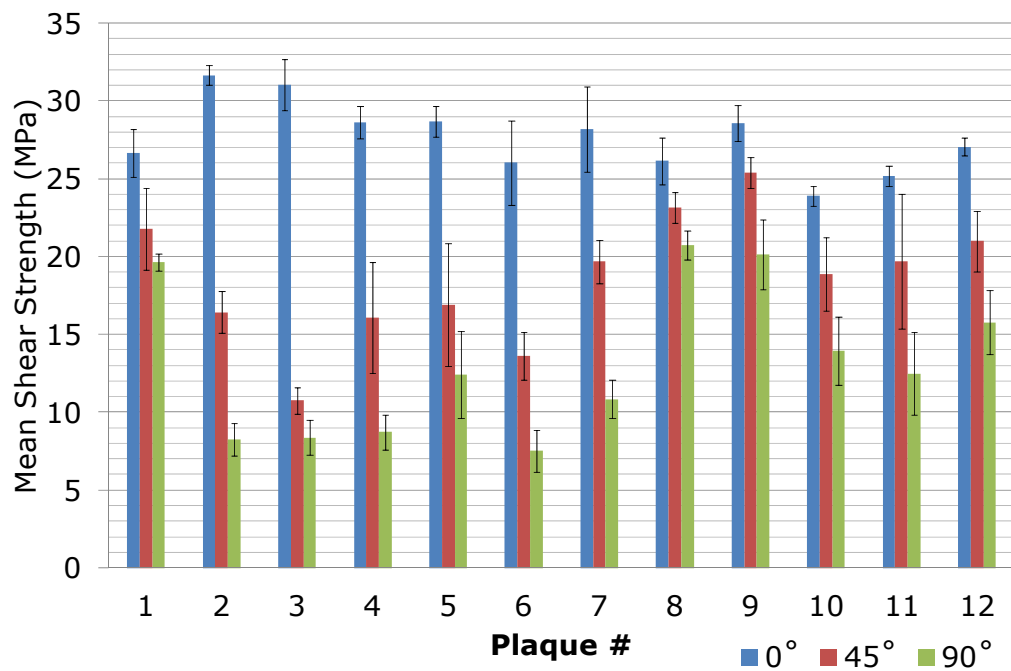
Mixed Failure – Cohesive/Matrix

Substrate Failure for 45° Specimens

Figure 56 Example of Common Specimen Failure Modes for ODCFP SLS Joints

F.2 Influence of Fibre Orientation on Shear Strength

The results for the shear strength of the ODCFP SLS joints are presented in Figure 57; whilst the ANOVA for the shear strength of the samples is presented in Table 45, overleaf.



Plaque #	0°		45°		90°	
	Shear Strength (MPa)	Rel Error (%)	Shear Strength(MPa)	Rel Error (%)	Shear Strength(MPa)	Rel Error (%)
1	26.7	5.74	21.8	12.0	19.6	2.77
2	31.7	2.00	16.4	8.19	8.25	12.4
3	31.1	5.27	10.7	7.78	8.37	13.4
4	28.6	3.61	16.1	22.0	8.71	12.9
5	28.7	3.43	16.9	23.4	12.4	22.4
6	26.0	10.5	13.6	11.3	7.52	17.9
7	28.2	9.67	19.7	7.17	10.8	11.2
8	26.1	5.71	23.1	4.23	20.7	4.50
9	28.6	4.04	25.4	3.8	20.1	11.1
10	23.9	2.58	18.9	12.5	13.9	15.8
11	25.2	2.62	19.7	21.9	12.5	21.3
12	27.1	2.08	21.0	9.29	15.8	13.0

Figure 57 Shear Strength of ODCFP SLS Joints tested at 3 fibre orientations

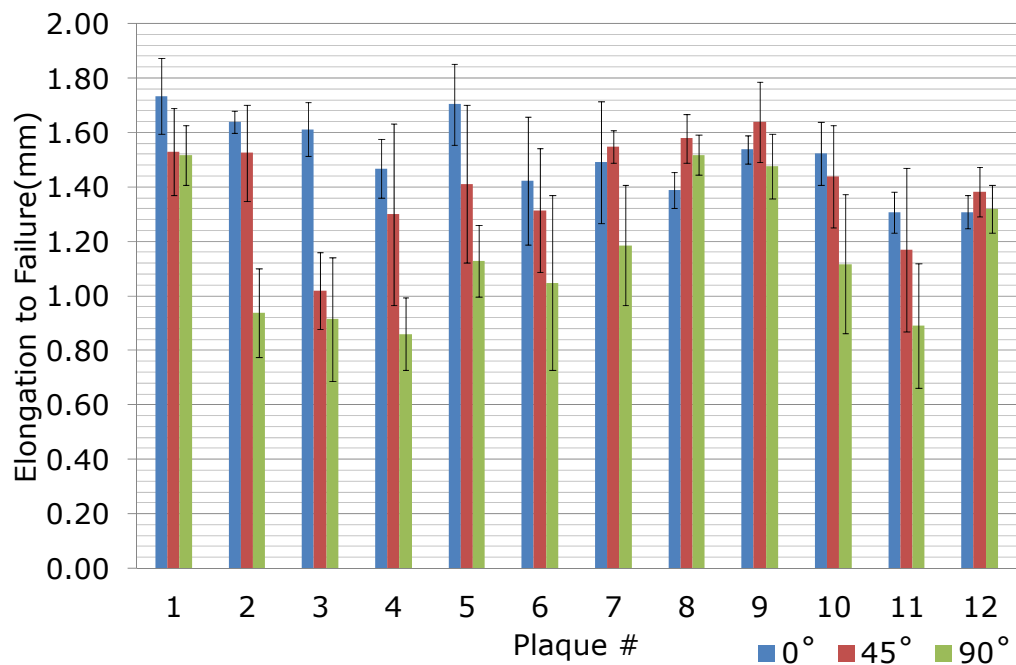
Appendix F – Investigation of SLS Joints manufactured using ODCFP Substrate

Table 45 Analysis of Variance for shear strength of ODCFP SLS adhesive joints

Source	DF	Seq SS	Adj SS	Adj MS	F	P	% Contribution
Main Effects	4	6510	6660	1670	287	0	77.0
Tow Size	1	416	533	533	91.9	0	4.9
Fibre Length	1	273	305	305	52.6	0	3.2
Chopper Height	1	85.9	120	120	20.6	0	1.0
Fibre Orientation	1	573	5860	5860	1010	0	67.8
2-Way Interactions	6	816	816	136	23.5	0	9.7
Tow Size*Fibre Length	1	40.7	38.6	38.6	6.65	0.011	0.5
Tow Size*Chopper Height	1	2.84	0.7	0.7	0.12	0.729	0.0
Tow Size*Fibre Orientation	1	143	143	143	4.72	0	1.7
Fibre Length*Chopper Height	1	11.1	14.1	14.1	2.43	0.121	0.1
Fibre Length*Fibre Orientation	1	333	310	310	53.5	0	3.9
Chopper Height*Fibre Orientation	1	286	299	299	51.5	0	3.4
3-Way Interactions	4	201	196	49.0	8.44	0	2.4
Tow Size*Fibre Length*Chopper Height	1	5.26	5.2	5.2	0.9	0.345	0.1
Tow Size*Fibre Length*Fibre Orientation	1	98.8	99.9	99.9	17.2	0	1.2
Tow Size*Chopper Height*Fibre Orientation	1	30.7	30.8	30.8	5.31	0.023	0.4
Fibre Length*Chopper Height*Fibre Orientation	1	66.4	61.6	61.6	10.6	0.001	0.8
4-Way Interactions	1	47.5	47.5	47.5	8.2	0.005	0.6
Tow Size*Fibre Length*Chopper Height*Fibre Orientation	1	47.5	47.5	47.5	8.2	0.005	0.6
Residual Error	152	881	881	5.8			10.4
Lack of Fit	20	484	483	24.2	8.02	0	5.7
Pure Error	132	398	398	3.01			4.7
Total	167	8450					

F.3 Influence of Fibre Orientation on Elongation to Failure

The results for the elongation to failure of the ODCFP SLS joints are presented in Figure 58; whilst the ANOVA is presented in Table 46. Owing to the very high residual error of the ANOVA, the analysis was only presented for reference and was not carried out extensively. The pure error observed in the investigation was 27.7%; whilst the lack of fit owing to overlooked factors was 13.4%.



Plaque #	0°		45°		90°	
	Elongation to Failure (mm)	Rel Error (%)	Elongation to Failure (mm)	Rel Error (%)	Elongation to Failure (mm)	Rel Error (%)
1	1.73	8.01	1.53	10.5	1.52	7.17
2	1.64	2.43	1.52	11.6	0.94	17.3
3	1.61	6.10	1.02	13.7	0.91	24.9
4	1.47	7.36	1.30	25.7	0.86	15.5
5	1.70	8.73	1.41	20.5	1.13	11.5
6	1.42	16.5	1.31	17.2	1.05	30.6
7	1.49	15.0	1.55	3.89	1.19	18.6
8	1.39	4.82	1.58	5.66	1.52	4.88
9	1.54	3.36	1.64	9.03	1.48	8.12
10	1.52	7.61	1.44	13.1	1.12	22.9
11	1.31	5.75	1.17	25.7	0.89	25.7
12	1.31	4.60	1.38	6.57	1.32	6.57

Figure 58 Elongation to Failure of ODCFP SLS Joints tested at 3 fibre orientations

Appendix F – Investigation of SLS Joints manufactured using ODCFP Substrate

Table 46 Analysis of Variance for Elongation to Failure of ODCFP SLS adhesive joints

Source	DF	Seq SS	Adj SS	Adj MS	F	P	% Contribution
Main Effects	4	5.19	5.39	1.35	41.2	0	43.0
Tow Size	1	1.16	1.36	1.36	41.5	0	9.6
Fibre Length	1	0.98	0.96	0.96	29.5	0	8.1
Chopper Height	1	0.00	0.00	0.00	0.11	0.745	0.0
Fibre Orientation	1	3.06	3.22	3.22	98.5	0	25.4
2-Way Interactions	6	1.40	1.37	0.23	7.01	0	11.6
Tow Size*Fibre Length	1	0.02	0.03	0.03	0.77	0.381	0.2
Tow Size*Chopper Height	1	0.06	0.08	0.08	2.31	0.131	0.5
Tow Size*Fibre Orientation	1	0.61	0.61	0.61	18.8	0	5.1
Fibre Length*Chopper Height	1	0.04	0.04	0.04	1.21	0.274	0.3
Fibre Length*Fibre Orientation	1	0.10	0.09	0.09	2.73	0.101	0.9
Chopper Height*Fibre Orientation	1	0.56	0.55	0.55	17.0	0	4.7
3-Way Interactions	4	0.46	0.46	0.11	3.5	0.009	3.8
Tow Size*Fibre Length*Chopper Height	1	0.06	0.06	0.06	1.91	0.169	0.5
Tow Size*Fibre Length*Fibre Orientation	1	0.20	0.20	0.20	6.14	0.014	1.7
Tow Size*Chopper Height*Fibre Orientation	1	0.04	0.04	0.04	1.27	0.261	0.4
Fibre Length*Chopper Height*Fibre Orientation	1	0.15	0.14	0.14	4.32	0.039	1.2
4-Way Interactions	1	0.05	0.05	0.05	1.65	0.201	0.4
Tow Size*Fibre Length*Chopper Height*Fibre Orientation	1	0.05	0.05	0.05	1.65	0.201	0.4
Residual Error	152	4.97	4.97	0.03			41.2
Lack of Fit	20	1.62	1.62	0.08	3.19	0	13.4
Pure Error	132	3.35	3.35	0.03			27.7
Total	167	12.1					

F.4 Rankings

The ODCFP plaques' SLS joint performance were ranked according to the shear strength and elongation to failure in Table 47; whilst in

Table 48 the failure characteristics were also taken into account. Using these tables the optimum fibre architecture, as described in Chapter 6 was identified.

Table 47 Ranking of ODCFP Substrate Regardless of Fibre Orientation or Failure Mode

Plaque ID	Tow Size	Fibre Length	Chopper Height	Shear Strength Rank	Elongation to Failure Rank	Overall Rank
1	3k	30mm	0mm	3	1	2
2	3k	90mm	0mm	7	6	7
3	24k	90mm	0mm	11	10	11
4	24k	30mm	0mm	9	11	9
5	24k	30mm	75mm	5	4	4
6	24k	90mm	75mm	12	9	11
7	3k	90mm	75mm	6	5	5
8	3k	30mm	75mm	2	3	3
9	3k	30mm	150mm	1	2	1
10	24k	30mm	150mm	10	7	8
11	24k	90mm	150mm	8	12	9
12	3k	90mm	150mm	4	8	6

Table 48 Ranking of ODCFP Substrate Considering Failure Modes of Specimens

Plaque ID	Tow Size	Fibre Length	Chopper Height	Shear Strength Rank	Elongation to Failure Rank	Failure Mode Rank	Overall Rank
1	3k	30mm	0mm	8	1	7	5
2	3k	90mm	0mm	1	3	1	1
3	24k	90mm	0mm	2	4	5	2
4	24k	30mm	0mm	4	8	9	8
5	24k	30mm	75mm	3	2	12	6
6	24k	90mm	75mm	10	9	10	12
7	3k	90mm	75mm	6	7	1	3
8	3k	30mm	75mm	9	10	7	10
9	3k	30mm	150mm	5	5	5	4
10	24k	30mm	150mm	12	6	10	11
11	24k	90mm	150mm	11	12	1	9
12	3k	90mm	150mm	7	11	1	7